

Plasticized Polymer Coatings for SH-SAW Sensors for High Sensitivity and Long-Term Monitoring of BTEX Analytes in Liquid Phase

Pintu Adhikari
Marquette University

Recommended Citation

Adhikari, Pintu, "Plasticized Polymer Coatings for SH-SAW Sensors for High Sensitivity and Long-Term Monitoring of BTEX Analytes in Liquid Phase" (2016). *Master's Theses (2009 -)*. 391.
https://epublications.marquette.edu/theses_open/391

**PLASTICIZED POLYMER COATINGS FOR SH-SAW SENSORS
FOR HIGH SENSITIVITY AND LONG-TERM MONITORING OF
BTEX ANALYTES IN LIQUID PHASE**

by

PINTU ADHIKARI

**A Thesis submitted to the Faculty of the Graduate School,
Marquette University,
in Partial Fulfillment of the Requirements for
the Degree of Masters of Science (Electrical and Computer Engineering).**

Milwaukee, Wisconsin

December 2016

ABSTRACT
PLASTICIZED POLYMER COATINGS FOR SH-SAW SENSORS FOR HIGH SENSITIVITY AND LONG-TERM MONITORING OF BTEX ANALYTES IN LIQUID PHASE

PINTU ADHIKARI
MARQUETTE UNIVERSITY, 2016

BTEX compounds (benzene, toluene, ethylbenzene, and xylene) are constituents of crude oil and hazardous to human health. Among them, benzene has the lowest maximum contaminant level for drinking water because of its carcinogenicity. Spills or leakage from underground storage tanks or hazardous waste sites can contaminate nearby groundwater with these volatile organic compounds. Therefore, it is very important to detect the presence of BTEX contamination as early as possible in order to start the remediation process and maintain a healthy environment.

To develop an in-situ continuous monitoring sensor system, shear horizontal surface acoustic wave (SH-SAW) sensor devices are being investigated and have shown promising results with the use of suitable coatings for BTEX analyte sorption. However, commercially available polymers that can be used as suitable coatings for BTEX detection directly in the aqueous phase are limited in sensitivity and long-term stability. To improve the sensitivity of a suitable polymer, the addition of a plasticizer is a convenient means to lower the glass transition temperature and thus increase sensitivity. The best coatings for acoustic-wave chemical sensors will be those which are rubbery in the low-frequency range, resulting in good analyte sorption, but glassy at the operating frequency of the sensor device, resulting in low acoustic-wave attenuation. Plasticized polymer coatings allow adjustment of the shear modulus of the coating by varying the polymer-plasticizer mixing ratio; this enables the use of thicker coatings with larger analyte sorption capacity and, ultimately, higher sensitivity. This work investigates polymer-plasticizer blends as sensor coatings for detection of BTEX in water at low concentrations (parts per billion range). Two polymers and two plasticizers were studied. For each polymer-plasticizer combination, the influence of the mixing ratio of the blend on the sensor response was investigated. The sensitivity to benzene for each polymer-plasticizer blend was compared with commercially available polymers that had been used for BTEX detection in previous work. The highest sensitivity and lowest detection limit for benzene were found for a 1.25 μm -thick sensor coating of 17.5% diisooctyl azelate-polystyrene. This work demonstrates that by varying type of plasticizer, mixing ratio and coating thickness, the properties of the coating can be conveniently tailored for BTEX analyte sorption. Thus, the addition of plasticizers increases significantly the number of suitable coatings available for use with a single sensor or a sensor array.

ACKNOWLEDGEMENTS

PINTU ADHIKARI

First and foremost, I am grateful to the Almighty (Supreme Soul) for my good health and wellbeing that were essential to complete this research. Also, I am thankful to the Almighty for guiding me throughout my entire life.

I would like to express my deepest gratitude to my advisor professor, Dr. Fabien Josse for his guidance, support and advice over the past two and half year. His scholarly guidance, constant supervision, and valuable criticism from the beginning to the end of the research work have made the completion of the research possible.

I would like to thank Dr. Florian Bender for his guidance, insightful explanation, and direction throughout this work. He is my 2nd research advisors and his experience made my journey smooth. This thesis would not have been complete without the innumerable hours of valuable discussion on both methodological approach and writing style with Dr. Fabien Josse and Dr. Florian Bender.

I would like to thank the members of my thesis committee Dr. Fabien Josse, Dr. Florian Bender, and Dr. Chung Hoon Lee. Thank you for being a part of my success at Marquette University. Also, thank you so much for reviewing and making constructing suggestions on my thesis that help me to grow not only as a good researcher but also as a good technical writer. I also would like to thank all the group members (including Laura Alderson, Jude Coompson, Karthick Sothivelr, Shamitha Dissanayake and Nick Post) of the Microsensor Research Laboratory at Marquette University for their help throughout this journey.

Last but not least, a very special thanks to my parents and younger brother for their lifelong support, unconditional love, sacrifice, and encouragement in all my endeavors.

TABLE OF CONTENTS

ACKNOWLEDGEMENTS	I
LIST OF FIGURES	V
LIST OF TABLES	IX
1. INTRODUCTION	1
1.1 Importance of Monitoring for BTEX	1
1.2 General Background of Sensor Techniques	3
1.2.1 Sensors and Sensor Systems:	3
1.2.2 Categories of Sensors:	4
1.2.3 Chemical Sensors Overview:	4
1.2.4 Acoustic Waves	7
1.3 Acoustic Wave Sensors	9
1.3.1 Thickness Shear Mode (TSM) Resonators:	11
1.3.2 Surface Acoustic Wave (SAW) Sensors:	12
1.3.3 Shear Horizontal Surface Acoustic Wave (SH-SAW):	13
1.3.4 Shear Horizontal Acoustic Plate Mode (SH-APM) Sensors:	13
1.3.5 Flexural Plate Wave (FPW) Sensors:	14
1.4 SH-SAW Devices as Chemical Sensors	15
1.5 Importance of SH-SAW Sensor Coatings	16
1.6 Sensor Arrays	17
1.7 Problem Statement and Objective of Research	18
1.8 Present Status of the Problem and Solution Approach	18
1.9 Organization of the thesis	19
2. THEORETICAL REVIEW OF SH-SAW	21
2.1 Introduction to SH-SAW Devices	21
2.2 Sensor Geometries and Fabrication	22
2.3 Review of IDT Geometry	24
2.4 Review of Acoustic Wave Theory	27
2.5 Transduction and Sensing Mechanism	28
2.6 Analyte Absorption, Mass Loading and Viscoelastic Effect	34

3.	POLYMER AND PLASTICIZER THEORIES.....	36
3.1	Introduction	36
3.2	Polymers.....	36
3.2.1	Basic Properties and Characterization of Polymers:.....	36
3.2.2	Viscoelastic Properties of Polymers:	38
3.2.3	Glass Transition Temperature:	40
3.3	Plasticizers.....	44
3.3.1	Introduction:.....	44
3.3.2	Properties of Plasticizers:.....	45
3.3.3	Types of Plasticizers:	46
3.3.4	Plasticizer Theories:	47
3.4	Effect of Plasticization on Sensing Parameters	50
3.5	Solubility Parameters	51
3.6	Selection Criteria for Polymer and Plasticizer	53
3.7	Chemical Structure & other properties of Polymer.....	54
3.8	Compatibility and Efficiency of Plasticizer	55
3.9	Stability of Plasticizer in Water (Permanence/Leaching).....	56
3.10	Anti-plasticization	58
3.11	Polymer and Plasticizer Used in this Work	58
4.	EXPERIMENTAL PROCEDURE	64
4.1	Introduction	64
4.2	Apparatus and Materials.....	64
4.2.1	Sensing Device:	64
4.2.2	Chemical Materials:	66
4.2.3	Spin Coater:	66
4.2.4	Thickness Characterization:.....	67
4.2.5	Flow Cell:.....	68
4.2.6	Peristaltic Pump:	69
4.2.7	Vector Network Analyzer:.....	70
4.2.8	GC-PID:	70
4.2.9	Plasma System, PE-50:	71
4.3	Experimental Set Up and Procedures	72
4.3.1	Experimental Set Up:.....	72
4.3.2	Device Preparation:.....	73

4.3.3	Analyte Sample Preparing:	79
4.4	Measurement Procedures	81
4.4.1	Thickness Characterization:	81
4.4.2	Device Response:	82
4.4.3	Concentration Confirmation:	83
4.5	Data Processing	84
5.	RESULTS AND DISCUSSION	87
5.1	Introduction	87
5.2	Studied Range of Plasticizer Percentage in the Blend	89
5.3	Thickness of Coating.....	90
5.4	Results for DIOA-PS Coatings	90
5.4.1	22.9% DIOA-PS 7.9% in THF:	92
5.4.2	17% DIOA-PS 10% in THF:	96
5.4.3	17.5% DIOA-PS 11.5% in THF:.....	99
5.4.4	Reproducibility and Repeatability:	103
5.4.5	Reproduced 17.5% DIOA-PS 11.5% in THF for BTEX	106
5.5	DIOA-PMMA and DINCH-PMMA.....	112
5.6	Ideal Plasticizer Percentage of Sensor Coatings	113
5.7	Pinhole Formation and Polymer Creep	115
5.8	Improving Stability by Oxygen Plasma Treatment (OPT).....	117
5.9	Selectivity.....	119
5.10	Sensitivity Comparison	122
6.	SUMMARY, CONCLUSIONS AND FUTURE WORK	126
6.1	Summary	126
6.2	Conclusions	129
6.3	Future Work.....	131
	REFERENCES	133

LIST OF FIGURES

Figure 1.1: BTEX compounds of gasoline (% weight) [2].....	1
Figure 1.2: A schematic diagram of a sensor system.	4
Figure 1.3: schematic representation of acoustic waves in solids [9].....	9
Figure 1.4: Pictorial representation of TSM, SAW, FPW and APM acoustic sensors [13]	11
Figure 2.1: A schematic diagram of SH-SAW sensor with different layers.....	22
Figure 2.2: Schematic view of four-layer and three-layer sensor geometries.	22
Figure 2.3: A schematic view of general three-layer sensor geometry with the coordinate system.	23
Figure 2.4: Single pair IDT finger geometry	24
Figure 2.5: Schematic diagram of double electrodes and two-ten electrodes with their measured pass band frequency spectrum [7].	26
Figure 2.6: Schematic of a three-layer SH-SAW sensor system with coordinates.	28
Figure 3.1: Schematic view of cyclic stress and strain vs time for various types of materials [8].	39
Figure 3.2: First order and second order change of crystalline and amorphous materials [10].....	41
Figure 3.3: Schematic of various regions of a polymer over a broad range of temperature [11].....	42
Figure 3.4: A relationship among compatibility, efficiency, and permanence of plasticizer [18].....	57
Figure 4.1: A SH-SAW device used for this work with a coin to compare the size of the device.	65
Figure 4.2: Parts of the flow cell used for this work. Top, Plexiglas cover with gasket and inlet/outlet tubes; lower left, bottom part of the flow cell to house the device; lower right, brass middle part with contact pins including grounding pins.	69

Figure 4.3: A Schematic of the experimental set-up used in this work.....	72
Figure 5.1: Frequency response of SH-SAW device coated with 0.7 μm -thick ($h = 0.0175 \lambda$) 22.9% DIOA-PS coating to 1 ppm (1 mg/L) benzene in water with error bars.	92
Figure 5.2: Frequency shift vs benzene concentration with a linear fit and zero intercept to extract sensitivity for a 0.7 μm -thick ($h = 0.0175 \lambda$) 22.9% DIOA-PS coated SH-SAW sensor.....	94
Figure 5.3: Loss spectrum of an SH-SAW sensor device with 0.7 μm -thick ($h = 0.0175 \lambda$) 22.9% DIOA-PS coating. The inset shows the loss tracked at the operating frequency. .	95
Figure 5.4: Frequency response of SH-SAW device coated with 1.0 μm -thick ($h = 0.025 \lambda$) 17% DIOA-PS coating to a concentration of 1 ppm benzene in water. Error bars represent the standard deviation of 9 measurements performed over 36 days.	97
Figure 5.5: Frequency shift vs benzene concentration with a linear fit and zero y-intercept used for extracting sensitivity for a 1.0 μm -thick ($h = 0.025 \lambda$) 17% DIOA-PS coated SH-SAW sensor.	98
Figure 5.6: Device insertion loss at the operating frequency for the 1.0 μm -thick 17% DIOA-PS coated SH-SAW sensor tracked over a period of 40 days.....	99
Figure 5.7: Frequency response of SH-SAW device coated with 1.25 μm -thick ($h = 0.031 \lambda$) 17.5% DIOA-PS coating to various concentrations of benzene in water. Concentrations are indicated in the graph (1 ppb = 1 $\mu\text{g/L}$). The analyte was flushed out with DI water between individual sample measurements and the graph combines individual sensor responses recorded on different days. The signal was corrected for baseline drift.	100
Figure 5.8: Frequency responses of the 1.25 μm -thick ($h = 0.031 \lambda$) 17.5% DIOA-PS coated SH-SAW sensor normalized to 1 ppm benzene. The data shows repeatability of the frequency response of the devices.	101
Figure 5.9: Frequency shift vs benzene concentration with a linear fit and zero y-intercept used for extracting sensitivity for a 1.25 μm -thick ($h = 0.031 \lambda$) 17.5% DIOA-PS coated SH-SAW sensor.....	102
Figure 5.10: Device insertion loss at the operating frequency for the 1.25 μm -thick ($h = 0.031 \lambda$) 17.5% DIOA-PS coated SH-SAW sensor tracked over a period of 32 days.	103
Figure 5.11: The average frequency response of SH-SAW device coated with the reproduced 1.25 μm -thick ($h = 0.031 \lambda$) 17.5% DIOA-PS coating to a concentration of 1 ppm (1 mg/L) benzene in water with error bars representing the standard deviation of the measurements.....	104

- Figure 5.12: Frequency shift vs benzene concentration with a linear fit and zero y-intercept used for extracting sensitivity for the reproduced 1.25 μm -thick ($h = 0.031 \lambda$) 17.5% DIOA-PS coated SH-SAW sensor. 105
- Figure 5.13: Device insertion loss at the operating frequency for the reproduced 1.25 μm -thick 17.5% DIOA-PS coated SH-SAW sensor tracked over a period of 37 days. 106
- Figure 5.14: The average frequency response of SH-SAW device coated with the reproduced 1.25 μm -thick ($h = 0.031 \lambda$) 17.5% DIOA-PS coating normalized to a concentration of 1 ppm (1 mg/L) toluene in water with error bars representing the standard deviation of the measurements. 107
- Figure 5.15: The average frequency response of SH-SAW device coated with the reproduced 1.25 μm -thick ($h = 0.031 \lambda$) 17.5% DIOA-PS coating normalized to a concentration of 1 ppm (1 mg/L) ethylbenzene in water with error bars that represent the standard deviation of the measurements. 108
- Figure 5.16: The average frequency response of SH-SAW device coated with the reproduced 1.25 μm -thick ($h = 0.031 \lambda$) 17.5% DIOA-PS coating normalized to a concentration of 1 ppm (1 mg/L) xylene in water with error bars representing the standard deviation of the measurements. 109
- Figure 5.17: Measured frequency shift vs toluene concentration with a linear fit and zero intercept used for extracting sensitivity for the reproduced 1.25 μm -thick ($h = 0.031 \lambda$) 17.5% DIOA-PS coated SH-SAW sensor. 110
- Figure 5.18: Measured frequency shift vs ethylbenzene concentration with a linear fit and zero intercept used for extracting sensitivity for the reproduced 1.25 μm -thick ($h = 0.031 \lambda$) 17.5% DIOA-PS coated SH-SAW sensor. 111
- Figure 5.19: Measured frequency shift vs xylene concentration with a linear fit and zero intercept used for extracting sensitivity for the reproduced 1.25 μm -thick ($h = 0.031 \lambda$) 17.5% DIOA-PS coated SH-SAW sensor. 111
- Figure 5.20: Results for coatings with various thicknesses and polymer-plasticizer (DIOA-PS) mixing ratios showing the stability of the coatings. All red points represent unstable coatings and all points on or below the dotted line are stable coatings that can produce repeatable sensor response. 114
- Figure 5.21: Left side: surface of a SH-SAW device coated with 1.25 μm -thick 17.5% DIOA-PS coating before the measurements; right side: surface of the same device after one month of measurements, seen under an optical microscope. Scale: the width of the IDT fingers (narrow golden lines) is about 5 μm 116
- Figure 5.22: Change in insertion loss versus time, left: change in loss for a device without oxygen plasma treatment; right: change in loss for a device with oxygen plasma treatment. 118

Figure 5.23: Partial selectivity comparison among various coatings (1.25 μm -thick 17.5 % DIOA-PS, 0.7 μm -thick 22.9 % DIOA-PS, 1.0 μm -thick 23% DINCH-PS, 0.6 μm -thick PECH and 0.8 μm -thick PIB). 120

Figure 5.24: Radial plot showing the response time constant, τ (in units of 100 s), and the ratios of frequency shift, Δf of devices coated with various coatings for benzene, toluene and ethylbenzene..... 121

Figure 5.25: Comparison of frequency shift response as a function of benzene concentration for SH-SAW devices coated with various investigated polymer-plasticizer coatings and commercially available polymer coatings. Thickness of each coating is given in parenthesis..... 123

LIST OF TABLES

Table 1: Commonly used Piezoelectric Crystal materials with their characteristics [19], [20].....	15
Table 2: Chemical properties of the materials used in this work [according to manufacturer's specifications (Sigma Aldrich, Scientific Polymer Products.)]	60
Table 3: Hansen solubility parameter of the materials used in this work [22], [36], [37], [38].....	62
Table 4: Solubility Calculation between two materials	62
Table 5: Sensitivity to Benzene for various coatings of DINCH-PMMA and DIOA-PMMA with Several Coating Thickness.....	112
Table 6: Summary of the investigated coatings along existing coatings showing response time constants and sensitivities for BTEX compounds	122

1. INTRODUCTION

1.1 Importance of Monitoring for BTEX

The acronym BTEX stands for the four volatile organic compounds (VOCs) Benzene, Toluene, Ethylbenzene and Xylene usually found in petroleum products. BTEX compounds are naturally found in crude oil, and also occur in petroleum products such as gasoline and diesel fuel [1]. These four BTEX components are often found together in contamination sites and the average percentages (% weight of total amount of BTEX compounds) of these chemicals in gasoline are given below (note that xylene exists in the form of three chemical isomers: o-, m-, and p-xylene). Note that these four compounds will not always be found together. These chemicals can also be found in the environment individually.

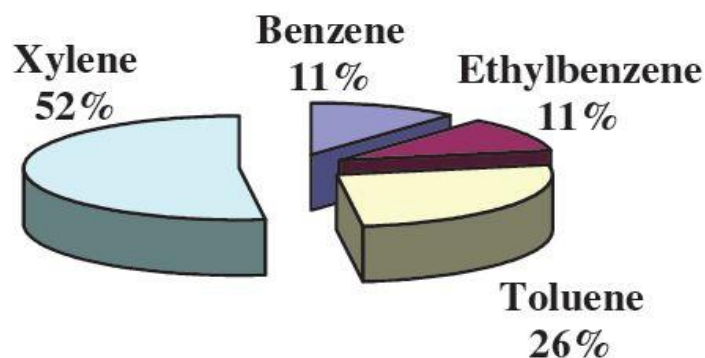


Figure 1.1: BTEX compounds of gasoline (% weight) [2].

Benzene can be found in gasoline as well as in products such as synthetic rubber, plastic, nylon, insecticides, furniture wax, cosmetics, etc. It can also be found in automobile exhaust and smoke. Around 20% of the total nationwide exposure to benzene

is found in automobile exhaust and industrial exposure. Tobacco smoke accounts for about 50% of the nationwide exposure to benzene [1].

Toluene can be found naturally in petroleum products and it is used as a solvent for paints, coatings, gums and oils. Similar to toluene, ethylbenzene can be found in gasoline but it is also used as aeronautics fuel additive. It can also be found in consumer products such as paints, plastics, pesticides etc. Xylene can be found in petroleum as well as in paints, rubber and leather industries [1].

BTEX compounds are almost ubiquitous in ambient air at small concentrations because these are volatile chemicals and most importantly benzene can be found in auto exhaust and smoke. But high concentrations of BTEX pose a danger to the environment. BTEX contamination can occur from different sources. One of the main sources of BTEX pollution is the accidental release of gasoline from faulty and poorly maintained underground storage tanks [2]. In addition, overfilling of storage tanks, surface spills, pipeline leaks, fuel spills from vehicle accidents and landfills can be sources of BTEX contamination. BTEX compounds can easily pollute the environment by evaporation, and can contaminate groundwater and public and private drinking water systems by moving through soil and dissolving into water [1].

BTEX can be hazardous to human health depending on how much, how long and how often a person is exposed to it. Exposure to BTEX can occur by drinking contaminated water, breathing contaminated air or absorption through the skin, potentially resulting in face skin and sensory irritation, central nervous system (CNS) problems such as tiredness, dizziness, headache, loss of coordination, etc. It can also have effects on the respiratory system and cause eye and nose irritation. Extended exposure to

these chemicals has effects on kidney, liver and body systems. Most importantly, the U.S. Environmental Protection Agency (U.S. EPA) has identified benzene as a human carcinogen [2].

The Safe Drinking Water Act (SDWA) protects human health by guaranteeing the quality of drinking water whether from above ground or underground in the USA [3]. Because of SDWA and the health hazards of BTEX, the U.S. EPA has set up Maximum Contaminant Levels (MCLs) for chemical contamination in drinking water. The MCL set by U.S. EPA is 5 parts per billion (ppb) or $5\mu\text{g/L}$ for benzene, 1 part per million (ppm) or 1mg/L for toluene, 10 ppm for ethylbenzene and 700 ppb for xylene, respectively.

1.2 General Background of Sensor Techniques

1.2.1 Sensors and Sensor Systems

In a broader sense, a sensor is a device that receives a signal or stimulus that could be physical, chemical or biological, and responds usually with an electrical signal [4]. The electrical response signal of the sensor can be in the form of a voltage, current, amplitude, resistance, frequency, and/or phase. This signal can be processed by an electronic device such as a network analyzer and/or computer. Thus, a sensor can work as an interface between the real world and electronic devices.

A sensor is usually a part of a larger data acquisition system which may consist of detectors, signal processor, signal conditioner, data recorders, memory devices, actuators and some other devices. The measurands of a sensor or sensor system can be physical, mechanical, thermal, chemical or bio-chemical. A sensor system may be very complex; a typical sensor system is illustrated in the Fig.1.2.

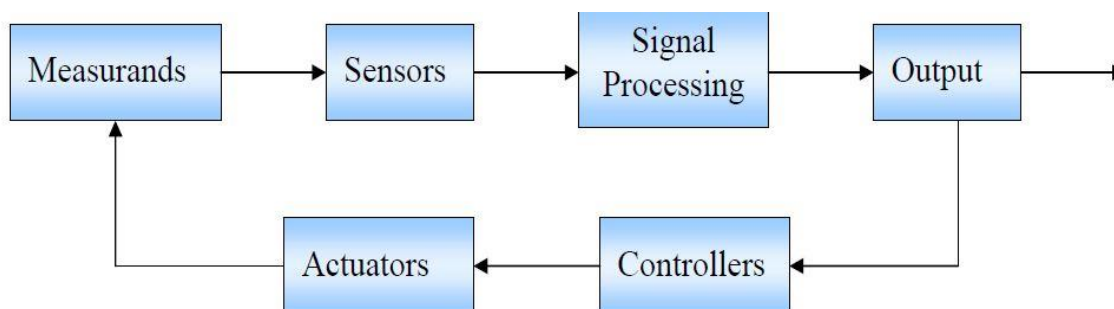


Figure 1.2: A schematic diagram of a sensor system.

1.2.2 Categories of Sensors

Sensors can be divided into many different categories such as natural and man-made sensors, active and passive sensors, contacting and non-contacting sensors etc. Alternatively, according to the applications and measuring quantities sensors can be classified into many different types, for example: pressure sensor, position sensor, level sensor, strain sensor, flow sensor, temperature sensor, chemical sensor, bio-chemical sensor etc. In this research work, the main focus is on chemical sensors.

1.2.3 Chemical Sensors Overview

A chemical sensor is a device that can determine the detectable presence, concentration or quantity of a given chemical analyte in liquid or gas phase [5]. Basically, chemical sensors can identify and/or quantify chemical species. Like all other sensor systems, a chemical sensor is a part of a larger data acquisition system. It consists of a recognition element (often a coating), a transduction element (that can convert energy or signal from one form to another) and a data collection technology that is used to monitor the changes of chemical concentrations. The choice of the recognition element of a

chemical sensor – which is typically a coating or film that will interact with the chemical(s) of interest – depends on various factors.

Many different sensor platforms can be used to identify and quantify the changes caused by the interaction of a chemical analyte with the coating element. The platforms can be resistive, capacitive, optical or acoustic wave-based. The acoustic wave sensor platform is studied in this thesis. Chemical sensors can be characterized by some parameters regardless of these platforms. Those parameters are sensitivity, selectivity, response time constant, dynamic range, linearity, stability, repeatability and detection limit.

- Sensitivity is defined as the change in the measured signal per unit concentration of analyte, such as $\Delta f/\Delta c$, where Δf is frequency shift and Δc is the change in analyte concentration [6]. In other words, it can be defined as the change in sensor output signal divided by the change in the concentration or mass of the analyte, i.e. the slope of the response vs concentration curve. For chemical sensors, it is mainly the product of the sensitivity of the coating element to the analyte and the sensitivity of the transduction element to its operating characteristic.
- Selectivity is the ability to distinguish between the target analyte and non-target analytes. This property mainly depends on the coating or film of the sensor. In general, bio-chemical sensors are more selective than chemical sensors.
- Response time constant is the time taken by a sensor to reach 63% of its final value of the response after exposing to a step change in

concentration. Usually, it is denoted by τ_s . Alternatively, τ_{90} (the time taken by the sensor signal to reach 90% of its final value when exposed to a step change in concentration) can be used [7]. Response time relies on the sorption rate and properties of analyte-coating interactions. For exponential sensor responses, $\tau_{90} = 2.3 * \tau_s$.

- Detection limit is often expressed as limit of detection (LOD) and defined as the smallest concentration of analyte that can be detected reliably by a chemical sensor. The response change by this smallest concentration should be no smaller than three times the root-mean-square (RMS) noise level of the baseline [8].
 - Dynamic range is defined as the range of analyte concentrations where the sensor shows a significant sensitivity (i.e., a significant change in sensor output with a change in analyte concentration) [7].
 - Linearity: The relative deviation between an experimentally determined calibration and an ideal straight line in the dynamic range is stated as linearity [7].
 - Stability can be described as the ability to uphold its performance during a particular period of time.
 - Repeatability is stated as the degree in which a sensor can repeatedly provide the same response for the same analyte concentration while the measurement has been taken place under the same conditions [8].
- Reliability is similar to repeatability except the measurements are taken

under a variety of conditions to test whether the sensor device will show the same response for the same analyte concentration.

- **Reproducibility:** Although it is often confused with repeatability, it is defined as the ability of fabricating identical sensor devices or sensor coatings (films) by the same procedure but at different times or at different places with different instruments or facilities, yielding the same sensor response for the same analyte concentration. If a sensor coating has a high degree of reproducibility, then a single coated sensor from a batch of sensors is capable to yield calibration data that are valid for all other sensors in that batch [8].

1.2.4 Acoustic Waves

An acoustic wave is a disturbance in an elastic medium that propagates in space and time, thus transferring the energy supplied by an excitation source along the medium in the form of oscillation or vibration [9]. Unlike electromagnetic waves, acoustic waves propagate through a medium and their speed depends on the mechanical properties of the medium. Theoretically, all materials support acoustic wave propagation but piezoelectric materials offer the advantage of simple excitation and detection of the acoustic wave. As a result, piezoelectric materials are often chosen as acoustic substrate for many acoustic wave devices because of their electromagnetic energy conversion properties.

There are mainly two types of acoustic waves, one is surface acoustic waves (SAW) and the other is bulk acoustic waves (BAW). A surface acoustic wave (SAW) is a wave that propagates along the surface of the material and is confined to that surface, and

a bulk acoustic wave (BAW) is a wave that propagates through the bulk of the material. Variations of these two waves are found in many different waves such as longitudinal, shear, mixed longitudinal-shear Rayleigh waves, Love waves, Lamb waves, etc. Although the velocity of an acoustic wave depends on the properties of the medium, in general it is much slower than electromagnetic waves. Fig. 3 shows schematic illustrations of acoustic waves with their typical range of wave velocities. In (a) and (b) bulk waves are shown where bulk longitudinal waves have particle displacement parallel to the wave propagation direction and bulk transverse waves have particle displacement normal to the wave propagation direction. In case of surface waves, shear horizontal surface acoustic waves have particle displacement polarized normal to the wave propagation direction and parallel to the wave propagation surface whereas shear vertical surface acoustic waves have particle displacement polarized normal to the propagation direction and perpendicular to the surface [8].

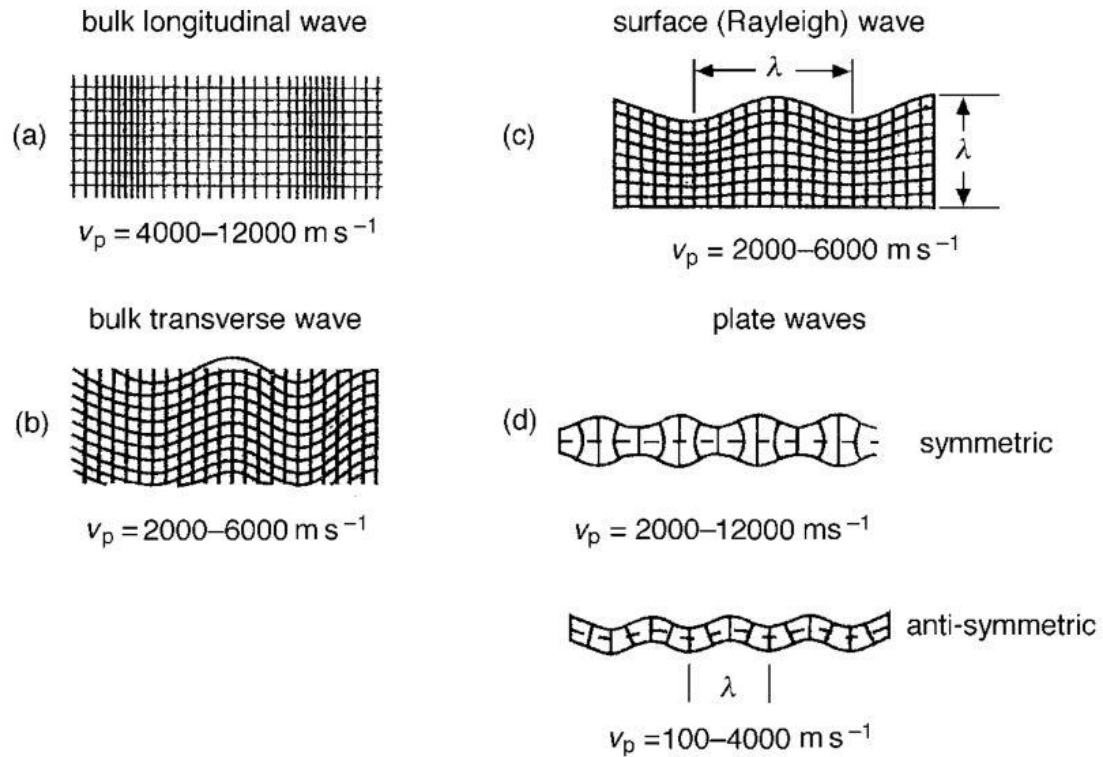


Figure 1.3: Schematic representation of acoustic waves in solids [8].

1.3 Acoustic Wave Sensors

Acoustic wave devices have been used since world war I and the first application of piezoelectric acoustic devices was sonar (**s**ound **n**avigation and **r**anging) application in 1917 [10]. After that, the improvement of interdigital transducers (IDTs) made acoustic wave based sensors much easier to fabricate. In the 1960s, acoustic transduction of IDTs based on SAW and other modes of acoustic wave propagation was first demonstrated by White & Voltmer [11]. In the 1980s, SAW devices compatible with VLSI technology had reached their maturity and have been commercially used since then.

Both SAW and BAW are widely used in acoustic wave sensors. In SAW devices the energy conversion (acoustic to electric) is happening on the side of the material that is in

contact with the sensing medium but in BAW devices the energy conversion can happen on the other side of the acoustic material [12]. When the acoustic wave is travelling through the device or on the surface of the device, any kind of perturbation will affect the velocity, amplitude and/or phase of the wave. These changes are related to frequency, insertion loss or phase of the response signal of the device. By monitoring any of these changes it is possible to identify and/or quantify the physical or chemical quantity which is the reason for the perturbation.

There exist various acoustic wave sensors such as thickness shear mode (TSM) resonator, surface acoustic wave (SAW) device, shear horizontal surface acoustic wave (SH-SAW) device, shear horizontal acoustic plate mode (SH-APM) device and flexural plate wave (FPW) device. All acoustic wave sensors work properly in vacuum or gaseous phase but only few of them work properly in liquid phase. Those devices that have shear horizontal particle displacement work well in liquid and include TSM, SH-SAW and SH-APM. The other devices that have compressional wave components to couple with liquids dissipate substantial amounts of energy into liquids. Although FPW sensors have such a component, they can work well in liquid phase because the velocity of the wave is considerably lower than the compressional velocity of sound in liquids. A brief review of these four types of sensor and a pictorial representation are given below [8].

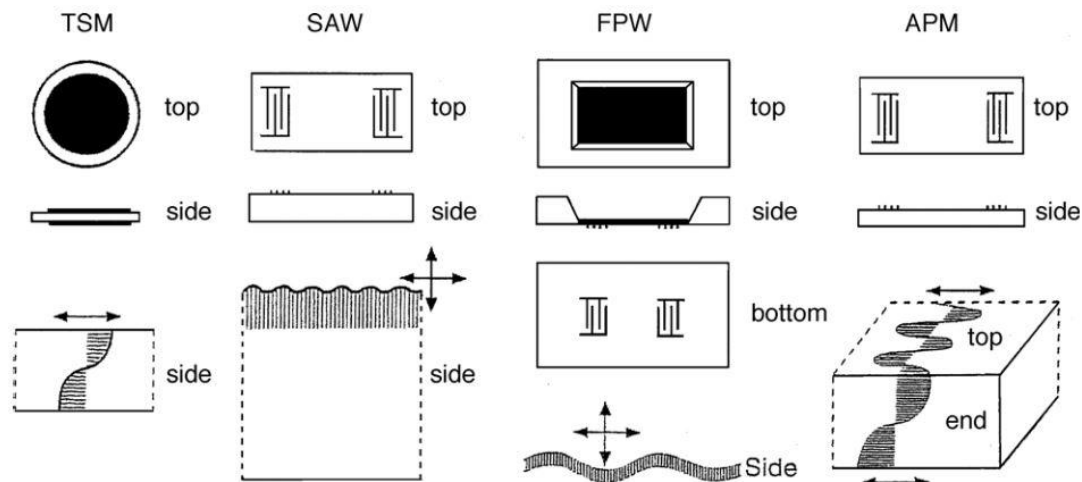


Figure 1.4: Schematic representation of TSM, SAW, FPW and APM acoustic sensors [13].

1.3.1 Thickness Shear Mode (TSM) Resonators

The oldest and simplest acoustic wave device is the Thickness Shear Mode (TSM) Resonator [14], also widely known as quartz crystal microbalance (QCM). Usually, this device consists of a thin disk of AT-cut quartz crystal with parallel circular metal electrodes patterned on both sides of the crystal [15]. The TSM resonator supports a standing bulk shear acoustic wave between the two surfaces of the plate, and the particle displacement is parallel to the surface of the device. As the displacement is maximum at the crystal surface of a TSM resonator, it is used as a gravimetric mass sensor. It can also be used as a chemical sensor by using a chemically sensitive coating on the surface of the QCM that will absorb the target analyte. Consequently, the absorbed added mass will change the resonance frequency and therefore be detected by the sensor.

1.3.2 Surface Acoustic Wave (SAW) Sensors

SAW sensors exploit SAW propagation and electromagnetic transduction performed by two or more metallic electrodes and a piezoelectric substrate/layer [16]. In SAW sensors metallic electrodes also known as IDTs are fabricated in a 'delay line' configuration as shown in Fig. 4. When an alternating voltage is applied between two successive electrodes, a periodic mechanical strain is produced in the piezoelectric crystal due to the periodic electric field of the alternating voltage. As a result of mechanical strain, a surface acoustic wave will be generated that can propagate from the input transducer to the output transducer. The velocity of this wave depends on the material, orientation and cut of the crystal. The properties of this wave such as velocity and amplitude will change by any perturbation on the surface of the device. The typical frequencies of SAW resonator based applications are in the UHF band and below 1GHz but some commercial SAW devices have frequencies up to 3GHz [16]. Particularly, the typical frequencies of operation of SAW sensors are 30 to 1000MHz. The fundamental frequency of SAW sensors depends on the pitch of the IDTs and velocity of the acoustic wave. The pitch is basically the transducer periodicity, d referred as the center-to-center distance between the successive fingers of one comb of the IDT and this pitch is chosen as equal to the wave length of the SAW wave, λ . Thus, the fundamental frequency of the SAW device is defined as, $f_0 = v/\lambda$, where v is the velocity of the wave [8]. However, SAW sensors have both vertical and horizontal components. The vertical component can couple with any media in contact with the device. This will not produce significant attenuation in the gas phase but will lead to unacceptable insertion loss in the liquid

phase. For liquid phase sensor application, a special case of SAW, called SH-SAW has generally been used and has much better performance as described below.

1.3.3 Shear Horizontal Surface Acoustic Wave (SH-SAW)

The SH-SAW sensor is a device which has particle displacement parallel to the surface of the device and normal to the wave propagation direction. This device uses a piezoelectric substrate with a special crystal orientation, and the wave is generated and received in input and output IDTs like on a SAW device. To perform well in liquid, the SH-SAW should not have any particle displacement component perpendicular to the crystal surface. However, common piezoelectric materials do not yield pure shear waves and additionally, the SH-SAW propagates slightly deeper ($1\sim 5 \lambda$) within the substrate [17], resulting in lower sensitivity and increased insertion loss. To increase the sensitivity and trap the energy near the surface, a guiding layer is often used that can work as an acoustic waveguide. A material which has lower acoustic velocity has to be used for the guiding layer. This design operates effectively in liquid. SH-SAW devices can be made more sensitive than TSM devices because most of the energy is trapped near the surface of the device where the sensing takes place. The back side of the device can be bonded to the sensor package whereas in TSM devices both sides interact with the bulk wave and can be used for sensing.

1.3.4 Shear Horizontal Acoustic Plate Mode (SH-APM) Sensors

SH-APM sensors use a single piezoelectric crystal as waveguide that confines the acoustic wave in between the upper and lower surface of the crystal. Both surfaces of the device can be used for sensing in contrast to SH-SAWs where only one surface is used

for sensing [14]. The thickness of the plate is typically around 10 wavelengths. Similar as for an SH-SAW, this wave also has particle displacement parallel to the surface and normal to the propagation direction. The absence of the vertical component allows this wave to propagate along the surfaces of the device without coupling excessive energy into an adjacent liquid [8]. The SH-APM has higher sensitivity than TSMs but lower than SH-SAWs because the acoustic energy is not confined to the surface. Moreover, the sensitivity of the sensor increases with decreasing thickness of the plate which is limited by the need for robustness of the device and by the manufacturing process.

1.3.5 Flexural Plate Wave (FPW) Sensors

The Flexural Plate Wave device is an acoustic wave device where the acoustic wave is produced in a thinned membrane [8]. This device is fabricated in a standard silicon wafer. On one side of the wafer a membrane layer (silicon nitride, silicon dioxide, oxy-nitride, aluminum nitride or diamond) is deposited, then piezoelectric material (zinc oxide) is sputtered on the surface of the membrane and finally metal electrodes (IDTs) are patterned on top of the surface. On the backside of the wafer, the silicon is etched to release the membrane [18]. The thickness of the membrane is much less than the acoustic wavelength. The wave has elliptical particle displacement similar to Rayleigh waves and it is referred to as Lamb wave. The FPW propagates from one IDTs to the other in a delay line configuration and any perturbation on the surface changes the properties of the wave such as velocity or amplitude. FPW sensors have many advantages on chemical sensing and can be operated in liquid phase because the wave velocity is lower than that of compressional waves in water (operating frequencies are in 100's of KHz to few MHz). But the big disadvantage of the device is the thin membrane that tends to be fragile.

1.4 SH-SAW Devices as Chemical Sensors

Acoustic wave devices have been available for commercial use for 65 years and have many applications in chemical and bio-chemical sensing. The most common piezoelectric materials used to fabricate the AW devices are lithium niobate (LiNbO_3), lithium tantalate (LiTaO_3) and quartz (SiO_2). Every crystal has its own advantages. SH-SAW sensors perform very well in liquid phase and, for this case, have the highest sensitivity among the other AW devices mentioned in this chapter. To generate this mode, a specific crystal orientation is needed. Some commonly used piezoelectric materials with their crystal orientation and other properties are given below.

Table 1: Commonly used piezoelectric crystal materials with their characteristics [19],[20].

Piezoelectric crystal	Orientation	SH-SAW Velocity (m/s)	Temperature Coefficient (ppm/°C)	Electromagnetic coupling coefficient (%)
64°/41° YX-LiNbO ₃	64°/41° rotated, Y-cut, X-propagating	4478/4389	81/80	11.3/17.2
36° YX-LiTaO ₃	36° rotated, Y-cut, X-propagating	4112	32	4.7
LST-quartz	15° rotated, Y-cut, X-propagating	4990	0	0.11

SH-SAW sensors can detect chemicals in trace concentrations (ppm to ppb levels) in liquid phase. They can be used as small, in situ, portable and continuous chemical identifying and quantifying systems.

1.5 Importance of SH-SAW Sensor Coatings

As mentioned above, to trap all the acoustic energy near the surface of the device, a thin film that acts as a guiding layer is coated on the surface of the SH-SAW sensor, made of a material that has a lower acoustic wave velocity than the substrate. If the film is (bio)chemically sensitive, it will turn the device into a (bio)chemical sensor. This film will determine the selectivity of the device and contribute to the sensitivity of the sensor. For a chemically sorptive film, the presence of chemical species changes the physical properties of the film. Thus, this film works as a chemical to physical transducer by inducing changes in its physical properties in the presence of a specific chemical analyte in the sensing medium. Selecting the materials for this film or coating is one of the most important steps to optimize a sensor for a particular application. Depending on the coating materials, the sensor can be used for a variety of applications such as environmental monitoring (e.g., detecting pesticides), in-situ industrial process monitoring and control (to detect a specific chemical), counterterrorism (in airport security, chemical and biochemical weapons detection), personal health safety, etc. As an example, to detect BTEX chemicals, a specific type of material is needed for the coating, possessing suitable properties such as chemical structure, glass transition temperature, etc. The performance of the SH-SAW sensor will depend on the choice of the coating material. As the theory behind SH-SAW sensors has already been established, selecting and blending the right coating materials is the main objective of the research for this thesis.

1.6 Sensor Arrays

The selectivity of a chemical sensor varies for different coatings and usually is lower than for biosensors. To solve the selectivity issue, one approach that had been proposed by Zaromb and Stetter in 1984 is to use an array of sensors with various coatings [21]. Different sensor coatings have different sensitivities for the same chemical analyte. Therefore, an array of chemical sensors with various coatings, each possessing partial selectivity to the analytes, can be designed to detect and quantify chemicals in a sample containing multiple analytes. Sometimes one sensor is enough to detect and quantify the analytes, specifically if more than one sensing parameter is used, but a sensor array is always better for the confirmation of the result obtained from the first sensor. In addition, if each coating is selected to give high sensitivity for a specific analyte, a sensor array exposed to a mixture of these analytes will give better results compared to a single sensor. As an example, for detection and quantification of mixtures of BTEX compounds in water, a sensor array of four coatings with different partial selectivities (i.e., different ratios of sensitivities to different BTEX compounds) can be designed to obtain precise concentration measurements of each BTEX analyte from the mixture. Furthermore, it is important to select coatings materials that are stable in water and capable to sorb specific analytes rapidly and reversibly. The investigation of diverse SH-SAW sensor coatings is a high priority in the development of an in-situ continuous BTEX identification and quantification system for groundwater monitoring. However, because of the limited number of commercially available polymer coatings showing good performance in BTEX detection, finding additional coatings based on polymer-plasticizer

blends provides an opportunity to greatly improve this BTEX monitoring sensor technology.

1.7 Problem Statement and Objective of Research

Section I described the various sources of contamination with BTEX and the hazards associated with such contamination. The objective of this research is to detect and quantify the presence of BTEX contamination in groundwater as early as possible, with the goal to minimize contamination, to permit rapid remediation, and to maintain a healthy environment. To perform the research work, the SH-SAW sensor platform has been used to establish a real time in-situ and cost effective BTEX monitoring system. The primary objective of this research is to develop sensor coatings based on suitable polymer-plasticizer blends that can detect BTEX compounds in groundwater in a very low concentration range (ppb to low ppm). Also investigated were the repeatability, reproducibility and long term stability of the coatings.

1.8 Present Status of the Problem and Solution Approach

At present, the standard for analyzing a groundwater sample [22] is to collect the groundwater sample and transport it to a laboratory where the sample can be tested and analyzed. This procedure is time consuming and expensive. In addition, as the BTEX compounds are volatile and can be degraded by microorganisms [23], there is a possibility of analyte loss during transport to the laboratory for analysis. Therefore, an urgent need exists to develop an in-situ BTEX measurement technique to analyze groundwater and to protect the environment from possible hazardous impacts. For this methodology, sensor devices are being investigated and shear horizontal surface acoustic

wave (SH-SAW) sensor devices have shown promising results with the use of suitable polymer coatings for analyte sorption [24]. So far, only two polymers have shown promising results in long-term measurements on BTEX detection; however, to implement a sensor array and to confirm the presence of BTEX in aqueous phase in the presence of potential interferents, a larger variety of coatings is needed. To select polymers as coatings for SH-SAW devices, the glass transition temperature of the polymer has to be considered. If the polymer is too glassy, it will not effectively absorb the analyte, and if it is too rubbery, it will strongly attenuate the SH-SAW. By varying the mixing ratio of plasticizer to polymer, the glass transition temperature can be adjusted to the desired value. Blending diisooctyl azelate (DIOA) plasticizer with polystyrene polymer is showing promising results for BTEX detection. Some plasticizers are not suitable for aqueous environment because of leaching. Plasticizers that have very slow or undetectable leaching rates and also have the ability to lower the glass transition temperature of polymers have been proposed for use in SH-SAW sensor coatings. Plasticizer-polymer combinations (DIOA-PS, DIOA-PMMA, DINCH-PMMA) are being investigated to create a stable and sensitive coating for SH-SAW sensors to detect BTEX compounds in groundwater.

1.9 Organization of the thesis

This thesis is comprised of six chapters. Chapter 1 is an introduction that describes the problem of BTEX exposure, general background of sensor systems, current status of the problem and objective of this research. Along with SH-SAW sensors, several other types of sensor devices have been reviewed briefly in this chapter. The importance of coatings for SH-SAW sensors has been explained. Chapter 2 discusses a theoretical review

of SH-SAWs, various geometries of IDTs for SH-SAW sensors, sensing mechanism and effect of analyte sorption on coating parameters. Chapter 3 offers a detailed theoretical discussion of coating materials. Properties of polymer and plasticizer materials, glass transition temperature of the materials, solubility parameters and polymer-plasticizer selection criteria are discussed in this chapter. Plasticizer theories and effect of plasticization on coating materials are also discussed in chapter three. In chapter 4, experimental methods, setup and procedure are discussed in detail. Along with the description of the instruments used for this research, coating solution preparation, device preparation and analyte sample preparation are also discussed in chapter four. Chapter 5 contains the results and discussion. Detailed characterizations of devices with specific coatings are presented in this chapter, as well as a comparison of coating sensitivities found in this research with existing coatings. Finally, in Chapter 6, a summary of the results and the conclusion are presented along with suggestions for future work.

2. THEORETICAL REVIEW OF SH-SAW

2.1 Introduction to SH-SAW Devices

In the first chapter, a general overview of acoustic wave sensors has been given. In this chapter, only shear horizontal surface acoustic wave (SH-SAW) sensors will be discussed as this research work is based on this type of sensor. As discussed in chapter one, guided SH-SAW sensors are based on a piezoelectric crystal (e.g., LiTaO₃) substrate, metal electrodes (IDTs) and a thin film to guide the shear horizontal surface acoustic wave. This film (coating) can be selected to act as both the guiding layer and chemically sensitive layer. For bio-chemical sensing, biologically sensitive receptors can be deposited on the coating to provide bio-chemical selectivity to the sensor. For this research, only chemical sensing will be discussed. In order to understand the response of the sensor to the target chemical analyte, it is essential to look at the function of each layer of the sensor before understanding the sensor system as a whole. In addition, it is important to understand the characteristics of the perturbed acoustic wave. In this chapter, a theoretical review of the SH-SAW sensor platform is presented based on acoustic wave theory. In addition, the geometry and fabrication of SH-SAW sensors, mass loading and viscoelastic effects, as well as transduction and sensing mechanisms of SH-SAWs are reviewed in detail.

2.2 Sensor Geometries and Fabrication

A schematic diagram of the two-port SH-SAW sensor device is shown below.

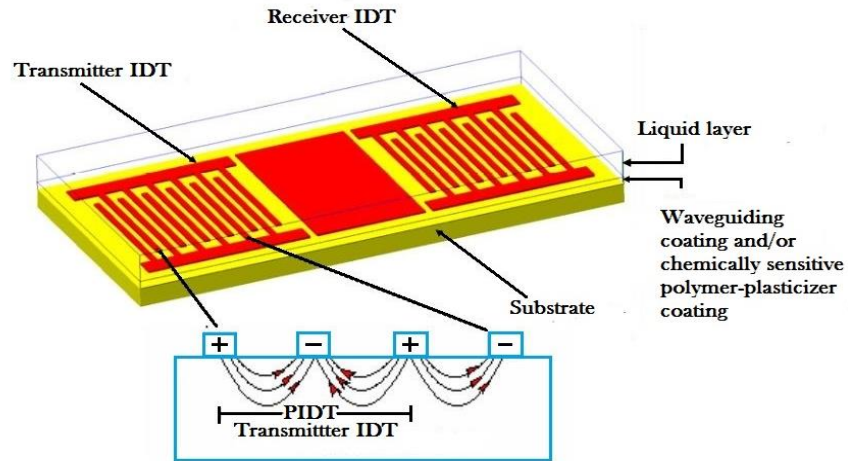


Figure 2.1: A schematic diagram of SH-SAW sensor with different layers [19].

The sensor geometry used in this work consists of a piezoelectric crystal substrate, a film, and a liquid layer. It is a three-layer geometry because the film acts as both waveguide and chemically sensitive layer. If a sensor needs two films, one for wave guiding and another for sensing, it is said to have a four-layer geometry. A schematic view of three layer and four layer geometries is shown in the Fig.2.2.

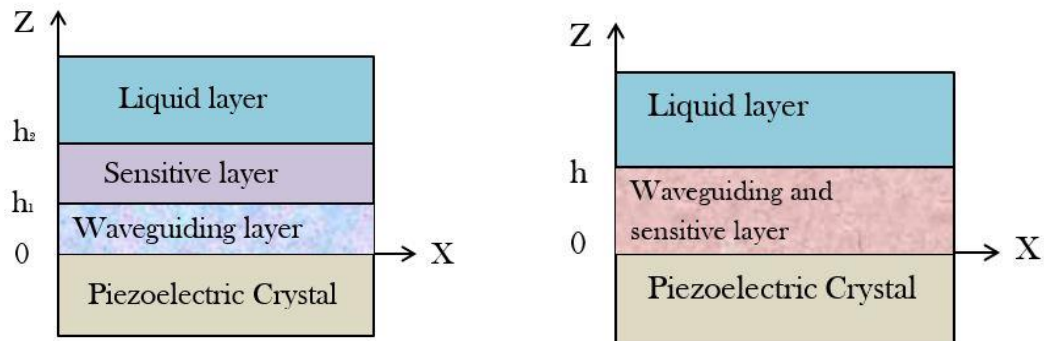


Figure 2.2: Schematic view of four-layer and three-layer sensor geometries.

There are various kinds of piezoelectric crystals available as SH-SAW sensor substrates, and because of a better electromechanical coupling coefficient, high dielectric constant and acceptable temperature coefficient of delay (TCD), 36° rotated Y-cut X-propagating lithium tantalate (LiTaO_3) is used in this work. By using this orientation of the crystal, the particle displacement will be in the y direction which is parallel to the surface and wave propagation direction will be in the x direction. A three-layer structure along with the coordinate system is given below [20], [25], [26].

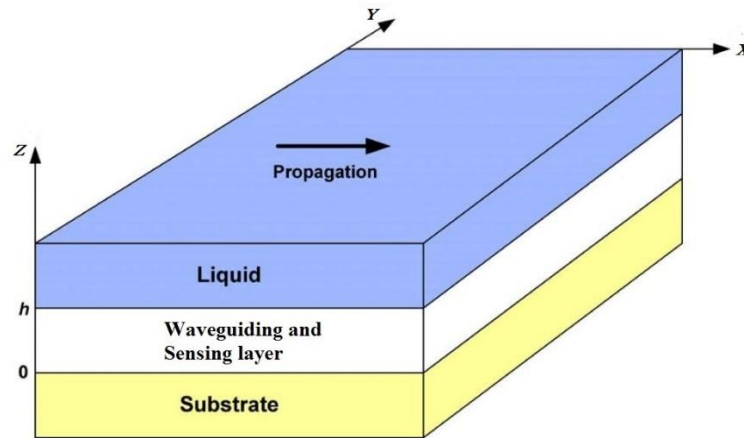


Figure 2.3: A schematic view of general three-layer sensor geometry with the coordinate system.

In this three-layer geometry, the 2nd layer, shown above as the wave-guiding and sensing layer with thickness h , is coated on top of the surface of the device. This layer is made of polymer materials or a polymer-plasticizer blend, and a detailed discussion about polymers and plasticizers is given in chapter 3.

The 3rd layer of this geometry is the liquid layer and is assumed to be a Newtonian fluid where the viscosity is constant with respect to frequency. The liquid contains the target chemical analyte to be detected, and the concentration of the chemical analyte will

be very low (ppm or ppb range) for this research. Here, low concentration means the absorption of the analyte obeys the linear sorption isotherm equation [27]. As a result, the frequency response can be assumed to be linear with the change in concentration [27]. In this sensor geometry, the liquid layer and substrate are assumed as semi-infinite layers (thickness $\rightarrow\infty$) but the coating layer is considered as a finite layer with thickness h . The fabrication process of the SH-SAW sensor is similar to that of MEMS devices. After choosing a 36° rotated Y-cut X-propagating LiTaO₃ crystal as substrate, the metal electrode pattern is deposited in the form of a transmitting and a receiving transducer by using standard photolithography. The metal IDT can be deposited onto the substrate surface by using lithography, metal deposition and etching techniques [11].

2.3 Review of IDT Geometry

It is important to have an optimum IDT finger arrangement for a specific application. General SAW devices have a one-one IDT finger pair geometry shown in the Fig.2.4 below with acoustic wave generation from the IDTs.

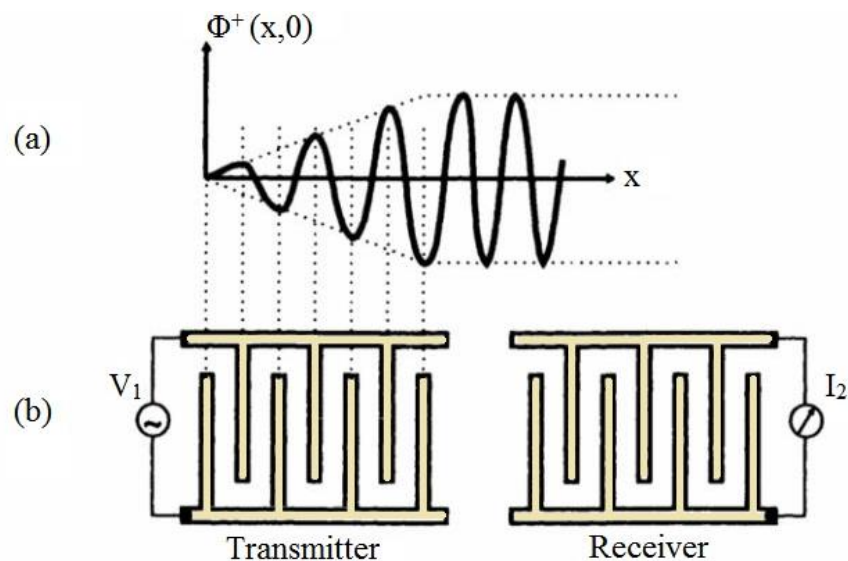


Figure 2.4: Single pair IDT finger geometry [19].

However, it is possible to reduce the unwanted acoustic wave reflections and phase distortions in an SH-SAW device. A multi-electrode transducer can be used to reduce baseline noise. The number and polarities of electrode fingers in multi-electrode transducers need to be arranged in such a way that most of the reflected waves will cancel each other [28]. In SH-SAW devices an Au metal electrode is used in a transducer structure on the surface of a piezoelectric substrate. In IDTs, every electrode finger is a potential source (reflection edge) of acoustic wave reflection. Both changes in mechanical and electrical boundary conditions can lead to reflections and distort the signal. If the piezoelectric material has a high coupling factor, this signal distortion will be significant. Some common piezoelectric materials used for SH-SAW devices, LiNbO_3 and LiTaO_3 , have high coupling factors. In order to reduce unwanted reflections, double-electrode IDTs (“split-finger”/ “two-two finger pair”) are used [29]. A double-electrode IDT has four electrode fingers per electric period ($S_e=4$) which cause a 180° phase difference for reflections from adjacent electrode fingers, meaning that the reflections effectively cancel each other. For weak piezoelectric coupling materials where the amplitudes of the reflected waves from adjacent electrodes are approximately equal, a double-electrode IDT is sufficient for reducing unwanted reflections, but for strong piezoelectric coupling materials, there still remains significant reflection even if using double-electrode IDTs. In liquid phase, because of their high dielectric constants, LiNbO_3 or LiTaO_3 substrates are used for SH-SAW devices, but their high coupling factors lead to unwanted wave reflection even if using double-electrode IDTs. To improve the SH-SAW pass band, the number of electrodes can be reduced to minimize overall reflection, but this will lead to a larger SH-SAW bandwidth and increased mode overlap. A more

promising approach is to change the polarity of some electrodes in order to make them opposite in phase to the SH-SAW, thus reducing the overall coupling of the SH-SAW to the IDT while still obtaining a narrow bandwidth. A detailed design approach has been discussed in a previous work of this research group [30] to achieve the desired transfer function based on multi-electrode IDTs [31]. The SH-SAW device used for this work has a two-ten electrode fingers arrangement. The double-electrode and two-ten-electrode IDTs with their associated measured passband are shown in the Fig.2.5 below [30]. Fig. 2.5b shows a less distorted SH-SAW passband and reduced interference between adjacent modes.

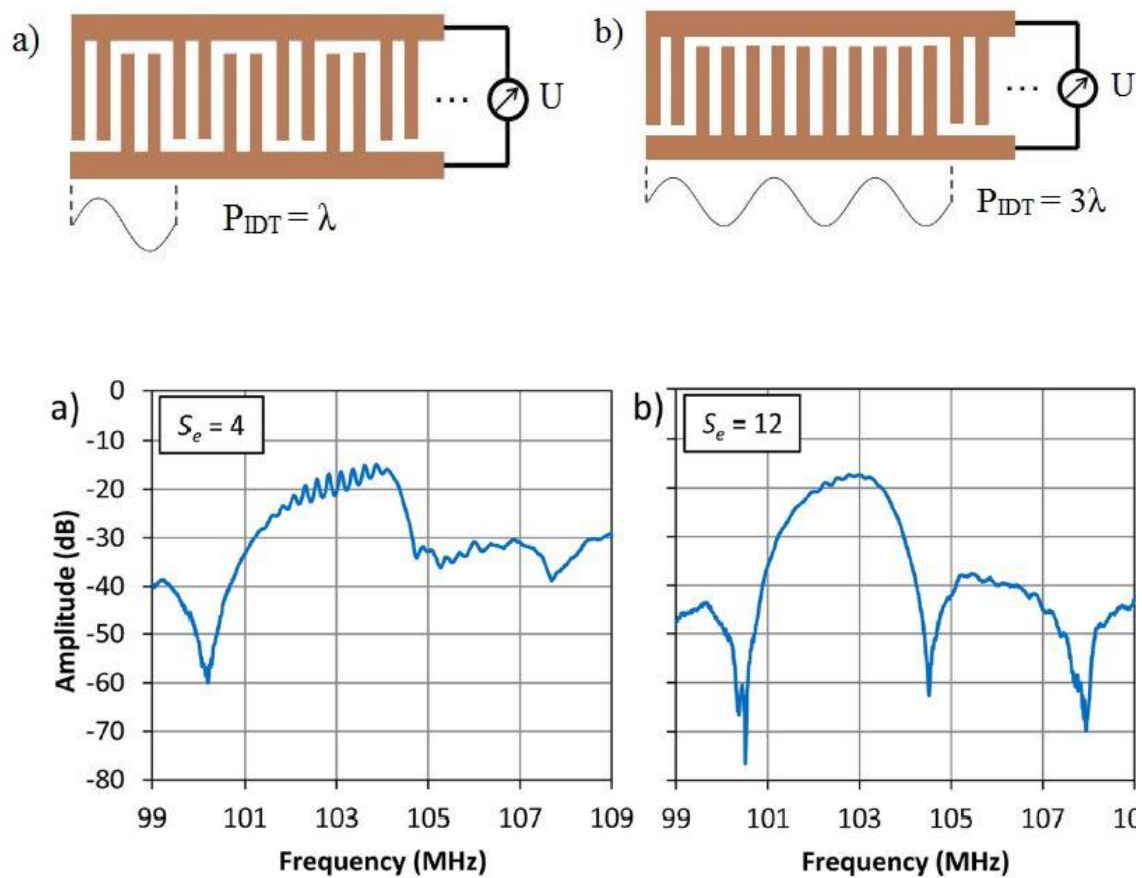


Figure 2.5: Schematic diagram of a) double electrodes and b) two-ten electrodes with their measured pass band frequency spectrum [30].

The SH-SAW sensor platform used in this work was previously described in [30], [24]. It is a two-ten finger IDT and the IDT periodicity is 120 μm . The third harmonic of the SH-SAW was used for this work, resulting in a wavelength of $\lambda = 40 \mu\text{m}$ and a frequency of 103-MHz. A 36° YX-LiTaO₃ piezoelectric crystal serves as a substrate for the sensor platform. The center-to-center IDT separation is 8 mm (200λ).

2.4 Review of Acoustic Wave Theory

Before utilizing the acoustic wave device as a sensor, it is important to review the theoretical modeling of the device and analyze the acoustic mode in the system. It is also important to review the changes of the characteristics of the acoustic wave as a result of any perturbation on the sensor surface. In this research, a composite sensor system with three-layer geometry will be used. The overall sensor sensitivity to mechanical and electrical perturbations from the analyte solutions of interest can be analyzed using two methods. As described in detail in the dissertations of former students of our research group [19], [32], the first method involves numerical analysis and the second is based on perturbation theory. Although the rigorous numerical analysis method is effective and accurate, it is difficult to relate the numerical changes used in this model with the physical changes of the sensor system. On the other hand, the perturbation method attributes all the small physical changes in the sensor system to specific changes in ambient parameters, and involves the calculation of resulting changes in acoustic wave properties. This method is one of the most commonly used methods in liquid and gas phase sensing and will be used in this work. It is described in more detail in the following section.

2.5 Transduction and Sensing Mechanism

With a chemically sensitive guiding layer, shear horizontal surface acoustic wave sensors are very effective chemical sensors in liquid phase because of the shear horizontal movement of the particles.

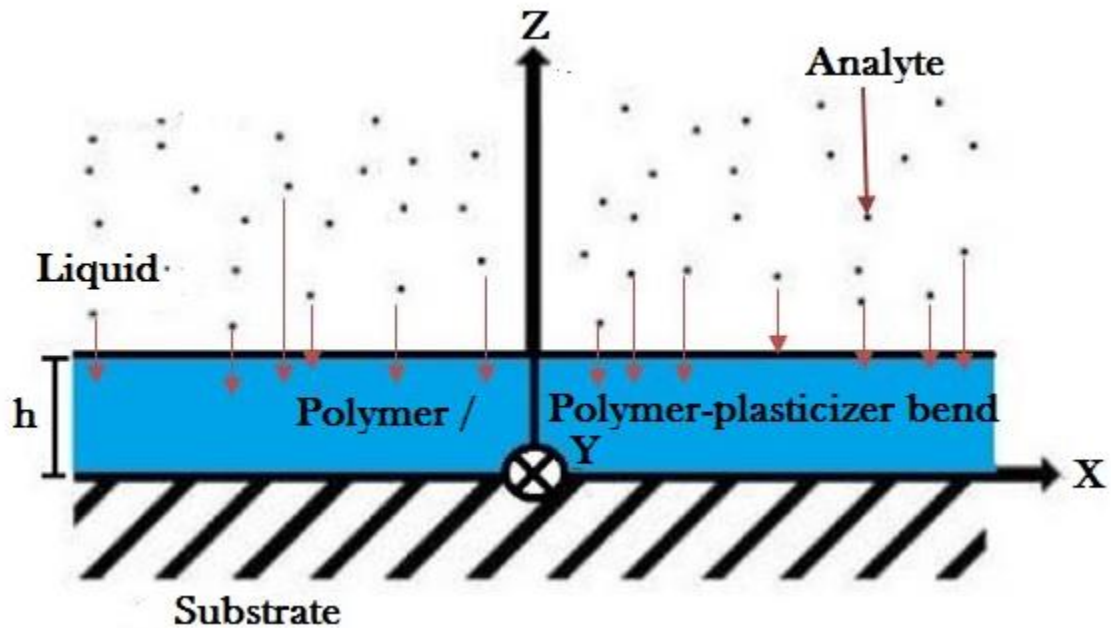


Figure 2.6: Schematic of a three-layer SH-SAW sensor system with coordinates.

The three-layer geometry of a SH-SAW sensor, shown in the above Fig.2.6, indicates that the sensing and guiding polymer / polymer-plasticizer layer (coating/film) has contact with both the liquid environment and substrate layer. The properties of the coating affect the acoustic wave, and the coating confines the wave to the surface of the substrate. The liquid contains analyte molecules, which are absorbed (and adsorbed) by the coating from the liquid sample by the process of diffusion. This absorption of analyte molecules changes the properties of the coating. As a result, the velocity and attenuation of the acoustic wave will also change. This velocity and attenuation change can be related to the

measured frequency shift and loss change, respectively [19], [32]. The shear horizontal surface acoustic wave travelling along the surface of the device has particle displacement in the y direction; for this wave, particle displacement is a function of x , y and time and the wave can be described by the following expression [33],

$$u_y(x, y, t) = u_y(z, t)e^{j\omega t - \gamma x} \quad (2.1)$$

where, $\omega = 2\pi f$ represents the angular frequency of the wave and γ is the complex coefficient of the propagating wave, encompassing the attenuation (α) and wave number (k) of the wave [8],

$$\gamma = \alpha + jk = \alpha + j\frac{\omega}{v} \quad (2.2)$$

The wavenumber (k) is defined as the angular frequency (ω) divided by wave velocity (v). The change of the properties of the propagating wave at a specific frequency can be characterized by measuring the change of attenuation (α) and velocity (v) of the wave. Therefore, the changing complex coefficient of the wave is a function of changing attenuation and velocity of the wave and can be expressed as

$$\Delta\gamma = \Delta\alpha + j\Delta k = \Delta\alpha - jk_0 \frac{\Delta v}{v_0} \quad (2.3)$$

where k_0 and v_0 are the wavenumber and phase velocity of the wave before perturbation, respectively. The above expression is usually written in normalized form by dividing by the unperturbed wavenumber as

$$\Delta\gamma' = \frac{\Delta\gamma}{k_0} = \frac{\Delta\alpha}{k_0} - j \frac{\Delta v}{v_0} \quad (2.4)$$

A network analyzer is used to measure the frequency spectrum of the device. The relationship between the frequency and velocity is given below as,

$$f = \frac{v}{P} \quad (2.5)$$

where P is the periodicity of the IDT of the SH-SAW sensor device. The vector network analyzer is used in continuous monitoring of the frequency spectrum while the sensor device is exposed to the analyte, and because of the sorption of analyte into the coating, the velocity and attenuation of the wave change. If P is constant for a particular device, the normalized frequency change is equal to the normalized change in the wave velocity, assuming phase velocity and group velocity are equal.

$$\frac{\Delta f}{f} = \frac{\Delta v}{v} \quad (2.6)$$

By measuring the frequency change, the change in velocity due to film perturbation can be measured, thus enabling analyte detection and quantification.

Changes in velocity and attenuation are due to the change in mass (m), viscoelastic constant (c), dielectric constant (ϵ), conductivity (σ), temperature (T) and pressure (P) for

an SH-SAW device. The total change in velocity and attenuation, for small perturbation, can be expressed as a sum of partial derivatives with respect to these parameters as [32],

$$\Delta v = \frac{\delta v}{\delta m} \Delta m + \frac{\delta v}{\delta c} \Delta c + \frac{\delta v}{\delta \varepsilon} \Delta \varepsilon + \frac{\delta v}{\delta \sigma} \Delta \sigma + \frac{\delta v}{\delta T} \Delta T + \frac{\delta v}{\delta P} \Delta P. \quad (2.7)$$

$$\Delta \alpha = \frac{\delta \alpha}{\delta c} \Delta c + \frac{\delta \alpha}{\delta \varepsilon} \Delta \varepsilon + \frac{\delta \alpha}{\delta \sigma} \Delta \sigma + \frac{\delta \alpha}{\delta T} \Delta T + \frac{\delta \alpha}{\delta P} \Delta P. \quad (2.8)$$

These two equations are basically the sum of all the parameters that cause the change in velocity and attenuation, except attenuation is either not a function of mass accumulation (gas phase) or depends only weakly on mass accumulation (liquid phase) [32]. However, by using an appropriate experimental design, some terms in the above equations can be minimized or eliminated. A grounded metalized delay line can eliminate the acoustoelectric interactions, and as a result $\Delta \varepsilon$ and $\Delta \sigma$ become zero. The experiment can be performed at a constant temperature in a temperature controlled setting such as using a cooler box. Finally, by using a dual delay line configuration of the device, it is possible to eliminate the temperature (ΔT) and pressure (ΔP) effects from the equation by making a differential measurement. Note that SH-SAW devices are very sensitive to temperature; specifically, devices fabricated on a lithium tantalate crystal substrate have a temperature frequency coefficient of between $-30 \text{ ppm}/^\circ\text{C}$ and $-40 \text{ ppm}/^\circ\text{C}$ [34]. Temperature changes on the order of tens of millidegrees will not significantly affect the frequency shift and small ambient pressure changes will also not produce a change in frequency because of the shear horizontal motion of the SH-SAW. By eliminating those terms from the above two equations, the equations can be simplified to

$$\Delta v = \frac{\delta v}{\delta c} \Delta c + \frac{\delta v}{\delta m} \Delta m \quad (2.9)$$

$$\Delta \alpha = \frac{\delta \alpha}{\delta c} \Delta c \quad (2.10)$$

i.e., the change in velocity depends on both the change in viscoelastic coefficient and mass loading, but the change in attenuation only depends on the change in viscoelastic coefficient. The sensor response is solely dependent on the coating because the mass loading and viscoelastic changes are due to analyte sorption of the coating.

Changes in viscoelastic properties (Δc) of the coating can be characterized by the material's modulus changes. For an SH-SAW, the coating undergoes a shear deformation, so only the shear modulus (G) has to be considered, which is a complex term that can be expressed as

$$G = G' + jG'' \quad (2.11)$$

where G' and G'' are the storage modulus and loss modulus, respectively. The storage modulus is associated with the energy stored and released as the coating displacement occurs with the oscillation of the shear horizontal surface acoustic wave. The loss modulus is associated with the energy that is being lost from the system, usually in the form of heat because of the deformation of the material. From equation (2.6), the frequency shift is related to the change in velocity. Assuming that the shear modulus is

the only component of viscoelastic changes, the frequency shift and attenuation change can be expressed as a function of shear modulus [32]:

$$\Delta f = f_1(\Delta m, \Delta G', \Delta G'') \quad (2.12)$$

$$\Delta \alpha = f_2(\Delta G', \Delta G'') \quad (2.13)$$

Because of the adsorption of analyte, the shear modulus of the coating changes and that change contributes to the response of the sensor.

For this experimental work, a network analyzer is used to measure insertion loss instead of attenuation. However, the change in insertion loss is directly related to the change in attenuation by the equation below [29]

$$\frac{\Delta \alpha}{k} = \frac{\Delta L}{54.6} N \quad (2.14)$$

where ΔL and N are change in insertion loss and length of the transmission line in units of wavelength, respectively. Because the size of the device and wavelength are constant for this experimental work, change in insertion loss can be used to calculate change in attenuation.

2.6 Analyte Absorption, Mass Loading and Viscoelastic Effect

The response of a polymer coated SH-SAW device depends on both mass loading and change of polymer modulus [32]. The characteristic response of the device is a function of the nature of the interaction between the chemically sensitive layer and analyte and the mass transport (sorption) process. The sorption process is a combination of adsorption and absorption processes. Analyte sorption by the coating from the liquid environment results in mechanical loading which is a combination of added mass and change in the complex modulus of the coating [8], [19]. It is difficult to evaluate the contribution of the change of polymer modulus due to the unknown actual value of polymer modulus before and after the analyte sorption. The mass loading is expressed as the change in the product of the coating density and thickness, $\Delta(\rho h)$, after exposure to analyte solution. The coating thickness and density vary with the absorption of the analyte solution, and this has been analyzed in the references [19], [32]. Although mass loading often provides the dominant contribution to the sensor response for polymer coated acoustic sensor devices, some studies have shown that the viscoelastic effect can have an equal or greater contribution in both gas and liquid phase [35], [36], [37]. Analyte sorption causes the polymer coating to swell and soften, or plasticize, and as a consequence the viscoelasticity of the coating changes. In a glassy, highly cross-linked or crystalline polymer, these changes are minimal, but in a lightly cross-linked or rubbery polymer these changes are significant. In the plasticized polymers used in this work, viscoelastic changes can be quite significant. The viscoelastic change in a plasticized polymer coating indicates a change in the shear modulus, resulting in changes in both phase velocity and attenuation. When the plasticized polymer coating is exposed to the sample, the absorption (and adsorption) of analytes from

the sample changes the mass as well as the viscoelastic properties of the coating, resulting in changes in SH-SAW frequency, phase and loss.

3. POLYMER AND PLASTICIZER THEORIES

3.1 Introduction

The response of a sensor eventually depends on the properties of the coating materials. The sensitivity and selectivity of a chemical or bio-chemical sensor are governed by the interactions between the coating materials and the target analytes. Therefore, in order to predict the sensor response, it is important to understand the physical and chemical properties of the coating materials. In this research, polymer-plasticizer blends are used as coating materials. In this chapter, basic physical and chemical properties, viscoelastic properties, glass transition temperature of polymer-plasticizer blends, effect of plasticization on polymers and solubility parameters of the materials will be discussed in details. Finally, the selection criteria of polymers and plasticizers for BTEX detection as well as the polymers and plasticizers used in this work will be discussed.

3.2 Polymers

3.2.1 Basic Properties and Characterization of Polymers

In order to gain control over the sensing characteristics of a polymer-coated SH-SAW sensor, an understanding of the properties of the polymer is first required. The properties of a polymer are influenced by various factors such as inter and intra molecular forces that bind the polymer molecules together, size of the polymer chain and the average molecular weight of the polymer [8]. Inter molecular forces are the attraction produced between neighboring molecules as a result of synchronization of electron

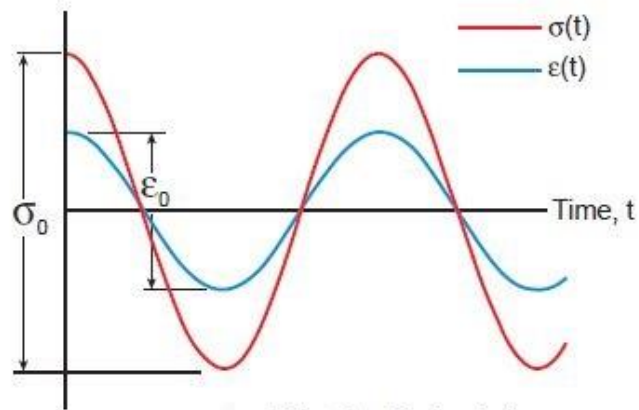
motion in the interacting atoms. Physical properties of the polymer mainly depend on this force. Intra-molecular forces on the other hand are covalent bonds that hold the repeating units or monomers of polymer together.

Polymers can be divided into three main groups, which are thermoplastics, thermosets and elastomers [38]. Thermoplastics can be further divided into two types: crystalline and amorphous. Crystalline polymers are more rigid, have higher melting point temperature and are less affected by solvent penetration as compared to amorphous polymers. Overall, thermoplastic materials have relatively weak inter-molecular force which is why this material softens when exposed to heat, and usually returns back to its original state upon cooling. Thermoplastic polymers are homogeneous, non-volatile and can be repeatedly softened and solidified by heating and cooling, and therefore can be used as coatings in acoustic wave (bio-) chemical sensors [39]. Thermoplastic polymers have only secondary bonds between polymer chains but no cross-links. Examples of thermoplastic polymers are polyvinyl chloride (PVC), polystyrene (PS) etc. Unlike thermoplastics, thermosets are irreversibly softened and solidified when heated and cooled, respectively. Thermoset polymers are usually three dimensional networked polymers, which have a greater number of cross-links, making them more rigid. For this reason, they have slower response times and longer recovery times which is undesired for sensing. Examples of thermoset polymers are epoxides, polyesters, etc. The other group of polymers, elastomers, are basically rubbery polymers which can be easily stretched and will return to their original shape by applying and removing stress. This type of polymer has less cross-link density than thermosets, but these cross-links are enough to

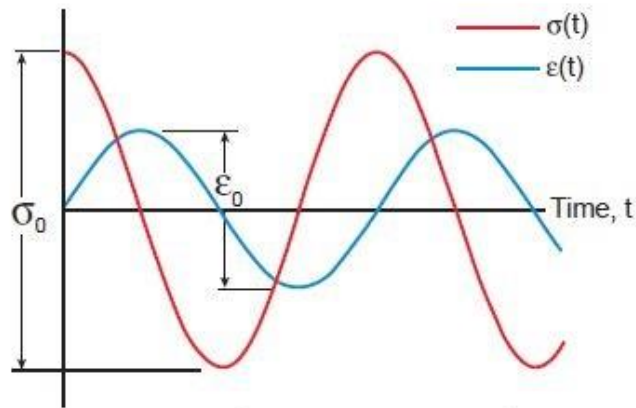
prevent polymer chains to move permanently relative to each other [32]. Examples of elastomers are natural rubber, polyurethanes, polybutadiene, neoprene, etc. [40].

3.2.2 Viscoelastic Properties of Polymers

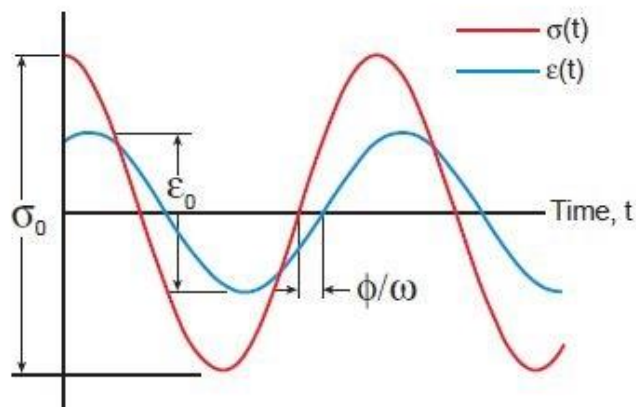
Viscoelasticity is a property of materials that combine both the viscous and elastic properties of a liquid and solid, respectively [41]. An elastic solid has a definite shape but deforms and restores its original shape when external forces are applied and removed. A viscous liquid shows resistance to shear flow but has no definite shape, i.e. it flows irreversibly when external forces are applied [42]. The viscoelastic behavior of a polymer can include all intermediate ranges of properties between an elastic solid and a viscous liquid. Additionally, viscoelastic properties depend on temperature and experimental time scale, which means the material possesses a memory (fading) of past events, i.e. mechanical properties are a function of time because of the intrinsic nature of polymers. Viscoelasticity of a polymer describes the polymer deformation when stress is applied. In an acoustic wave sensor, the stress is caused by the passage of an acoustic wave. The relationship of stress and strain for different materials is shown in the Fig.3.1 below. From the Fig.3.1 it is clearly seen that polymer materials combine the behavior of elastic and viscous materials. The loading frequency ω is in phase with the strain for elastic materials, 90° out of phase for viscous materials and for viscoelastic material, it is out of phase by an angle ϕ , where $0 < \phi < 90^\circ$.



a. Elastic Material



b. Viscous Material



c. Viscoelastic Material

Figure 3.1: Schematic view of cyclic stress and strain vs time for various types of materials [43].

A polymer's basic mechanical properties depend on the bulk modulus (K) and shear modulus (G). Both parameters are complex and can be expressed as:

$$K = K' + jK'' \quad (3.1)$$

$$G = G' + jG'' \quad (3.2)$$

where K' and G' are storage moduli that represent the elastic behavior of the material and K'' and G'' are loss moduli, which represent the viscous behavior of the material. For SH-SAW sensors, the shear deformation is dominant and that is why only the shear modulus of the polymer is considered. Therefore, any change in the viscoelastic behavior of the polymer will influence the shear modulus of the polymer coating, which will affect the sensor response.

3.2.3 Glass Transition Temperature

One of the most important properties of a polymer is its (static) glass transition temperature (T_g). The glass transition temperature is the temperature range where the polymer transitions from a hard, rigid or glassy material to a soft, rubbery material. Although it is a (usually narrow) temperature range where the mobility of the polymer chains increases substantially, the convention is to describe it as a single temperature defined as the midpoint of this temperature range [44]. The glass transition temperature depends on several factors such as the chemical structure of the polymer, the molecular weight of the polymer, the thermal history, age and other factors. The transition occurs

only in the amorphous region of the polymer. If the polymer has any crystalline region, it will remain crystalline during the glass transition.

The glass transition temperature (T_g) is often confused with melting point (T_m), but there are some clear differences between these phase transitions. Glass transition occurs in the amorphous region whereas melting happens in the crystalline region. Below and above T_g , disordered amorphous materials have immobile molecules and partially mobile molecules, respectively. On the other hand, below and above T_m the crystalline region is solid and deformed due to melting respectively. Additionally, T_m is a first order phase transition and T_g is a second-order transition [45]. The Fig.3.2 shows the first and second order transition of crystalline and amorphous materials.

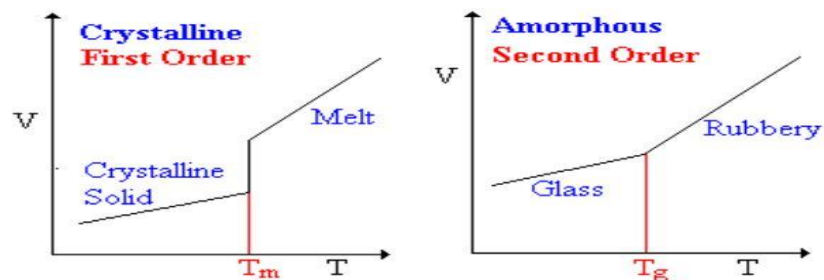


Figure 3.2: First order and second order change of crystalline and amorphous materials [45].

Typically, over a broad temperature range most polymer materials can be found in four different regions of state or phase, referred as glassy, transition, rubbery and viscous, as shown in Fig. 3.3, which shows a modulus vs temperature curve for linear and cross-linked amorphous polymer materials.

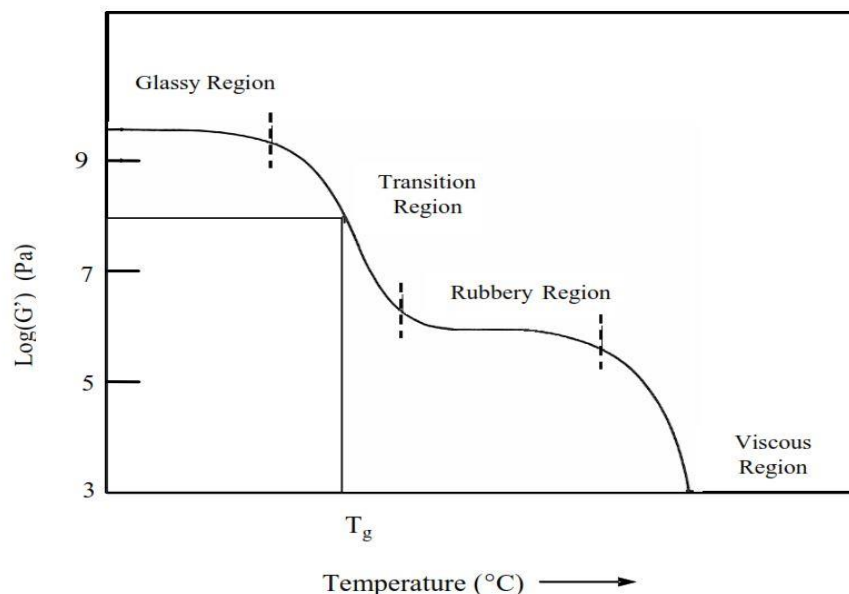


Figure 3.3: Schematic of various phase regions of a polymer over a broad range of temperature [46].

This transition of polymer material is called the (static) glass-rubber transition or simply the glass transition. At the glass transition temperature, physical properties of the material such as the Young's and shear moduli, specific heat, coefficient of expansion and dielectric constant are changed [47]. Below this temperature, the molecular chains of the polymer are immobile and there is no rotational or translational motion of the molecule. This behavior of polymers is reflected in their storage and loss modulus. For this region (glassy) the loss modulus is much lower than the storage modulus, such that for a typical glassy polymer film, $G' \approx 10^9 \text{ Pa}$ and $G'' \ll G'$ [32]. At this region, polymers become hard, brittle and glassy because the energy barrier for inter-chain motions of the polymer is greater than the thermal energy of the polymer molecule, which is why the chain of the molecule can no longer move or wiggle around. When the temperature increases to a point above the glass transition temperature, the loss modulus also increases and storage modulus decreases. Above T_g , the polymer becomes soft, rubbery and viscoelastic. A

typical rubbery film exists when $G' \leq 10^7$ Pa and $G'' \leq G'$ [32]. Moreover, the polymer's glassy or rubbery behavior can be determined by its relaxation time. Most particles in a material eventually reach equilibrium state regardless of their initial states, and the time to reach equilibrium is called relaxation time, τ . Given a material is probed with the angular frequency, ω , then if $\omega\tau \gg 1$ it behaves like a glassy material, and if $\omega\tau \ll 1$ it behaves like a rubbery material, and when $\omega\tau \approx 1$, then the material is in the transition region [48], [49].

Based on this frequency dependent behavior, a dynamic glass transition temperature can also be defined over $\tau(T_g) = 1/\omega$ [48]. The same polymer can behave rubbery at low (near static) frequencies but glassy at higher frequencies, such as the frequency of measurement, f , which is on the order of 100 MHz for the sensors used in this work. For one of the polymers used for comparison in this research, poly(isobutylene) (PIB), this is reported to be the case [48], [50]. At this frequency, it is desirable that the polymer is glassy in order to minimize acoustic-wave attenuation due to inter-chain motion. Thus, the best coatings for acoustic-wave chemical sensors will be those which are rubbery in the low frequency range, resulting in good analyte sorption, but glassy at the operating frequency of the sensor device, resulting in low acoustic-wave attenuation and a good signal-to-noise ratio. If the polymer used as a SH-SAW sensor coating has a very high static glass transition temperature, this coating will be glassy during normal experimental temperature. This glassy coating will have low and slow analyte adsorption rates, and as a result, the sensor will have a longer response time and lower sensitivity. On the other hand, if the polymer coating is in the rubbery state at measurement frequency, i.e. has low glass transition temperature, then the coating will

have fast and high adsorption rate of analyte. As a result, the sensor will have high sensitivity but may also have high insertion loss, which will produce high baseline noise. Therefore, to be an ideal coating for acoustic-wave sensors, the polymer needs to be a compromise between these two extremes, and the static glass transition temperature needs to be slightly below ambient temperatures. In that case, there is a high probability that the polymer will behave glassy at the operating frequency of the acoustic wave.

For a polymer which has a high glass transition temperature, adding a plasticizer can lower the glass transition temperature. The plasticizer gives the polymer molecules a higher mobility, turning the polymer into a suitable film for the sensor in chemical sensing applications. Plasticizers and the theory of plasticization will be discussed in the next section.

3.3 Plasticizers

3.3.1 Introduction

A plasticizer is a chemical substance which, when added to a material (usually polymer), increases the fluidity, plasticity, flexibility or resiliency of the material [51]. Plasticizers have many different uses in various applications. There are more than 300 plasticizers that exist and 50 to 100 of them have commercial applications. In general, a plasticizer works by increasing the free space between the polymer chains, as a result lowering the glass transition temperature of the polymer and making it softer. Various theories have been published to explain the plasticizing mechanism [52].

3.3.2 Properties of Plasticizers

Plasticizers have the ability to change the thermal and mechanical properties of a polymer. A plasticizer lowers the rigidity of a polymer at room temperature so that the polymer can be easily deformed without large forces. It also increases the elongation necessary to break the polymer at room temperature and extends the range of high polymer toughness to lower temperatures. This can be achieved when the polymer is blended with a lower molecular weight compound (a plasticizer) that reduces the crystallizability and increases the chain flexibility [53]. A plasticizer's properties are defined in terms of the polymer-plasticizer system. As an example, a property might be defined for a compound that gives intermediate flexibility to the coating, i.e. not too rubbery and not too glassy. Another example might be a plasticizer that, if added to elastomeric materials, has the characteristic to reduce the stiffness of the polymer. It is ultimately not possible to exactly characterize the behavior of a plasticizer in terms of fundamental properties because a plasticizer's behavior strongly depends on the polymer it is added to, and the properties of the polymer slightly depend on its previous history. As an example, two samples of film prepared from the same batch of polymer-plasticizer might not have exactly the same behavior because the orientation of the polymer chains, the effect of the plasticizer, or a combination of those might be different. Although it is very difficult to get exactly the same behavior from the polymer-plasticizer blend, by always preparing the polymer-plasticizer solution in exactly the same way, it is possible to get nearly reproducible properties for the resulting coatings.

3.3.3 Types of Plasticizers

Plasticizers can be divided into two groups: internal plasticizers and external plasticizers. *Internal plasticizer* is a monomer that is copolymerized into the polymer structure, making it less ordered and more flexible. For this reason, the polymer becomes softer, and will have a lower modulus and glass transition temperature (T_g). Another internal plasticization may consist of a side chain that can be either a substituent or grafted branch [53]. For example, BPA-HMTS (bisphenol A-hexamethyltrisiloxane): in this internal plasticization, HMTS acts as porous backbone that increases the free volume and flexibility [54]. *External plasticizers* are chemical compounds which have low vapor pressure and can interact with the polymer to reduce its glass transition temperature (T_g) without involving chemical reactions, by means of their solvent or swelling potential [53]. External plasticizers are more important because their combination with polymers gives more satisfactory properties and flexibility for formulation. Additionally, external plasticizers are used more for commercial applications and in this project, only external plasticizer will be used. There is another classification of plasticizers which divides the plasticizers into primary and secondary plasticizers. Primary plasticizers are chemical plasticizers which, when added to the polymer, change the properties of elongation and softness of the polymer; secondary plasticizers are referred to as plasticizing oil. The secondary plasticizers are not used alone and usually used in combination with primary plasticizers resulting in an enhancement of the plasticizing performance of the primary plasticizer.

3.3.4 Plasticizer Theories

There are several plasticizer theories that can explain the plasticization mechanism, but all of them agree that the addition of a plasticizer to a polymer material results in increased flexibility or mobility of rigid polymer molecules and makes them softer. The main four plasticizer theories are lubricity theory, gel theory, free volume theory and mechanistic theory. Those theories are explained in the following sections.

3.3.4.1 Lubricity Theory:

According to lubricity theory, “Plasticizer works as a lubricant to ease the intermolecular friction between polymer molecules liable for rigidity of the polymer” [55]. This theory states that the rigidity of a polymer depends on the intermolecular friction force between the polymer molecules, and the addition of plasticizer decreases this friction force, reducing the rigidity. It increases the mobility of the polymer chains and decreases the resistance of a polymer to deformation. Addition of plasticizer reduces cohesion forces between polymer molecules and intensifies the movement and rotation of the molecules which increases the overall flexibility of the polymer [52]. The lubricity theory presumes that the bonding among polymer-plasticizer molecules is very weak and the bonding among the macromolecules of the polymer beyond the surface irregularities is almost zero [56]. Briefly, a polymer without plasticizer is rigid due to the friction between the chains of the polymer and when plasticizer is added, the smaller molecules of the plasticizer are able to slide in between the chains of the polymer and act as a lubricant between the chains, allowing them to ‘slip’.

3.3.4.2 Gel Theory:

Gel Theory states that polymers are formed by an internal three dimensional honeycomb-like structure and this three dimensional structure is the main reason for their rigidity. The plasticizer molecules reduce this rigidity by breaking the polymer-polymer interaction between the chains of the polymer. According to this theory, polymer-polymer interactions occur at centers of attachment and plasticizer molecules break the attachment and mask these centers from each other, preventing re-formation of a polymer's honeycomb-like structure. By adding the plasticizer to the polymer, the number of centers of attachment is reduced, permitting an increase in the regions of aggregation of polymer molecules. This will enable the polymer chains to move, thus increasing the overall flexibility of the polymer. However, this theory is not sufficient to describe the interaction between polymer chains and the resulting increased flexibility, therefore it needs to be combined with lubricity theory.

3.3.4.3 Free Volume Theory:

Free volume is defined as the fraction of volume not occupied by the polymer. According to free volume theory, a plasticizer lowers the glass transition temperature of a polymer, and as a result increases the movement of polymer chains and flexibility of the polymer [55]. Actually, the free volume of a polymer is an internal empty space that is available for the movement of the polymer chains and this free volume is seen at its maximum at the glass transition temperature. Usually, plasticizer molecules are smaller than the polymer molecules and have lower glass transition temperatures [52]. By adding a plasticizer to polymer, the glass transition temperature of the polymer decreases,

resulting in increased flexibility at room temperature and a polymer that is softer and rubbery.

The volume of a polymer is decreasing linearly with temperature below the glass transition temperature. For all polymers, the volume changes between absolute zero and the transition temperature is a constant $0.0646 \text{ cm}^3/\text{g}$ [52]. The free volume of a polymer can be calculated by taking the difference between the volume of polymer at absolute zero temperature and the volume at a specific temperature. This can be expressed by the following equation,

$$v_f = v_t - v_0 \quad (3.3)$$

where v_f is the free volume of the polymer, v_t is the volume at a specific temperature and v_0 is volume of the polymer at absolute zero temperature. The inclusion of plasticizer decreases the glass transition temperature, which increases the free volume, resulting in increased flexibility and ability to absorb analyte species.

3.3.4.4 Mechanistic Theory:

The mechanistic theory states that plasticizer molecules are not bound permanently to the polymer molecules in a specific form. They could be inserted between the chains of the polymer or anywhere in the polymer structure, preventing the polymer molecules or chains from being bound tightly among themselves. As a consequence, flexibility improves, increasing softness and decreasing the glass transition temperature of the polymer-plasticizer mixture [55].

3.4 Effect of Plasticization on Sensing Parameters

All the plasticizer theories discussed in the above section can be used to explain the condition of a plasticized polymer. For SH-SAW chemical sensors or any other chemical sensor, it is important to know the effect of plasticization on the sensing parameters. All the theories showed almost the same type of behavior of plasticized polymer, in that flexibility is increased, or in other words, the polymer becomes softer. This flexibility can be increased by increasing the mobility of the chains of a polymer, by increasing free volume, or by decreasing the glass transition temperature. This effect of the addition of plasticizer is actually helpful in increasing the sensitivity of the chemical sensor where a polymer film is needed. Adding plasticizer to a polymer film has a positive effect on sensing parameters of a sensor. As an example, if a polymer is hard and rigid, it will be difficult for that polymer to absorb analyte. In this case, adding plasticizer to that polymer will help the coating absorb analyte because the plasticized polymer has increased free volume and increased chain mobility. This will allow for absorption of more analyte and a faster rate of analyte absorption. The extra analyte absorption will create added mass loading, which will increase the sensitivity of the sensor by increasing the frequency shift. In addition, the faster absorption rate might shorten the time response of the device.

The plasticized polymer has increased flexibility, which increases the sensitivity (or frequency shift) but at the same time will result in higher device insertion loss due to the increase in the loss modulus. If the coating of the SH-SAW sensor platform is rigid and hard, the device insertion loss is low because the coating oscillates synchronously with the substrate of the device. But with the addition of plasticizer to increase the

analyte absorption, the coating becomes more rubbery, leading to a phase lag across the thickness of the oscillating coating. The resulting periodic deformation of the coating causes an increase in loss. Therefore, a tradeoff between glassy and rubbery coating is very important so that the sensitivity of the device is increased but at the same time the insertion loss does not increase beyond a certain limit.

3.5 Solubility Parameters

Since the coatings of SH-SAW devices are prepared as solutions, solvent and solubility parameters of all coating materials have to be carefully considered. To obtain a repeatable and stable coating for the device, solubility parameters of the polymer, plasticizer, and solvent need to be known. To determine the solubility of materials, specifically for nonpolar materials such as many polymers, the Hildebrand solubility parameter (δ) is a good indicator. The Hansen solubility parameter enables even more reliable prediction of the miscibility of the materials in a solution. These methods of predicting solubility are based on a general rule of thumb, “like dissolves like” where “like” is defined by the molecular characteristics of two materials.

The first method indicates that a polymer will dissolve well in a solvent if their Hildebrand solubility parameters (δ) are very similar [57]. The Hildebrand solubility parameter is calculated from the cohesive energy density (c), which is the amount of energy needed to completely separate a unit volume of molecules from its neighbors like in an ideal gas. This parameter is the simplest indication of solubility and is calculated from the equation below,

$$\delta = \sqrt{c} = \left(\frac{\nabla H - RT}{V_m} \right)^{1/2} \quad (3.4)$$

where, ΔH is heat of vaporization, R is the universal gas constant, T is the temperature and V_m is molar volume [57].

A more accurate and detailed method to calculate the solubility parameter is to use the Hansen solubility parameters (HSP). HSP is named after Charles M. Hansen who developed this theory in his PhD dissertation in 1967. HSP starts from the idea of Hildebrand solubility and divides it into three components, which are usually measured in $(\text{MPa})^{0.5}$ [58]. The components are derived from energy from dispersion forces (δ_d), dipole forces (δ_p) and hydrogen bonds (δ_h) between molecules. Hansen solubility parameters relate to the sum of these three components, which can be considered as coordinates of a space called Hansen space.

$$\delta_t^2 = \delta_d^2 + \delta_p^2 + \delta_h^2 \quad (3.5)$$

Each individual component of this equation is compared between materials, and those that have comparable solubility parameters usually show good miscibility.

For two materials (e.g., solvent and polymer), the equation of a sphere was introduced by Skaarup [57] using partial solubility parameter components to calculate the ‘distance’, R_a between the Hansen parameters of the two materials in Hansen space.

$$(R_a)^2 = 4(\delta_{d2} - \delta_{d1})^2 + (\delta_{p2} - \delta_{p1})^2 + (\delta_{h2} - \delta_{h1})^2 \quad (3.6)$$

After calculating the distance, R_a , this value is compared with the experimentally determined radius of the solubility sphere, R_0 , which is also called the interaction radius. To be completely soluble or in other words for high affinity, the interaction radius R_0 must be greater than the calculated radius, R_a . The ratio between calculated radius R_a and interaction radius R_0 is defined as the relative energy difference (RED) of the system, as shown in the equation below.

$$RED = \frac{R_a}{R_0} \quad (3.7)$$

If RED is less than one ($RED < 1$), the molecules are alike and will be completely miscible or dissolve completely; if $RED > 1$, the system will not be miscible, and the case where RED is equal to one or close to one, which is the boundary condition for solubility, indicates a decrease in affinity between the materials and that system will partially dissolve [59].

3.6 Selection Criteria for Polymer and Plasticizer

The film, or coating, of the sensor is important for the partially selective detection of a specific analyte or a class of analyte, and choosing the coating materials is a critical issue for the chemical sensor. Interactions between the coating and analyte need to be well understood, and studies of chemical and physical properties of coating materials are necessary for this research. In order to achieve maximum sensitivity and optimum (partial) selectivity of a chemical sensor, covalent bonds between coating materials and analytes would be necessary. However, those bonds cause the analyte to become permanently attached to the sensor coating, resulting in irreversible sensor responses. For

a reversible response, the interactions between coating materials and analytes are limited to dispersion, dipolar and hydrogen-bonding interactions [60], [61]. For the purpose of a coating of an SH-SAW sensor, polymer and plasticizer materials should have certain specific properties. Chemical structure and other physical and chemical properties of the polymer are important for partially selective detection of a specific analyte. Before choosing a plasticizer, three criteria must be considered: compatibility of the plasticizer with the polymer, efficiency of the plasticizer and permanence of the plasticizer in the polymer or leaching of the plasticizer from the plasticized polymer. Moreover, anti-plasticization also needs to be considered.

3.7 Chemical Structure & other properties of Polymer

Materials that will make the sensor response fast, highly sensitive and selective are good candidates for the coating of the device. Before selecting a polymer as a coating, low material density, low crystallinity and rubbery properties of that polymer need to be considered, because these properties will dictate the polymer's high permeability and fast response [60]. The polymer needs to have a T_g below operating or ambient temperature to be a good candidate material. This is because the polymer needs to be in the rubbery regime for the sensor response to show good reversibility [62]. In addition, the polymer should show good adhesion and wetting properties with the surface of the device, otherwise acoustic wave coupling is poor, resulting in a loss in acoustic wave energy, an increase in the response time, and a lack of reproducibility of the sensor response [62].

The chemical structure of the polymer has a high impact on the sensitivity and selectivity of the sensor response for a specific analyte. Similarities in the chemical structures of polymer and analyte help to achieve good analyte absorption into the

coating. As an example, for the detection of BTEX compounds, a polymer which has a benzene ring in its structure is preferred as coating material because the BTEX compounds have a benzene ring in their chemical structure, and an attractive interaction between the delocalized π -electron systems of these benzene rings is expected (“ π stacking”) [63].

3.8 Compatibility and Efficiency of Plasticizer

When choosing the plasticizer, it is essential to check its compatibility with the selected polymer. Compatibility of a plasticizer relates to the structural configuration, polarity and molecular weight (Mw) of that plasticizer. Indications of good compatibility between a specific polymer and plasticizer are similar chemical structures and Hansen solubility parameters [56]. A suitable plasticizer needs to be non-toxic and should have low leaching rate in water as well as low vapor pressure. If the plasticizer is not compatible with the intended polymer, syneresis (leaching of plasticizer) occurs from their blend coating. A good way to evaluate the compatibility is to calculate the relative energy difference (RED) from the Hansen solubility parameters of polymer and plasticizer.

Efficiency of plasticizer is related to the amount of plasticizer required to achieve the desired modification of the properties of a given blend. For example, plasticizer efficiency can be evaluated by relating the decrease in glass transition temperature of the polymer to the volume fraction of the added plasticizer, to the weight percentage of the plasticizer, or to a given molar ratio [53]. However, there is no absolute value or established system to measure or express the efficiency of plasticizers because the modification is relative and also depends on the properties of the polymer. Molecular

weight (Mw), size or diffusion rate into the polymer matrix are also related to the efficiency of a plasticizer. The higher the diffusion rate of plasticizer molecules is into the polymer matrix, the higher the efficiency of the molecules is as plasticizer. Usually, smaller plasticizer molecules have higher diffusion rates, but have higher volatility, which leads to high leaching rates [64]. In general, a good plasticizer should have higher efficiency, giving high plasticization at low concentration, and little or no leaching from the blend.

3.9 Stability of Plasticizer in Water (Permanence/Leaching)

Plasticizer permanence means the tendency of the plasticizer to remain in the plasticized material and not leach out from the blend coating. One of the goals of this research is to find a coating that is suitable for long-term, repeatable measurements, thus requiring permanence of the plasticizer in the coating. Permanence of a plasticizer depends on the size of the plasticizer molecule and its diffusion rate in the polymer [53]. If the size of the plasticizer molecule is large, then its vapor pressure or volatility will be low. For application of plasticizers with low polarity in water, this means the leaching rate will also be very low, i.e. permanence will be high. The vapor pressure of the plasticizer also depends on the polarity and hydrogen bonding of the molecule. Another factor that determines the permanence of the plasticizer molecule is diffusion rate of the plasticizer in a polymer material. Unfortunately, while a high diffusion rate of the plasticizer gives greater efficiency, it leads to lower permanence of the plasticizer.

Studies have been done previously on leaching rates of plasticizers from plasticized polymers. Many commercially available plasticizers have high leaching rates.

Plasticizer such as diisooctyl phthalate (DOP or DEHP) has a leaching rate of 0.8% per week into the surrounding liquid environment [65]. Plasticizer leaching rate into the surrounding liquid is greatly dependent on the chemical structure of the plasticizer and polarities of the liquid and plasticizer. The higher the hydrophobicity of the plasticizer molecule is, the lower the leaching rate of the plasticizer is in aqueous phase. It was found that DINCH has a low or undetectable leaching rate because of its high hydrophobicity [65]. However, DIOA should also have a low or undetectable leaching rate because it has long carbon chains and high molecular weight. When selecting the plasticizer, it may be necessary to accept a compromise among some of its properties because of their conflicting nature. Molecular size, chemical structure, diffusion rate and compatibility all need to be considered together.

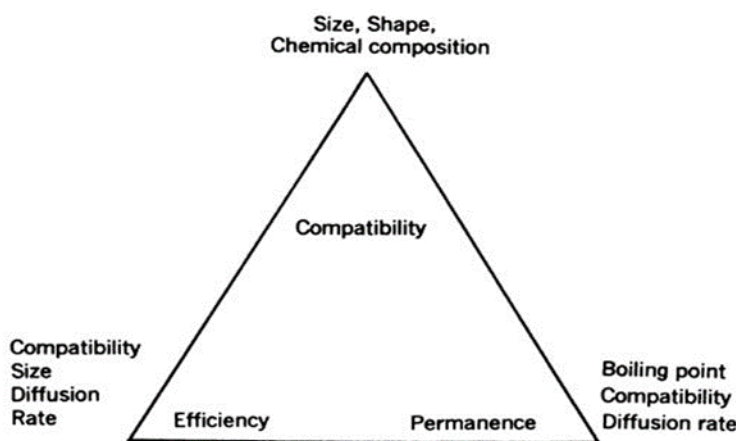


Figure 3.4: A relationship among compatibility, efficiency, and permanence of plasticizer [53].

It is important to analyze the permanence, efficiency and compatibility of the plasticizer with the intended polymer before choosing the plasticizer for the polymer-plasticizer blend.

3.10 Anti-plasticization

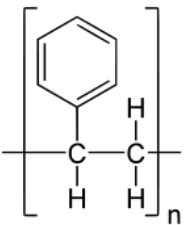
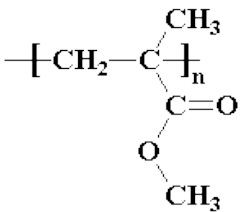
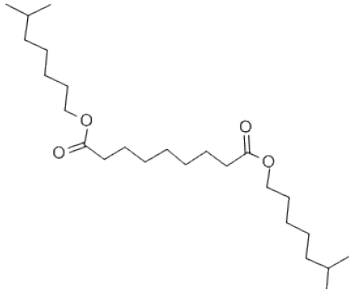
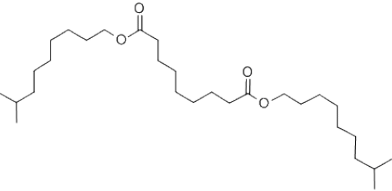
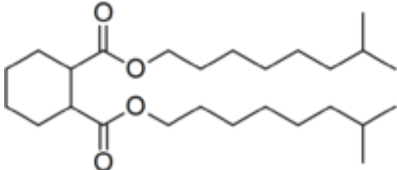
Sometimes, when a small amount of plasticizer is added to a polymer, the polymer becomes more ordered and compact and as a result the blend coating tends to become more crystalline. This affects the plasticization process in the opposite way. Because of the formation of crystals, the movement of the chains of the polymer decreases as does the flexibility of the plasticized material. Also, the polymer becomes a more rigid material with increased storage modulus. This effect is known as anti-plasticization. Anti-plasticization can occur not only at low plasticizer concentrations but also at high concentrations. As an example, when plasticizer is added to a specific polymer like poly vinyl chloride (PVC), crystallinity increases in the crystalline region but in the amorphous region it becomes softer. Usually, by adding a certain amount of plasticizer, the plasticized polymer becomes more flexible, has better elongation and lower tensile strength and brittleness [56].

3.11 Polymer and Plasticizer Used in this Work

Polymer and plasticizer materials are always used as a blend for a new coating in this work. The polymer-plasticizer blend is used as the SH-SAW sensor coating and serves as a waveguiding layer as well as a chemically sensitive layer for BTEX detection. From the results of [54], [66], [67], it is found that, in comparison to commercially available polymers, a plasticized polymer film has increased sensitivity to BTEX compounds in liquid environments for QCM and SH-SAW sensors. The specific polymers used in this work are polystyrene (PS) and poly (methylmethacrylate) (PMMA) and the plasticizers used are diisooctyl azelate (DIOA), 1,2-cyclohexane dicarboxylic

acid diisononyl ester (DINCH), and diisodecyl azelate (DIDA). PS and PMMA are both thermoplastic polymer materials. Chemical properties such as chemical structure, density at 25°C, molecular weight and glass transition temperature of the polymer and plasticizer materials used for this work are given in the Table 2.

Table 2: Chemical properties of the materials used in this work [according to manufacturer's specifications (Sigma Aldrich, Scientific Polymer Products)].

	Chemical Structure	Density at 25°C (g/cm ³)	T _g (°C)	Repeat unit	Molecular weight (Mw) investigated
PS		1.06	100	C ₈ H ₈	35000 & 280000
PMMA		1.19	105	C ₅ H ₈ O ₂	35000
DIOA		0.920		C ₂₅ H ₄₈ O ₄	413
DIDA		0.912		C ₂₉ H ₅₆ O ₄	469
DINCH		0.944 – 0.954		C ₂₆ H ₄₈ O ₄	425

By looking at the chemical structure of polystyrene, it can be assumed that this material is a potential candidate for BTEX detection because of the presence of a benzene ring (phenyl group). As all BTEX compounds have benzene rings, the presence of the benzene ring in PS suggests high affinity to BTEX compounds due to π stacking interaction [63]. Some BTEX compounds i.e., benzene, toluene, ethylbenzene and xylene, are sometimes used as a solvent for PS due to their high affinity to PS [68]. However, the glass transition temperature is not suitable for a sorbent coating material for SH-SAW sensors. As plasticizer can reduce the glass transition temperature of polymer, PS can be an ideal coating material for SH-SAW platforms to detect BTEX if it is plasticized. A previous study [54] showed that plasticized polystyrene has the highest sensitivity for benzene detection. PMMA can also be a good candidate material for the coating of a SH-SAW sensor if it is plasticized because the glass transition temperature of PMMA is similar to that of PS; PMMA is also a thermoplastic polymer.

Plasticizers are chosen based on their compatibility and leaching rate. DINCH is chosen because of its undetectable leaching rate [65]. DIOA is chosen because of its efficiency, compatibility, and because it is expected to have a low leaching rate due to its large molecular size.

The solubility parameter must be calculated for the materials before using them as coating materials. The solubility (miscibility) of all materials with one another was calculated using Hansen solubility parameters and equation (3.7). Hansen solubility parameters for all materials are listed in Table 2 and solubilities of each combination of polymer, plasticizer, solvent and analyte are listed in Table 3.

Table 3: Hansen solubility parameters of the materials used in this work [57], [69], [70], [71].

Materials	δ_d	δ_p	δ_h
PS	18.6	6.0	4.5
PMMA	18.6	10.5	7.5
DIOA**	16.7	1.4	4.8
DIDA**	16.5	1.3	4.5
DINCH	15.4	6.18	5.25
THF	16.8	5.7	8
TCE	18	3.1	5.3
Chloroform	17.8	3.1	5.7
Benzene	18.4	0	2.0
Toluene	18.0	1.4	2.0
Ethylbenzene	17.8	0.6	1.4
o-Xylene	17.8	1.0	3.1
m-Xylene	18.4	2.6	2.3
p-Xylene	17.6	1.0	3.1

** HSP values are collected from Reference [71]

Table 4: Solubility calculation between two materials.

First	Second	$\Delta\delta_d$	$\Delta\delta_p$	$\Delta\delta_h$	R_a	RED
THF	DIOA	0.6	1	-0.4	1.612	0.19
THF	DIDA	0.3	4.4	3.5	5.654	0.66
THF	DINCH	1.4	-0.48	2.75	3.954	0.46
THF	Polystyrene	1.8	-1.2	-5.1	6.357	0.74
THF	PMMA	1.8	4.8	-0.5	6.021	0.70
TCE	DINCH	1.4	-0.48	2.75	3.954	0.46
TCE	PMMA	-0.6	-7.4	-2.2	7.813	0.91
Chloroform	DIOA	1.6	-1.6	-2.7	4.482	0.52
Chloroform	DINCH	2.4	-3.08	0.45	5.721	0.67
Chloroform	PMMA	-0.8	-7.4	-1.8	7.782	0.90
Benzene	Polystyrene	-0.2	-4.5	-0.9	4.607	0.54
Toluene	Polystyrene	-0.6	-3.1	-0.9	3.444	0.40
Ethylbenzene	Polystyrene	-0.8	-3.9	-1.5	4.474	0.52
p-Xylene	Polystyrene	-1	-3.5	0.2	4.036	0.47
o-Xylene	Polystyrene	-0.8	-3.5	0.2	3.854	0.45
m-Xylene	Polystyrene	-0.2	-1.9	-0.6	2.032	0.24
Benzene	PMMA	-0.2	-10.5	-5.5	11.860	1.38
Toluene	PMMA	-0.6	-9.1	-5.5	10.700	1.24
Ethylbenzene	PMMA	-0.8	-9.9	-6.1	11.738	1.36

p-Xylene	PMMA	-1	-9.5	-4.4	10.659	1.24
o-Xylene	PMMA	-0.8	-9.5	-4.4	10.591	1.23
m-Xylene	PMMA	-0.2	-7.9	-5.2	9.466	1.10
Benzene	DINCH	3	-6.18	-3.25	9.206	1.07
Toluene	DINCH	2.6	-4.78	-3.25	7.775	0.90
Ethylbenzene	DINCH	2.4	-5.58	-3.85	8.307	0.97
p-Xylene	DINCH	2.2	-5.18	-2.15	7.128	0.83
m-Xylene	DINCH	2.4	-5.18	-2.15	7.382	0.86
o-Xylene	DINCH	3	-3.58	-2.95	7.584	0.88
Benzene	DIOA	-2.2	4.7	6.4	9.078	1.06
Toluene	DIOA	-1.8	3.3	6.4	8.050	0.94
Ethylbenzene	DIOA	-1.6	4.1	7	8.721	1.01
p-Xylene	DIOA	-1.4	3.7	5.3	7.044	0.82
m-Xylene	DIOA	-1.6	3.7	1.4	5.088	0.59
o-Xylene	DIOA	-2.2	3.7	-3.1	6.531	0.76
Benzene	DIDA	-1.9	1.3	2.5	4.731	0.55
Toluene	DIDA	-1.5	-0.1	2.5	3.906	0.45
Ethylbenzene	DIDA	-1.3	0.7	3.1	4.106	0.48
p-Xylene	DIDA	-1.1	0.1	1.4	2.625	0.31
m-Xylene	DIDA	-1.3	0.3	1.4	2.968	0.35
o-Xylene	DIDA	-1.9	-1.3	2.2	4.579	0.53
DINCH	PS	-3.2	1.68	2.35	7.022	0.82
DIOA	PS	-2.4	0.2	5.5	7.303	0.85
DINCH	PMMA	3.2	4.32	2.25	8.043	0.94
DIOA	PMMA	2.4	5.8	-0.9	7.582	0.88
DIDA	PS	-2.1	-3.2	1.6	5.517	0.65

The above table lists the solubility analysis for all materials used in this work. The values of RED less than one show clear solubility between the two materials. The values that are equal to 1 or close to 1 are borderline cases. The values that are clearly above 1 show little or no solubility between the materials.

4. EXPERIMENTAL PROCEDURE

4.1 Introduction

This chapter provides a detailed description of the experimental procedure for this research, consisting of a description of the equipment, materials, experimental procedure and processing of the collected data. The experimental procedure starts with preparing the desired coating solution, where a specific concentration of polymer-plasticizer blend is dissolved in an appropriate solvent. Next, the surface of a cleaned SH-SAW device is coated with this solution by means of a spin coater. Thickness of the coating is measured by a profilometer and confirmed by an ellipsometer. After that, the coated device is put into a flow cell specifically designed for this application and exposed to the analyte sample. A vector network analyzer is used to continuously monitor the frequency and attenuation during the exposure of analyte sample and reference sample and collects the data via the Agilent VEE (Virtual Engineering Environment) program. Details are given in the following sections.

4.2 Apparatus and Materials

4.2.1 Sensing Device

The heart of this research is the SH-SAW sensor device. This device was specially designed for chemical and biochemical sensing by the Microsensors Research Laboratory of Marquette University. The substrate material for this device is lithium tantalate (LiTaO_3) and the IDT pattern is made of gold on a thin adhesion layer of titanium or chromium deposited on the LiTaO_3 substrate surface [25], [72]. The IDT is patterned in a

two-ten electrode finger design to minimize the phase distortion in the passband [30]. The device has a dual delay line configuration and both delay lines are metalized and grounded to prevent any electrical interaction during the measurement in an aqueous environment. The typical operating frequency of this device for this particular measurement is around 103 MHz. The operating frequency depends on the linearity of the phase and must lie within the 3-dB passband.

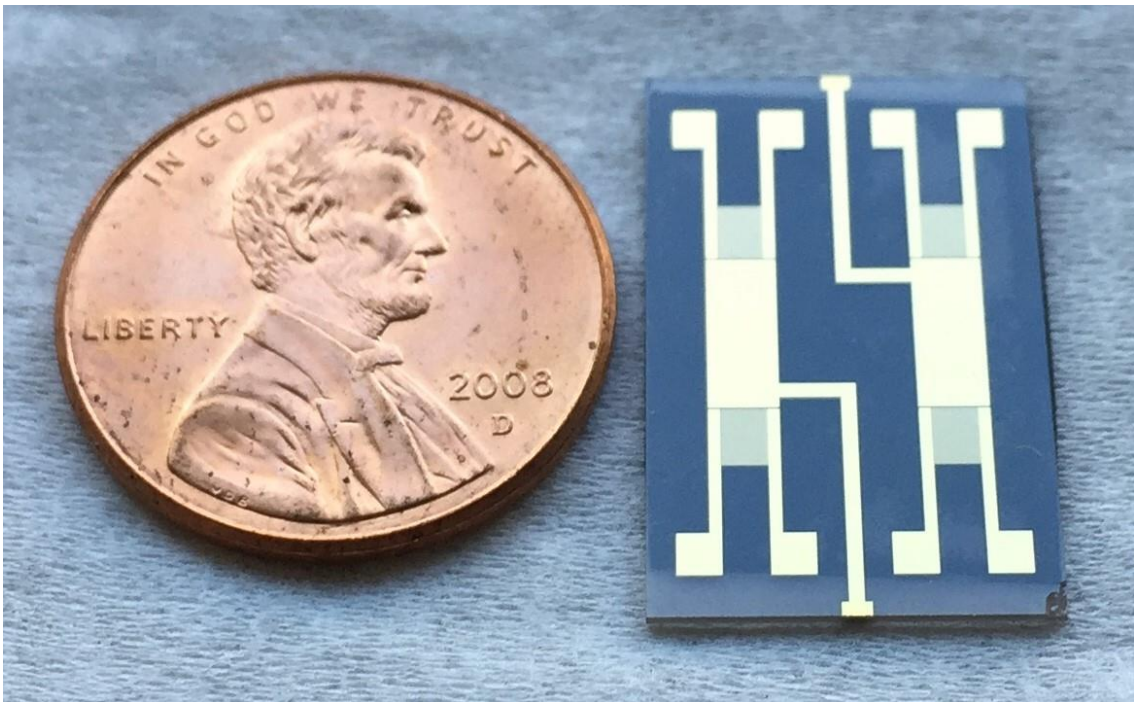


Figure 4.1: A SH-SAW device used for this work with a coin to compare the size of the device.

4.2.2 Chemical Materials

Polymer-plasticizer blends are used to coat the IDTs and delay lines of the device. Polystyrene and PMMA were used as polymers and were purchased from Sigma Aldrich. Both polymers have high glass transition temperatures (around 100°C and 105°C, respectively), requiring addition of a plasticizer to lower the glass transition temperature for effective analyte absorption. DIOA, DIDA and DINCH were used as plasticizers. All these plasticizers are commercially available. DIOA and DIDA were purchased from Scientific Polymer Products and DINCH was kindly provided by BASF Corporation. DIOA-PS and DIDA-PS blends were dissolved in tetrahydrofuran (THF), DINCH-PMMA and DIOA-PMMA were dissolved in chloroform. Chloroform (purity $\geq 99.8\%$), THF (purity $\geq 99.9\%$), and other cleaning solvents for the SH-SAW device were purchased from Sigma Aldrich. BTEX compounds, benzene (purity $\geq 98.5\%$), toluene (purity $\geq 99.3\%$), ethylbenzene (purity $\geq 99\%$), and xylene (purity $\geq 98.5\%$) were purchased from Sigma Aldrich. Analyte solution samples were prepared in degassed deionized water in the laboratory.

4.2.3 Spin Coater

To deposit the coating solution on the surface of the SH-SAW device, a spin coating system is used (Specialty Coating System (SCS) Model P6024). The coating process involves depositing a fixed volume of the viscous solution of polymer-plasticizer blend on top of the device and spinning the device at a selected high speed to ensure a uniform coating. The device is placed on the center of the chuck of the spin coater, which applies a vacuum to the back side of the device to hold it in place. Then the spin coater

operates following a preset routine or “recipe”. The user can set the “recipe” according to the requirements of the experiment by selecting the ramp up time, spin speed, spin time, and ramp down time to achieve a desired coating thickness [73]. Thickness of the coating not only depend on the settings of the spin coater but also on the properties of the coating solution such as concentration, viscosity and solvent evaporation rate. For this research, 0.5 μm to 1.4 μm -thick coatings were produced by spin coating and successfully tested for reproducibility.

4.2.4 Thickness Characterization

It is important to characterize the thickness of the coating to reproduce highly sensitive coatings for SH-SAW sensors. In the laboratory, two different thickness measurement methods are available for film characterization. One is a contact method (profilometry) and the other is a non-contact method (ellipsometry). Usually, the profilometer is used first to measure the thickness of the film, and then the ellipsometer is used to confirm the thickness.

4.2.4.1 Profilometer:

The profilometer used for this work is a KLA-Tencor Alpha-Step IQ instrument. A glass slide is first used for the thickness measurement instead of the actual sensor device. The glass slide goes through the same deposition process at the same time to replicate the coating on the actual device. For the soft and rubbery polymer coatings, a very low stylus force is often required to prevent penetration of the coating by the stylus, potentially resulting not only in scratching of the surface of the coating but also in inaccurate thickness measurements.

4.2.4.2 Ellipsometer:

The ellipsometer used for this work is a Gaertner Scientific Corporation L2WLSE544 instrument. The ellipsometer is a non-contact method which uses a laser beam to measure the thickness of a film. To avoid any measurement ambiguity, the ellipsometer uses two laser wavelengths (543.5 nm and 632.8 nm). It is critical for the thickness measurement that the probed surface be very smooth. A rough surface can give an inaccurate measurement due to the reflection from the rough surface. Therefore, in this work, a profilometer is used first to measure the coating thickness on a glass slide, and the ellipsometer is only used to confirm the thickness of the coating.

4.2.5 Flow Cell

A flow cell designed in-house is used to house the sensor device for the measurements [74]. The flow cell consists of three separate pieces shown in Fig. 4.2. The bottom piece and middle piece are made of brass. The bottom piece has a recessed area to hold the SH-SAW device. The middle piece contains spring-loaded contact pins that provide the connection for input and output transducers to the network analyzer through coaxial cables and also provide the ground connection for each delay line. These two pieces hold the device in its intended location and shield it from any electromagnetic interference. The top piece is a Plexiglas (PMMA) cover that has an inlet and an outlet to allow the liquid samples to flow over the device. A rubber gasket is used ensure a tight seal as well as to isolate the aqueous environment from the electrical contacts of the device. The cover is made of Plexiglas to allow visual inspection for bubbles while ensuring that it does not react with the solution. Of the sensor device, only the coated

IDTs and delay lines are exposed to the liquid environment. The interior volume of the flow cell is approximately 0.14 mL. The flow cell for this experiment is designed in such a way that only the IDTs and delay lines are exposed to the liquid environment.

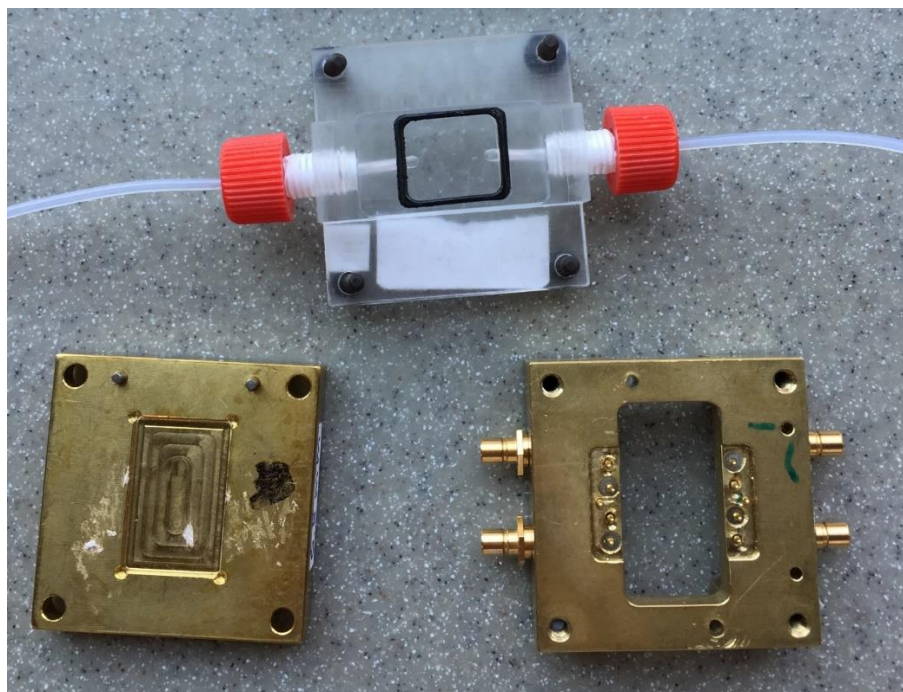


Figure 4.2: Parts of the flow cell used for this work. Top, Plexiglas cover with gasket and inlet/outlet tubes; lower left, bottom part of the flow cell to house the device; lower right, brass middle part with contact pins including grounding pins.

4.2.6 Peristaltic Pump

A peristaltic pump (Ismatec RS232; IDEX Corporation) is used to pump the analyte and reference solutions through the flow cell and over the sensor. As the analytes are volatile, analyte solutions are kept in a closed container with a PTFE-lined lid. Small PTFE tubes are inserted into the containers—analyte sample and reference liquid (degassed DI water)—and connected to the flow cell via a three-way valve. The pump pulls the liquid from the container through the flow cell to the waste container. With the

help of the three-way valve, which has three independent inlet/outlet switches, the pump is able to maintain a constant liquid flow rate while changing the solutions. The pump is selected to pump the liquid with minimum pulsation at a constant rate. For this research, the velocity of the pump was kept at $7\mu\text{l/s}$. The pump allows the user to select the flow rate, but for this experiment the flow rate was kept fixed to ensure a reproducible response time for a given coating/analyte combination.

4.2.7 Vector Network Analyzer

A vector network analyzer (VNA; Agilent E5061B) is used to send a signal through the SH-SAW device and measure the output signal of the device for a fixed frequency range in real-time. The VNA is connected to a switch control unit (Agilent 34980A) that alternates between the two delay lines of the SH-SAW device. An Agilent VEE (Virtual Engineering Environment) program is used to collect the data from the VNA and save them on an attached computer. Phase, frequency and amplitude data of the device are collected continuously throughout the measurement for each delay line.

4.2.8 GC-PID

For this work, a gas chromatography - photoionization detector (GC-PID) for detection of volatile organic compounds (VOC) in water [75] was used for independent measurement of BTEX concentrations. The instrument, a portable hand held micro GC system, is called FROG -4000 (Defiant Technologies). The GC-PID contains a micro preconcentrator, micro gas chromatographic (GC) column and a photoionization detector to determine the various organic compounds in water [75]. The micro preconcentrator is coated with a specially designed nanoporous material and the GC column has an

integrated heater for temperature ramp chromatography. The instrument contains a miniature PID (ionization potential: 10.6 eV). Although it is possible to measure concentrations from 0 ppb to 4000 ppb for BTEX compounds with the GC-PID, the linearity observed at low concentrations (below 500 ppb) was not as good as that at high concentrations (500 ppb to 4000 ppb).

4.2.9 Plasma System, PE-50

PE-50 is a plasma cleaning system that can be used for surface treatment by oxygen plasma. It was reported [76] that oxygen plasma treatment of a plasticized polymer film (PVC/phthalate) was shown to be effective in preventing or reducing plasticizer (phthalate) leaching from the plasticized polymer film. Therefore, in order to prevent leaching of plasticizer from plasticized polymer coatings of SH-SAW sensors, oxygen plasma treatment was applied in this work and showed promising results. The details of the oxygen plasma treatment on the coatings of SH-SAW sensors is discussed in the chapter on 'Results and Discussion'.

4.3 Experimental Set Up and Procedures

4.3.1 Experimental Set Up

A schematic view of the experimental set up used for this research is shown below.

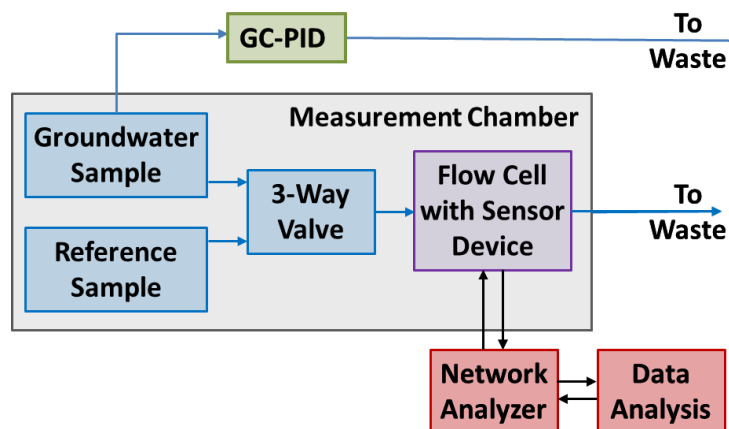


Figure 4.3: A Schematic of the experimental set-up used in this work.

Three closed containers are used for analyte solution, reference solution and waste. PTFE tubing from Kinesis is used to connect these containers to the flow cell. A peristaltic pump is pumping the analyte solution and reference solution through the flow cell to the waste container and the three-way valve is used to select the analyte solution or reference solution. The pump is set to a fixed flow rate of $7 \mu\text{l/s}$ for most of the experiment. To compare response times between different analytes or coatings, the flow rate needs to be constant for all measurements because response time depends on flow rate. The contact pads of the sensor device are connected through the contact pins of the flow cell to cable connectors, which are connected to the network analyzer through the coaxial cables. The network analyzer sends and receives the signal to measure the frequency and loss

response of the device. A switch control unit is used to switch the signal between the two delay lines of the device. The data is collected every 12 seconds via an Agilent VEE program on a computer attached to the network analyzer.

4.3.2 Device Preparation

There are various initial steps to be followed before using a new SH-SAW device for the measurements. These steps include filing the edges of the device, cleaning the device, preparing the coating solution and coating the device, applying black tape on the back side of the device and using silver paint on the contact pads. Important steps are described in details in the following.

4.3.2.1 Edge Filing:

Filing the edges is an important step for all new SH-SAW devices. It is performed in order to reduce the acoustic wave reflection from the edges of the substrate behind the transducers, resulting in reduced noise and improved signal to noise ratio (SNR) for the sensor response. A properly filed device will have very low passband ripple which helps to ensure experimental reproducibility. The filing steps include:

- i. Measure the insertion loss and save the frequency spectrum of the new unprepared SH-SAW device using network analyzer for later reference.
- ii. Bevel the width (short side) of the device substrate by using sandpaper (40 grit), at an angle of approximately 45° .
- iii. Again record the frequency spectrum and compare with the initial frequency spectrum to check if edge reflections have disappeared from the passband.

- iv. Furrow behind each of the IDTs using the sandpaper to further scatter any remaining reflected wave.
- v. After filing the device properly, it is ready for coating. Before putting the device in the flow cell, an insulating tape (black electrical tape) needs to be placed on the back side of the device. This black tape will absorb energy from incident bulk waves and reduce reflections from the back side.

4.3.2.2 Coating Solution Preparation:

The procedure to prepare the coating solutions is based on previous work done in the Microsensors Research Laboratory. The polymer-plasticizer ratio is calculated as weight percentage, as is the concentration of polymer-plasticizer blend in the solvent. Varying the plasticizer's percentage in the blend will affect the physical properties of the resulting coating, and varying the concentration of the blend in the solvent will affect the viscosity of the solution and the resulting coating thickness. The plasticizer percentage (weight/weight) is calculated using the equation below.

$$wt\% = \frac{\text{mass of plasticizer (g)}}{\text{total mass of plasticizer and polymer (g)}} \times 100 \quad (4.1)$$

The polymer-plasticizer blend in the solvent is calculated by the equation below.

$$wt\% = \frac{\text{mass of polymer and plasticizer (g)}}{\text{total mass of solution (g)}} \times 100 \quad (4.2)$$

The following steps are applied to prepare the coating solution.

- i. Take a clean vial and put a magnetic stir bar inside it. Place the vial with the stir bar on a microbalance.

- ii. Take anticipated amount of polymer and pour in the vial.
- iii. Calculate the weight of plasticizer needed to obtain the intended w/w percentage.
- iv. Add the calculated amount of plasticizer.
- v. Calculate the amount of solvent to obtain the intended w/w percentage of polymer-plasticizer blend in the solvent.
- vi. Add the calculated amount of solvent.
- vii. Quickly close the vial and seal with Teflon tape to avert solvent evaporation.
- viii. Stir the solution overnight at 600 to 700 rpm with the help of a magnetic stir plate.
- ix. The next day sonicate the solution for at least 4 hours.
- x. After sonication wait at least 2 hours so that the temperature of the solution returns to room temperature and also to allow for any bubbles to migrate to the top of the vial before coating. Finally, the solution is ready for coating.

4.3.2.3 Device Cleaning Procedure:

It is important to clean the device properly before coating to improve film adhesion and consistency between films. If there is any kind of contaminant on the surface of the device, improper coating adhesion, delamination, unevenness or formation of pinholes in the coating can occur. The device also needs to be properly cleaned before reuse to remove any polymer residue, tape residue, organic contaminants, finger grease or dust. The cleaning procedure includes three major steps. First, the device is cleaned with four different chemicals. Then, a mixture of ammonium hydroxide, hydrogen peroxide and water is used to clean the device. Last, the device is exposed to UV light. Details are described in the following:

The four chemical solvents that are used to clean the device are trichloroethylene, chloroform, acetone and 2-propanol. The device is immersed in these chemicals in that order, following the steps below:

- i. Place the solvent in a clean jar.
- ii. Put the device in the solvent jar carefully.
- iii. Place the jar with the device in a sonication bath and sonicate for 5 minutes.
- iv. Take out the device from the jar and rinse with DI water for first three solvents.
- v. Dry the device with nitrogen gas.
- vi. Repeat those steps for first three solvents and for fourth solvent skip the rinse with DI water and directly dry the device with nitrogen gas.

To remove ionic contaminants, trace organics, chemically or physically adsorbed monolayers of organics or any kind of organic monolayers that are not covalently bonded to the surface, a harsher chemical treatment can be used. This cleaning procedure includes the following steps:

- i. Prepare a solution of 5:1:1 H₂O: NH₄OH: H₂O₂ in a jar.
- ii. Fill the same amount of water into another jar.
- iii. Place both jars on a hot plate and heat the solution to approximately 65-70°C. Continuously measure the temperature from the water jar and keep the temperature around 65-70°C of the solution. Too high a temperature might damage the IDT during the cleaning procedure.
- iv. Place the device in the heated solution jar for 10 minutes.

- v. Take the device from the solution jar and rinse the device quickly with DI water for 30 seconds. Check if the device is wetting properly; a hydrophilic surface means a properly cleaned surface.
- vi. Finally dry the device with nitrogen gas.
- vii. An additional step can be applied to make sure that all water has been removed from the device surface. For this purpose, put the device into 2-propanol and again dry with nitrogen.

The final cleaning step to remove any remaining contaminants is UV cleaning. UV light can clean the surface by breaking the bonds of the contaminants with the surface of the device. This cleaning procedure includes the following steps:

- i. Put the device in the UV lamp chamber.
- ii. Place the device directly under the UV lamp approximately 1 cm away from the lamp.
- iii. Turn the lamp on and keep the device underneath the lamp for one hour. The temperature of the device will remain in a safe range.
- iv. After one hour, remove the device and coat as soon as possible.

It is noted that during the cleaning process it is important to follow proper safety procedures. The UV lamp chamber should never be opened with the lamp turned on because UV light might damage the eye.

4.3.2.4 Coating a Device:

Various polymer-plasticizer blends are used to coat the SH-SAW device that will work both as a guiding layer for the acoustic wave and chemically selective layer to absorb the intended analyte. The contact pads remain uncoated during the coating process. After preparing the polymer-plasticizer blend coating solution and cleaning the device, some specific steps have to be followed to coat the device. It is important to follow the same procedure every time to ensure reproducible and uniform coatings. The steps are given below:

- i. First, mask the contact pads with Kapton tape to prevent them from being coated with the coating solution.
- ii. Blow nitrogen gas on the surface of the device one last time to remove any dust or small particles that may be introduced from the air.
- iii. Place the device on the center of the chuck of the spin coater.
- iv. Set the spin coater's parameters (spin speed, ramp time, duration).
- v. To make a bigger opening, cut the top end of the plastic micropipette tip (100 – 1000 μ l) to allow faster deposition of the coating solution. This is particularly important when using a volatile solvent.
- vi. By using a micropipette deposit 450 μ l coating solution on the surface of the device. (Use more or less coating solution for solutions of higher or lower viscosity, respectively.)
- vii. Immediately close the cover of the spin coater and start spinning. Doing this step fast helps to minimize solvent evaporation and achieve better coating uniformity and reproducibility.

- viii. Take the device from the chuck of the spin coater and place in an aluminum foil box.
- ix. Place the box with the device in an oven for baking to remove all the solvent from the film and reduce internal stress in the film.
- x. Start baking the device for 60 minutes at 60°C to ensure all the solvent is removed from the coating.
- xi. After baking wait until the device returns to room temperature. Later remove the Kapton tape from the device.
- xii. Add a black tape on the back side of the device. While applying the black tape, make sure there is no bubble or debris between the device and the tape. Tape should be cut along the edge of the device, making sure that the device fits well into the recess in the flow cell.
- xiii. Add conductive silver paint on the contact pads of the device for better electrical connection between the device and the flow cell.

4.3.3 Analyte Sample Preparing

The analytes tested in this research are benzene, toluene, ethylbenzene and xylene (BTEX). For the experiment, these analytes are prepared as a solution in degassed DI water at various concentrations. The concentration range used for this experiment is 50 ppb to 2000 ppb and the solutions are prepared by using the equation below.

$$ppb = \frac{V_{solute} * d_{solute}}{V_{solute} * d_{solute} + V_{solvent} * d_{solvent}} * 10^9 \quad (4.3)$$

For the purposes of this experiment, this equation is further simplified. The solvent used for analyte solution preparation is water and the density of water is 1.0 g/ml. Usually, the sample is prepared in a 250 ml bottle, so the volume of the solvent is significantly larger than solute volume. Because of this, the denominator solute term can be ignored and the simplified equation can be written as,

$$ppb = \frac{V_{solute} * d_{solute}}{V_{solvent}} * 10^9 \quad (4.4)$$

Although analyte concentration is verified by using a GC-PID, it is important to prepare the analyte sample consistently and accurately to ensure the accuracy of the concentration. The best way to get more accurate concentration of the sample is to prepare a stock solution at higher concentration and dilute the sample to a desired concentration. Although it is possible to prepare analyte solution at low concentration directly, it is better to dilute from higher concentration to avoid large errors in concentration. The preparation of stock solution at higher concentration and diluting to the desired lower concentration involves the following steps.

- i. Generally, stock solution concentrations are in the range of 30 ppm to 10 ppm. First calculate the volume of the analyte according to the volume of solvent.
- ii. Take a clean jar and place a magnetic bar into the jar.
- iii. Pour degassed, deionized (DI) water of the desired volume. Usually water volume should be close to the jar volume, so that there is very little headspace to avoid analyte solute evaporation.

- iv. DI water is produced in-house and is boiled at least 3 hours for degassing. Before preparing sample make sure degassed DI water is at room temperature.
- v. Add calculated amount of analyte by using micro-pipette and close the cover of the jar quickly.
- vi. Place the jar on a stir plate and stir at 600-700 rpm for at least 4 hours (preferably overnight).
- vii. Dilute the analyte solution to desired concentration (100 ppb to 2000 ppb) using the above steps.
- viii. Stir the diluted solution for at least 2 hours.

Analyte samples are not prepared more than 2 days before the experiment. By the passage of time, analyte concentration can be changed due to evaporation and activity of microorganisms. Also, air can be re-dissolved in the degassed water, which may lead to bubble formation during the measurement.

4.4 Measurement Procedures

4.4.1 Thickness Characterization

It is important to measure the coating thickness of the device to reproduce the same coating and sensor response on later devices. Coating thickness was measured for every device. A glass slide was coated with the same coating solution in the same environment, at the same time and in the same way as the sensor device. This glass slide is used to measure the thickness by using a profilometer. First a glass slide is cut to a size close to the device dimensions and then the two ends are covered with Kapton tape. After

coating and baking, the Kapton tape is removed from the glass slide to expose uncoated reference areas for the thickness measurement. A profilometer scan is made that includes both the glass and polymer-plasticizer coated surfaces which allows for a differential measurement of the coating thickness.

At first, the scan settings (stylus force, scan length, scan speed and sampling rate) need to be selected for the profilometer. Usually the stylus force is kept in the range of 0.2 to 0.4 mg. Then the coating thickness is measured in at least three different positions and the average is taken. After each scan, the surface profile data is leveled and smoothed. Finally, a step height measurement is used to measure the thickness of the coating.

4.4.2 Device Response

A plasticized polymer coated SH-SAW device is used to measure the response for a specific analyte. After completing all the preparation steps, the coated device is carefully mounted inside a flow cell together with the gasket. It is necessary to insert the gasket properly to perform an uninterrupted bubble free measurement. Once the device is put in the flow cell, it should not be removed from the cell until all the necessary long term measurements are completed, because removing the cover and gasket might damage the coating by peeling the film off from the device.

Coaxial cables are used to connect the flow cell and network analyzer. Data is sent to the attached computer and processed by the Agilent VEE program. Reference samples and analyte samples are run through the flow cell via a pump and three-way valve. The pump is set to a fixed flow rate of 7 $\mu\text{l}/\text{second}$ for this research. The entire

setup is kept in a cooler box and before the measurement, the system is allowed to reach equilibrium temperature. Once the device has been exposed to DI water, an operating frequency needs to be determined. The operating frequency is selected in a linear phase region and also near 0° phase for both delay lines near the frequency where insertion loss is minimal, i.e., in the passband and near the device center frequency. The sensor is exposed to the analyte under test and reference sample long enough for the response to reach equilibrium for analyte absorption and return to the baseline for the analyte desorption. Device loss, frequency change and phase change are monitored by the Agilent VEE program on the attached computer and all the data is collected on the computer. After that, data is processed in excel and MatLab, which will be discussed below.

4.4.3 Concentration Confirmation

As the BTEX compounds are volatile, it is important to confirm the concentration of the analyte sample immediately after the measurement using the GC-PID (Gas Chromatograph – Photoionization Detector, Defiant FROG-4000). Before measuring the concentration of the analyte solution, the FROG is calibrated with standard BTEX samples from RESTEK or Sigma-Aldrich. It is recommended to calibrate the FROG once per month to ensure high accuracy. The concentration measurement error in GC-PID is around $\pm 7\%$ for the BTEX compounds [75]. Initially, the FROG was calibrated up to 1 ppm and later it was calibrated up to 4 ppm; thus, for sample concentrations higher than 4 ppm, the FROG shows non-linearity. If measurements need be made in this high concentration range, the solution is first diluted before the concentration is measured by the GC-PID, but dilution of the sample also adds to the error as the BTEX compounds are

volatile. For this research, sample concentrations are in the range of 100 ppb to 2000 ppb (2 ppm), and the concentration was measured directly without dilution.

4.5 Data Processing

Data is collected from the network analyzer through VEE program and stored as a comma-separated value (.csv) file in the computer. This .csv file can be imported into Microsoft Excel and the data can be processed as a spreadsheet. The first step after collecting data is to do the baseline correction because the sensor experiences a baseline drift during the measurement process. As for this research only frequency shift is used to calculate the sensitivity, the frequency shift data is corrected for baseline drift. Then, to see the long-term consistency of the sensor, this baseline corrected frequency data can be normalized using the equation below:

$$f_n = f_0 \left(\frac{C_n}{C_0} \right) \quad (4.5)$$

Here, f_n is the normalized frequency shift, f_0 is the actual raw frequency shift, C_n is the concentration to which the result is normalized, and C_0 is the actual concentration of analyte solution measured by the GC-PID. By using the equation (4.5), frequency shift response is normalized to a specific concentration (usually 1 ppm) to compare the responses of the sensor coating over a long period of time (sometimes up to 60 - 90 days). It is important to note that while normalizing the frequency shift, the noise is multiplied by the same factor. To compare the actual repeatability of the sensor response, the actual concentration of the analyte solution must not vary too much between experiments. Additionally, normalized data should not be used for noise calculation and detection limit

calculation. The actual raw data is used to calculate the noise and detection limit of the response.

For a single analyte, frequency response data can be fitted using a single exponential fitting program in MATLAB [77] based on the equation given below:

$$y(t) = y_0(1 - e^{-\frac{t}{\tau}}) \quad (4.6)$$

Here, τ is the response time constant, $y(t)$ and y_0 are the frequency at time t and equilibrium frequency shift, respectively. The time constant, τ , is defined as the time the sensor response takes to reach $(1 - \frac{1}{e}) \approx 63.2\%$ of the final equilibrium value starting with analyte exposure [78]. For this sensor system, the introduction of analyte is considered as a step input, i.e., the analyte concentration should change in a step-like manner (when the analyte is introduced). Time constant should not be confused with response time, which is the time to reach steady state condition. By using the MATLAB fitting program, two parameters, time constant and equilibrium frequency shift, can be extracted. The two parameters are used to characterize the sensor coating. Sensitivity is calculated by using the frequency shift [77]:

$$S = \frac{\Delta f}{c_0} \quad (4.7)$$

The detection limit is determined by:

$$LOD = \frac{3 * RMS \text{ Noise}}{Sensitivity} \quad (4.8)$$

where, LOD is the limit of detection, i.e. the lowest concentration that will induce a significant response in the sensor. RMS noise is simply calculated using standard deviation of the baseline corrected frequency response data. It is better to have a sensor coating that has high sensitivity and low RMS noise to achieve a low LOD. The main objective of this research is to find an optimal polymer-plasticizer coating with highest sensitivity and lowest detection limit.

5. RESULTS AND DISCUSSION

5.1 Introduction

In this research, the performance of SH-SAW sensor platforms coated with various polymer-plasticizer blends has been investigated. DIOA and DINCH as plasticizers were mixed with PS and PMMA polymers to create the polymer-plasticizer blend coatings. DIOA-PS, DIOA-PMMA and DINCH-PMMA blends were analyzed to find suitable coatings for SH-SAW sensors to detect BTEX chemicals in water at very low concentration (ppb range). The mixing ratio of polymer and plasticizer as well as the thickness of the coatings were varied, and sensitivity, response time constant, RMS noise level, detection limit and stability of the coated devices were studied. The objective of the research is to find an optimal SH-SAW sensor coating with high sensitivity, low detection limit and long term stability that will provide a valuable addition to a sensor array. The analyte concentration range studied for this work was 50 ppb to 2000 ppb.

Before collecting data, the device was exposed to DI water for the initial absorption of water and swelling of the coating. This initial swelling increases the thickness of the coating and changes the viscoelastic properties of the polymer-plasticizer blend. The device along with the analyte solution and DI water were kept in a temperature control box to maintain a constant ambient temperature before collecting data. A thermistor attached to the bottom of the flow cell is used in some measurements to track the temperature change during data collection. Temperature changes during the measurement process, possibly due to the switching to analyte solution from DI water or some other reason can have a significant effect on the response of the sensor. To minimize this effect, the analyte solution, DI water, and sensor were given time to reach

thermal equilibrium before measurements were taken. It was noticed from the thermistor data that the temperature changes when switching from analyte solution to DI water was negligible. Although sufficient time was allowed before the measurement to allow the temperature to reach equilibrium, there will still be a small drift in the loss, phase and frequency data collected by the vector network analyzer. This baseline drift was corrected using Excel after collecting the data.

The sensitivity, detection limit and response to all BTEX chemicals was measured for various concentrations by using SH-SAW devices with various plasticized polymer coatings. Initially, an operating frequency was selected to track the change in frequency at a constant phase and this operating frequency was kept fixed for all measurements for that specific coating. To investigate the repeatability of the sensor coating the responses were normalized to 1 ppm. After that, an average response curve of those normalized responses was created for visual representation with error bars representing the standard deviation, i.e. the spread of those measurements. The concentrations of all tested analyte samples were verified by GC-PID. The frequency responses were also plotted as a function of analyte concentrations as a calibration curve to extract the sensitivity of the coating for each BTEX analyte. After measuring the sensitivity to all BTEX chemicals, a graph was plotted to show the partial selectivity of the coatings. A comparison between all the tested coatings and commercially available coatings is shown at the end of this chapter.

5.2 Studied Range of Plasticizer Percentage in the Blend

In the literature [66], [67], polymer and plasticizer mixing ratios from 10% to 30% have been reported for various plasticizers in polymers for sensor coatings. This gives a general starting range for each plasticizer-polymer blend. Another important aspect for this work is the long-term stability of the coating, which depends on the rate of plasticizer leaching from the plasticized polymer coating [65] and also the polymer creep or deformation. The ideal plasticizer percentage is unique for each plasticizer-polymer blend due to the chemical nature of the materials. Generally, as described in chapter 3, increasing the percentage of plasticizer increases the flexibility and free volume of the coating, resulting in an increase in analyte absorption. At the same time, increasing the percentage of plasticizer increases the softness of the coating, resulting in an increase in acoustic-wave loss and decrease in stability. Therefore, plasticizer concentration was varied in the experiments and used to determine the optimum plasticizer-polymer ratio that gives high sensitivity while maintaining long-term stability. The previous studies of plasticized polymer coatings for SH-SAW sensors from [54], [79] reported that 23% DOP-PS and 23% DINCH-PS gave optimal performance for these polymer-plasticizer blends. Initially the mixing ratio of polymer-plasticizer blends for this work started at 23% and was adjusted depending on the observed sensitivity, repeatability and stability. Experiments were conducted to find the optimum DIOA percentage in the polymer-plasticizer blend.

5.3 Thickness of Coating

The thickness of the coating plays an important role in sensitivity and stability of the sensor and will be selected for optimum sensor performance. In general, by increasing the coating thickness up to a certain limit, the sensitivity increases because it increases the sorption capacity, but at the same time, this also increases acoustic wave attenuation. For this work, the coating thickness was in the range of about $h = 0.02 \lambda - 0.03 \lambda$ (acoustic wavelength, $\lambda = 40 \mu\text{m}$). From experimental observation, with the sensor design used in this work, a maximum coating thickness of 0.031λ can be tolerated for rubbery polymers before the wave attenuation becomes too high. At this thickness range, all the coatings are slightly in the acoustically thick regime [48], i.e. there will be a phase lag across the thickness of the vibrating coating. However, as long as this phase lag is small, the resulting increase in wave attenuation will not be prohibitive for the sensor signal. As a result, this range of coating thicknesses will allow a large analyte sorption capacity and low acoustic wave attenuation. Therefore, high sensitivity and a low detection limit are possible to achieve with these coatings. In the following section, the results and discussions of each plasticizer-polymer blend (DIOA-PS, DINCH-PS, DIOA-PMMA, and DINCH-PMMA) with variations of plasticizer concentration and thickness are reported.

5.4 Results for DIOA-PS Coatings

Polystyrene (PS) is selected for plasticized polymer coatings because of the chemical structure of the monomer, styrene, which includes a phenyl ring and is expected to have high affinity to BTEX. PS was used in previous work [54], [79], with DOP-PS

and DINCH-PS blends for benzene detection. As a plasticizer, DIOA is used because it has a long carbon chain, negligible leaching rate and favorable solubility parameters. Table 3 in chapter 3 shows the solubility of PS with DIOA, THF and all BTEX chemicals. All BTEX analytes are investigated for DIOA-PS coatings, but benzene is the main focus because of its carcinogenicity as well as its low detection limit. An optimal coating is found based on sensitivity to benzene, and then all the other BTEX chemicals are tested with that coating.

As stated earlier, based on [54], [79], 23% DOP-PS with a 1.1 μm thick coating and 23% DINCH-PS with a 1.0 μm thick coating were showing the best performance among DOP-PS and DINCH-PS blends. A device was prepared with 23% DIOA-PS with a 1.0 μm -thick coating and polymer-plasticizer mixing ratio and coating thickness were further adjusted depending on the observed sensitivity, repeatability and stability. For the DIOA-PS blends, it was observed that the long-term stability of the coating depends on the polymer-plasticizer mixing ratio as well as the thickness of the coating. Initially, various combinations of coating thickness and DIOA-PS mixing ratios were tested to determine stability of the coating and repeatability of the sensor response (frequency shift). An empirical figure of stable DIOA-PS coatings based on the mixing ratio and coating thickness is shown at the end of the DIOA-PS result section. Similarly, various mixing ratios with various coating thicknesses for DIOA-PMMA & DINCH-PMMA were analyzed and the results are shown in the respective sections.

5.4.1 22.9% DIOA-PS 7.9% in THF

As stated earlier, based on [54], [79], 23% DIOA-PS was prepared for a coating thickness of less than 1.0 μm . The exact percentage of DIOA in PS blend that was obtained was 22.9%. The thickness of the coating was measured to be 0.7 μm ($h = 0.0175 \lambda$) resulting in an initial insertion loss of 25 dB. Experiments were conducted to obtain the frequency response, and the loss was also tracked at the same operating frequency over the measurement period. The overlaid sensor responses to benzene over a measurement period of three months are shown in Fig. 5.1.

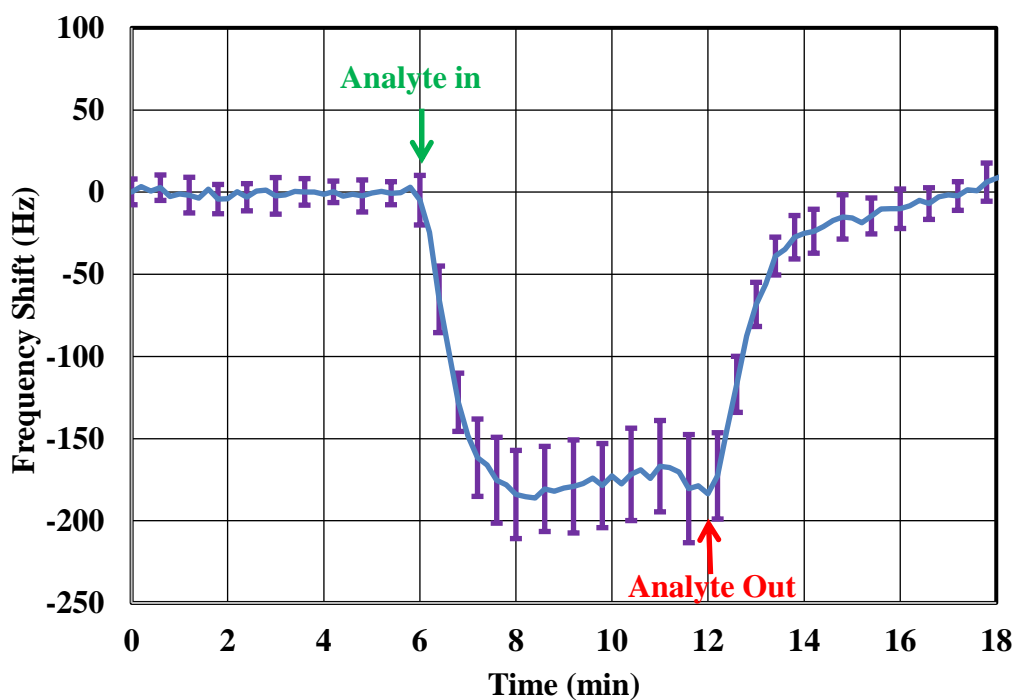


Figure 5.1: Frequency response of SH-SAW device coated with 0.7 μm -thick ($h = 0.0175 \lambda$) 22.9% DIOA-PS to 1 ppm (1 mg/L) benzene in water with error bars.

The measured responses were normalized to 1 ppm benzene using the concentration measured by the GC-PID immediately after the sensor measurement. The

headspace of the sample container jar was kept as low as possible to minimize analyte evaporation. After normalizing the responses to 1 ppm, an average response curve was produced by averaging all the data of the responses. Fig. 5.1 shows the average response curve of all the measurement with error bars. The error bars represent the standard deviation of all the response curves measured with the coating. The observed error bar is about $\pm 15\%$. Note that the measurement error of the GC-PID is about $\pm 7\%$ [80]. The mismatch between these values may be due to the volatility of the samples during the sample transfer from the sensor measurement to the GC-PID. Although the ambient temperature of the entire measurement system including analyte sample, reference sample and flow cell with sensor device should be stable, small changes in the temperature may be noticeable due to the low sensitivity of the coating, possibly contributing to the observed spread.

The sensitivity of the coating is referred to as the frequency shift response per unit concentration of analyte (Hz/ppm) and calculated from the baseline-corrected data. Using a single exponential fitting program in MATLAB, the frequency shift was extracted from the raw data and plotted as a function of analyte concentration. The slope of the curve represents the sensitivity of the coating for that specific analyte. The frequency shift as a function of benzene concentration was plotted for the 0.7 μm -thick 22.9% DIOA-PS coating and is shown below.

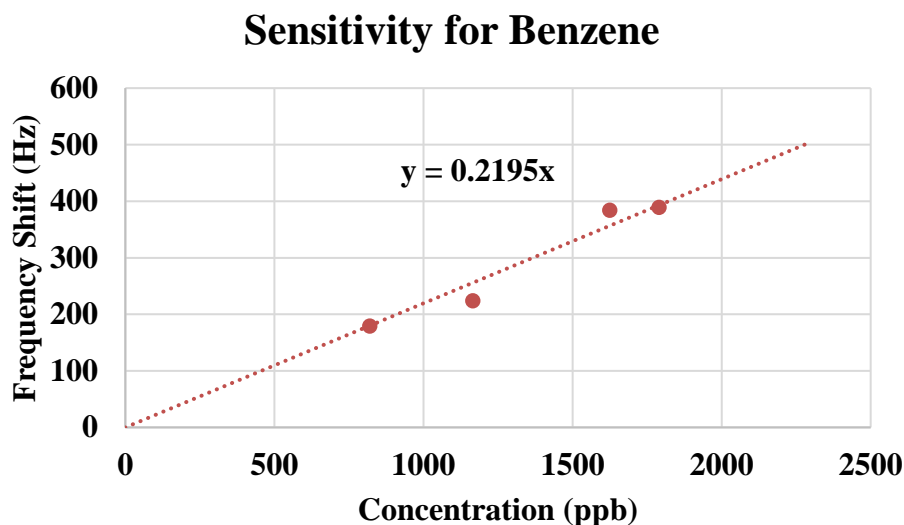


Figure 5.2: Frequency shift vs benzene concentration with a linear fit and zero intercept to extract sensitivity for a 0.7 μm -thick ($h = 0.0175 \lambda$) 22.9% DIOA-PS coated SH-SAW sensor.

The 0.7 μm -thick 22.9% DIOA-PS sensor coating had a sensitivity of 220 Hz/ppm shown in Fig. 5.2. The average RMS noise is 8 Hz, resulting in a limit of detection of 110 ppb. The goal of the research was to create a sensor coating that will have high sensitivity and low detection limit. To achieve this goal, further adjustment of the coating parameters was needed. To increase the sensitivity, either the thickness of the coating or the percentage of plasticizer can be increased. Increasing the percentage of plasticizer will soften the polymer, create an even more rubbery coating and increase the free volume, allowing more analyte to be absorbed by the coating. The plasticizer percentage can be optimized based on the loss spectrum of the device. The loss spectrum is shown in Fig. 5.3, with the tracked insertion loss at the operating frequency shown in the inset of the Fig.5.3.

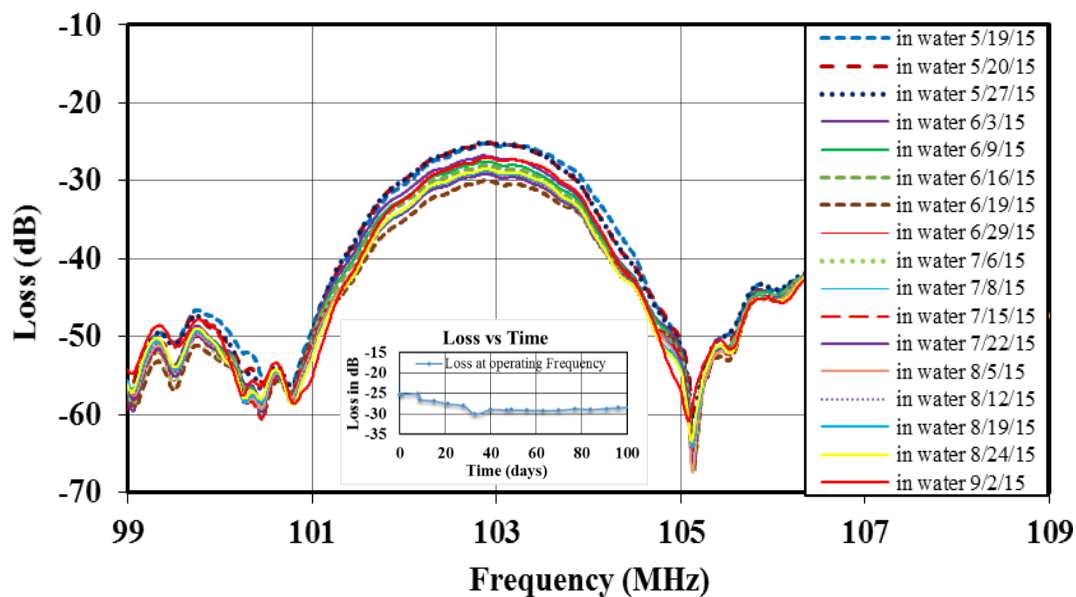


Figure 5.3: Loss spectrum of an SH-SAW sensor device with 0.7 μm -thick ($h = 0.0175 \lambda$) 22.9% DIOA-PS coating. The inset shows the loss tracked at the operating frequency.

Although the 0.7 μm -thick 22.9% DIOA-PS coating did not have high sensitivity, it was found to be stable for 100 days. The loss spectrum was collected for each measurement over 100 days. The insertion loss at the operating frequency of the device was tracked to see any indication for changes in the elastic characteristics of the coating over the measurement period. As seen in the above Fig.5.3, the loss of the device fluctuated by about 5 dB. The high insertion loss of the device suggests that the coating should not be made more rubbery. For the next blend, instead of increasing the plasticizer percentage, the coating thickness was increased, which should result in an increase in sensitivity. To keep the acoustic-wave attenuation low, the plasticizer percentage was simultaneously decreased.

5.4.2 17% DIOA-PS 10% in THF

In order to improve the sensitivity and the elastic characteristics of the DIOA-PS coating, several coatings with lower percentages of plasticizer and higher thickness (1.0 μm) were investigated. It was found that a 1.0 μm -thick ($h = 0.025 \lambda$) coating made from a solution of 17% DIOA-PS in 10% THF had high sensitivity (345 Hz/ppm) for benzene. The initial insertion loss (23 dB) suggests that it is possible to make this coating even thicker and more rubbery. Note that from experimental observation it is known that the signal-to-noise ratio of a sensor device deteriorates significantly if the device insertion loss exceeds about 35 dB; thus, for the 1.0 μm -thick ($h = 0.025 \lambda$) 17% DIOA-PS coating, there was still room for increased insertion loss. Experiments were conducted to determine the sensor response to benzene over the course of several weeks of sensor operation. Fig. 5.4 shows the average response of 9 measurements, with error bars representing standard deviation, of a sensor coated with 1.0 μm -thick ($h = 0.025 \lambda$) 17% DIOA-PS.

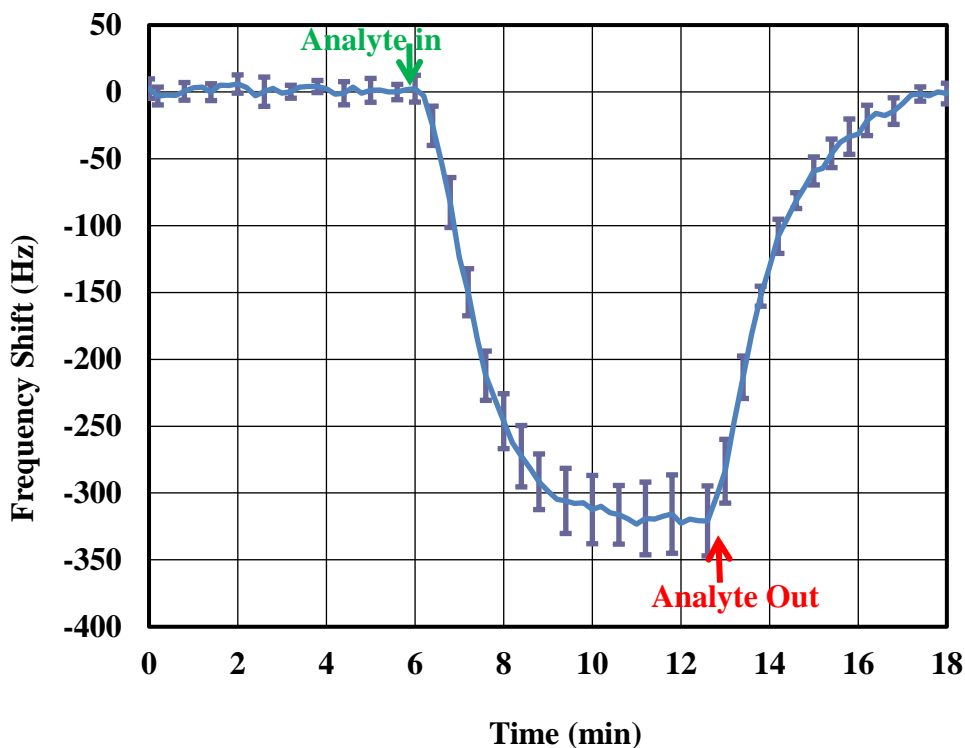


Figure 5.4: Frequency response of SH-SAW device coated with 1.0 μm -thick ($h = 0.025 \lambda$) 17% DIOA-PS to a concentration of 1 ppm benzene in water. Error bars represent the standard deviation of 9 measurements performed over 36 days.

Responses have been normalized to 1 ppm benzene using the independent concentration measurements of the GC-PID. Data was collected over the course of 36 days. The observed error bars in the equilibrium frequency shift are about $\pm 9\%$. Note that the measurement error of the GC-PID is about $\pm 7\%$ [80]. The small difference may be due to slight loss of the volatile samples during sample transfer between instruments. Also note that the error bars include the RMS noise of the SH-SAW sensor response as well.

The frequency shifts responses of the 1.0 μm -thick ($h = 0.025 \lambda$) 17% DIOA-PS coating for benzene were extracted from the raw data and plotted as a function of

benzene concentration. A linear fit with zero y-intercept was used to extract the sensitivity.

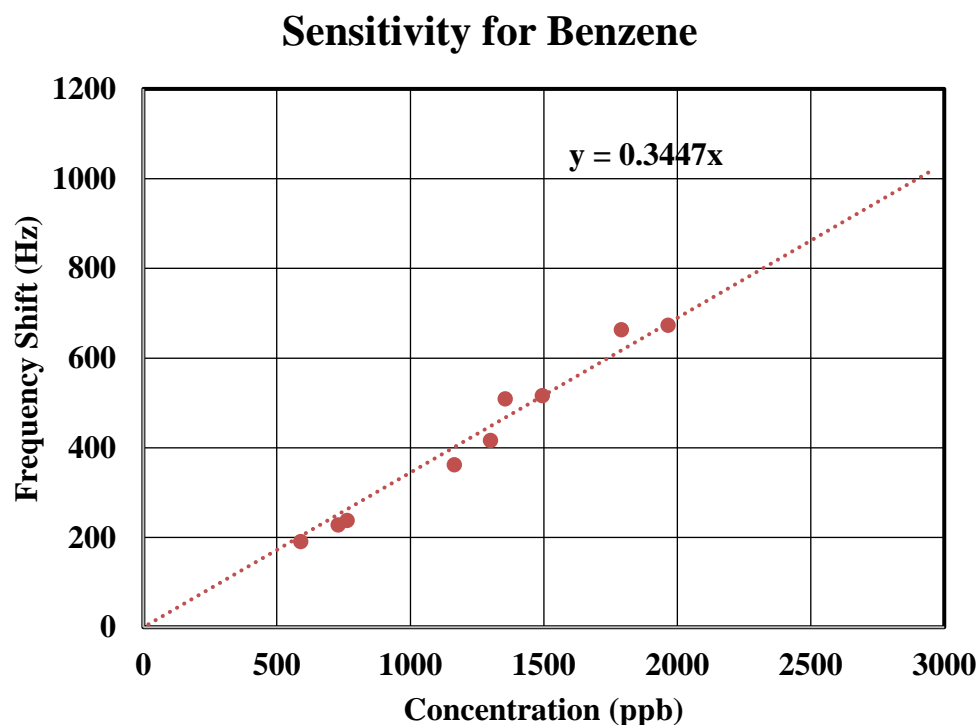


Figure 5.5: Frequency shift vs benzene concentration with a linear fit and zero y-intercept used for extracting sensitivity for a 1.0 μm -thick ($h = 0.025 \lambda$) 17% DIOA-PS coated SH-SAW sensor.

The 1.0 μm -thick 17.0% DIOA-PS sensor coating was found to have a sensitivity of 345 Hz/ppm, the average RMS noise was 7.3 Hz and the calculated limit of detection was 60 ppb.

The insertion loss at the operating frequency was tracked to determine any changes in the viscoelastic properties of the coating and is shown in Fig. 5.6. The loss remained stable at around 24 (± 1) dB for one month, indicating relative physical stability of the coating throughout the time of the experiments.

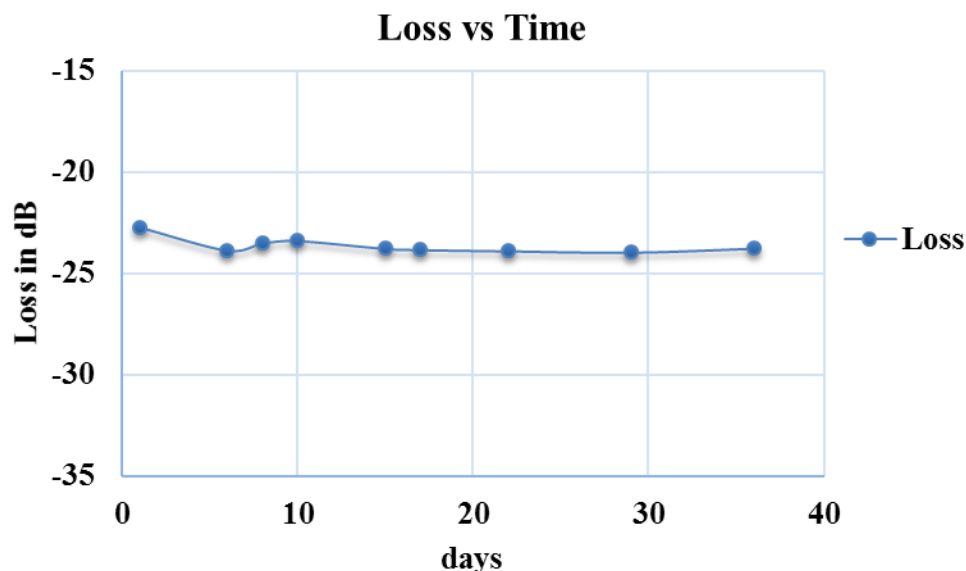


Figure 5.6: Device insertion loss at the operating frequency for the 1.0 μm -thick 17% DIOA-PS coated SH-SAW sensor tracked over a period of 40 days.

5.4.3 17.5% DIOA-PS 11.5% in THF

The percentage of DIOA and thickness of the coating have been further adjusted to change the sensing characteristics of the coating. It was observed that reducing the percentage of plasticizer increases the rigidity of the coating, making it glassier. The percentage was reduced to 16.0% DIOA-PS at 1.0 μm thickness, giving slightly reduced sensitivity and an increase in response time constant as expected for a glassier coating. Increasing the percentage of plasticizer with higher thickness (more than 1.0 μm) showed a trend towards reduced coating stability. To find the optimal balance between sensitivity and stability, the plasticizer percentage and coating thickness were increased slightly. Increasing coating thickness will increase the sorption capacity of the coating, which might also lead to an increased viscoelastic response and increased confinement of the SH-SAW

to the surface. Although at this thickness the rubbery coating is slightly in the acoustically thick regime [48], [81], (meaning that there will be a phase lag across the thickness of the vibrating coating), this phase lag is small and will not negatively affect the sensor signal. It was found that a 1.25 μm -thick ($h = 0.031 \lambda$) 17.5% DIOA-PS coating gave the highest sensitivity, as well as the lowest detection limit among all the investigated DIOA-PS coatings while maintaining stability for over one month. Fig. 5.7 shows the frequency response to benzene in the concentration range of 65 ppb to 990 ppb.

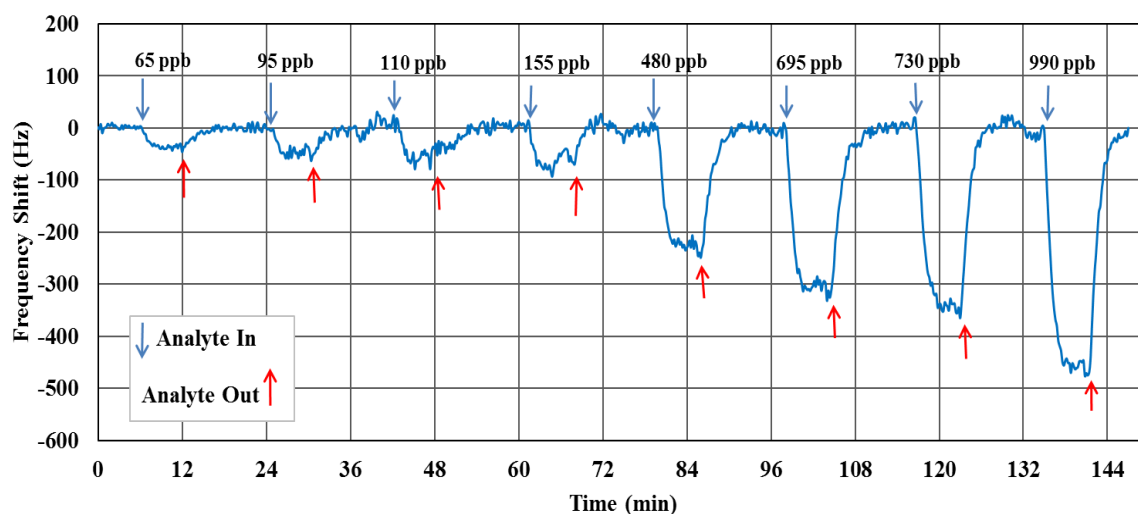


Figure 5.7: Frequency response of SH-SAW device coated with 1.25 μm -thick ($h = 0.031 \lambda$) 17.5% DIOA-PS to various concentrations of benzene in water. Concentrations are indicated in the graph (1 ppb = 1 $\mu\text{g/L}$). The analyte was flushed out with DI water between individual sample measurements and the graph combines individual sensor responses recorded on different days. The signal was corrected for baseline drift.

From Fig. 5.7, it can be seen that low concentrations of benzene (around 50 ppb) can be measured. The insertion loss at the operating frequency was tracked over the course of the experiments and was found to be stable throughout the experiments.

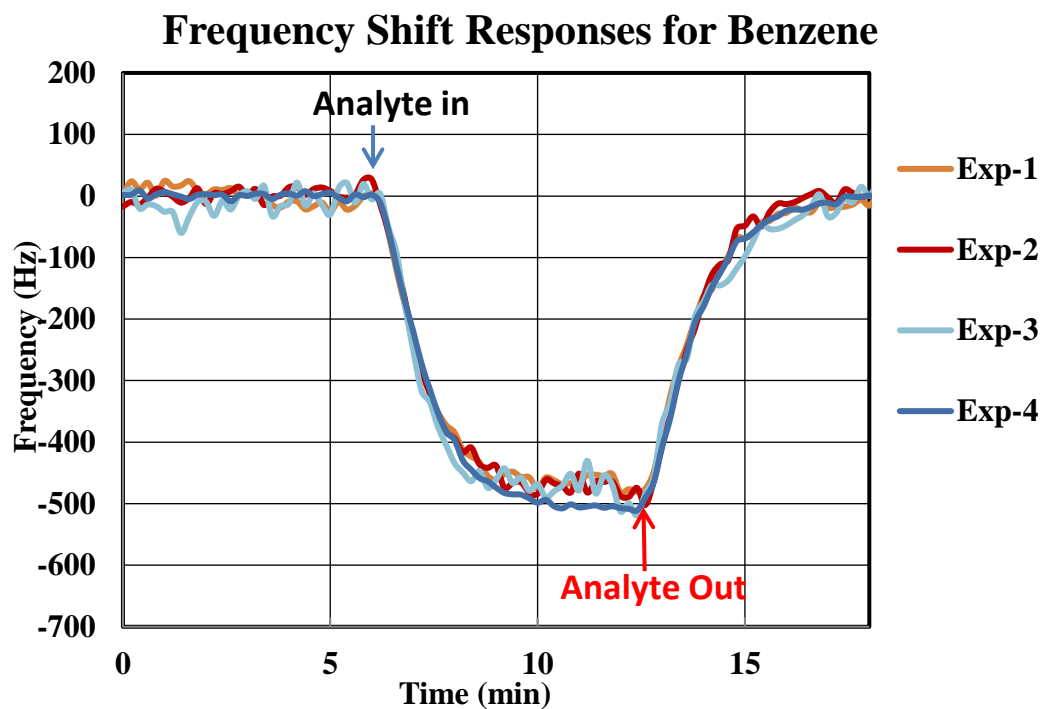


Figure 5.8: Frequency responses of the 1.25 μm -thick ($h = 0.031 \lambda$) 17.5% DIOA-PS coated SH-SAW sensor normalized to 1 ppm benzene. The data shows repeatability of the frequency response of the devices.

Fig. 5.8 shows the overlaid responses of a sensor coated with 1.25 μm -thick ($h = 0.031 \lambda$) 17.5% DIOA-PS. Responses have been normalized to 1 ppm benzene using the independent concentration measurements of the GC-PID.

Again, the sensitivity was extracted from the raw data. The slope of the frequency shifts versus benzene concentrations for 1.25 μm -thick ($h = 0.031 \lambda$) 17.5% DIOA-PS represents the sensitivity of the coating for benzene and the Fig. 5.9 is shown below.

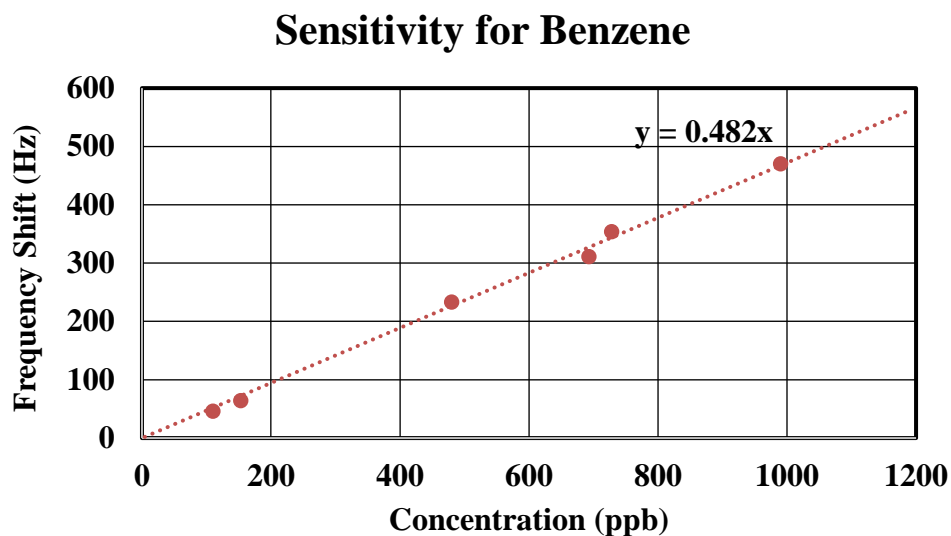


Figure 5.9: Frequency shift vs benzene concentration with a linear fit and zero y-intercept used for extracting sensitivity for a 1.25 μm -thick ($h = 0.031 \lambda$) 17.5% DIOA-PS coated SH-SAW sensor.

The sensitivity of the 1.25 μm -thick 17.5% DIOA-PS sensor coating was found to be 482 Hz/ppm, with a calculated limit of detection of 45 ppb, which was experimentally tested down to a concentration of 65 ppb of benzene as shown in Fig. 5.7. This figure also shows linearity between frequency shift and concentration for the concentration range investigated

To determine the stability of the 1.25 μm -thick 17.5% DIOA-PS sensor coating, the insertion loss at the operating frequency was tracked over the period of measurements. The initial loss was 24 dB, and over the period of measurements it changes only by 1 dB, which represents a very stable coating for this measurement period. Fig. 5.10 shows the insertion loss versus time curve.



Figure 5.10: Device insertion loss at the operating frequency for the 1.25 μm -thick ($h = 0.031 \lambda$) 17.5% DIOA-PS coated SH-SAW sensor tracked over a period of 32 days.

5.4.4 Reproducibility and Repeatability

The 1.25 μm -thick 17.5% DIOA-PS coated SH-SAW sensor showed highest sensitivity and good stability for at least one month. The sensor response of this coating showed repeatability over the period of the measurements. Later, the 1.25 μm -thick 17.5% DIOA-PS coating was reproduced four times to confirm the reproducibility of the coatings. The results of the repeated 1.25 μm -thick 17.5% DIOA-PS coated SH-SAW sensor are shown in Fig's 5.11, 5.12 and 5.13. The sensor response of the reproduced 1.25 μm -thick 17.5% DIOA-PS coating was similar to the first 1.25 μm -thick 17.5% DIOA-PS coating. Because of some procedural error, the thickness of the repeated coating was slightly thinner (1.23 μm) than the first coating, which is why the sensitivity was slightly lower. The sensitivity of the 1.25 μm -thick 17.5% DIOA-PS coating for benzene was 482 Hz/ppm and the sensitivity of the reproduced 1.25 μm -thick 17.5% DIOA-PS coating is 450 Hz/ppm. Fig. 5.11 shows the average frequency response of the

reproduced 1.25 μm -thick 17.5% DIOA-PS coating with error bars. The error bars represent standard deviation of all the measurements.

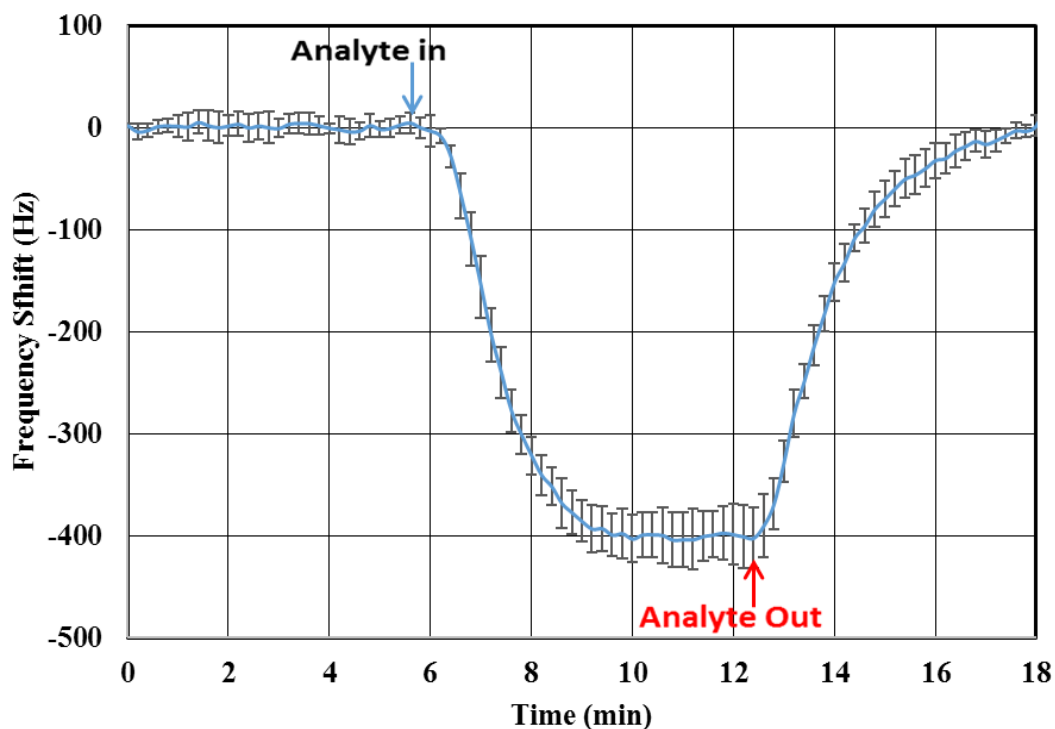


Figure 5.11: The average frequency response of SH-SAW device coated with the reproduced 1.25 μm -thick ($h = 0.031 \lambda$) 17.5% DIOA-PS coating to a concentration of 1 ppm (1 mg/L) benzene in water with error bars representing the standard deviation of the measurements.

Again, for the reproduced 1.25 μm -thick ($h = 0.031 \lambda$) 17.5% DIOA-PS coating, sensitivity was extracted from the raw data and plotted as a function of benzene concentration. Fig. 5.12 shows the frequency shift responses versus benzene concentration. The slope of the Fig.5.12 represents the sensitivity of the coating for benzene.

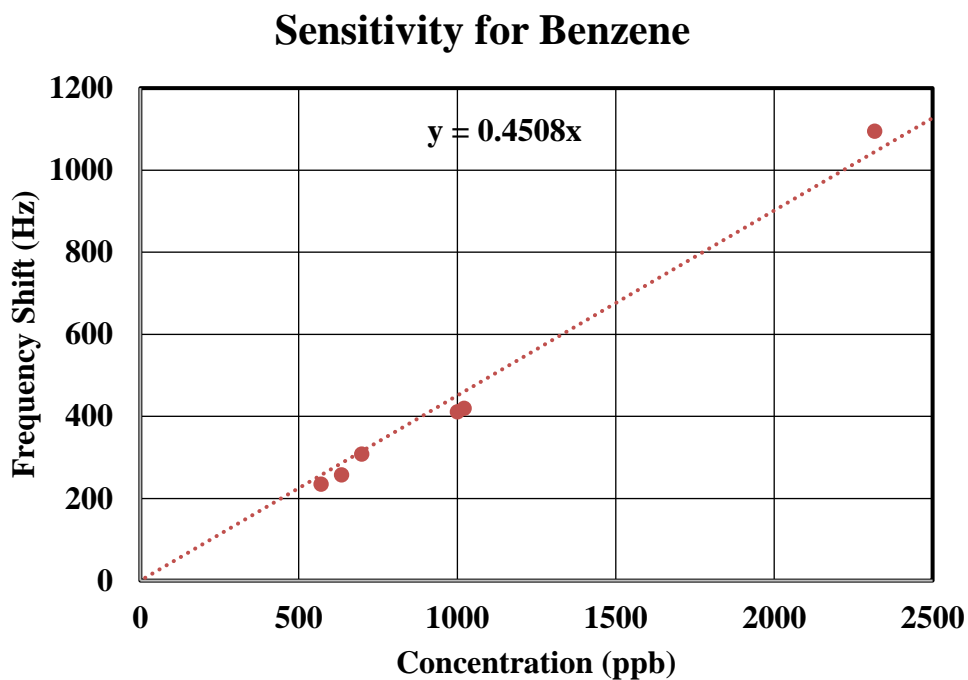


Figure 5.12: Frequency shift vs benzene concentration with a linear fit and zero y-intercept used for extracting sensitivity for the reproduced 1.25 μm -thick ($h = 0.031 \lambda$) 17.5% DIOA-PS coated SH-SAW sensor.

The loss tracked at the operating frequency for both 1.25 μm -thick 17.5% DIOA-PS and reproduced 1.25 μm -thick 17.5% DIOA-PS coated SH-SAW sensor devices was plotted and showed similar stability. Fig. 5.13 shows the loss changes during the one-month period of the measurements. This figure indicates similar behavior for both devices. After one week, the loss was stable throughout the measurement periods.

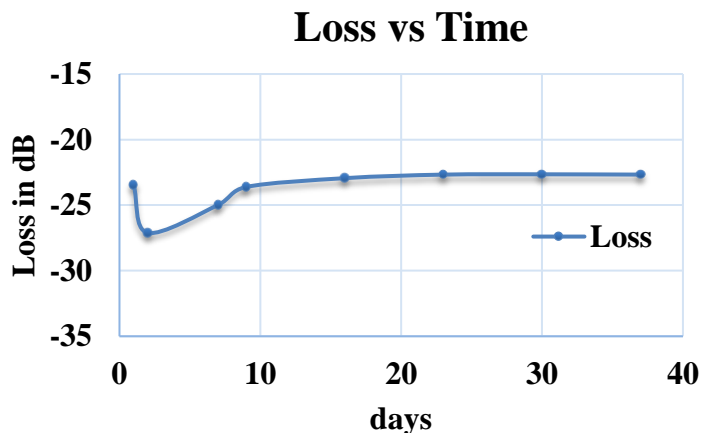


Figure 5.13: Device insertion loss at the operating frequency for the reproduced 1.25 μm -thick 17.5% DIOA-PS coated SH-SAW sensor tracked over a period of 37 days.

5.4.5 Reproduced 17.5% DIOA-PS 11.5% in THF for BTEX

Once the optimal DIOA percentage in the DIOA-PS blend and coating thickness were determined for benzene detection, the other BTEX chemicals, toluene, ethylbenzene and xylene were tested using the coating. As the 1.25 μm -thick ($h = 0.031 \lambda$) 17.5% DIOA-PS coating has the highest sensitivity and lowest detection limit for benzene, it was considered the optimum coating for DIOA-PS blends. The frequency responses of toluene, ethylbenzene and xylene for the reproduced 1.25 μm -thick 17.5% DIOA-PS coating are shown in Fig.'s 5.14, 5.15 and 5.16 respectively.

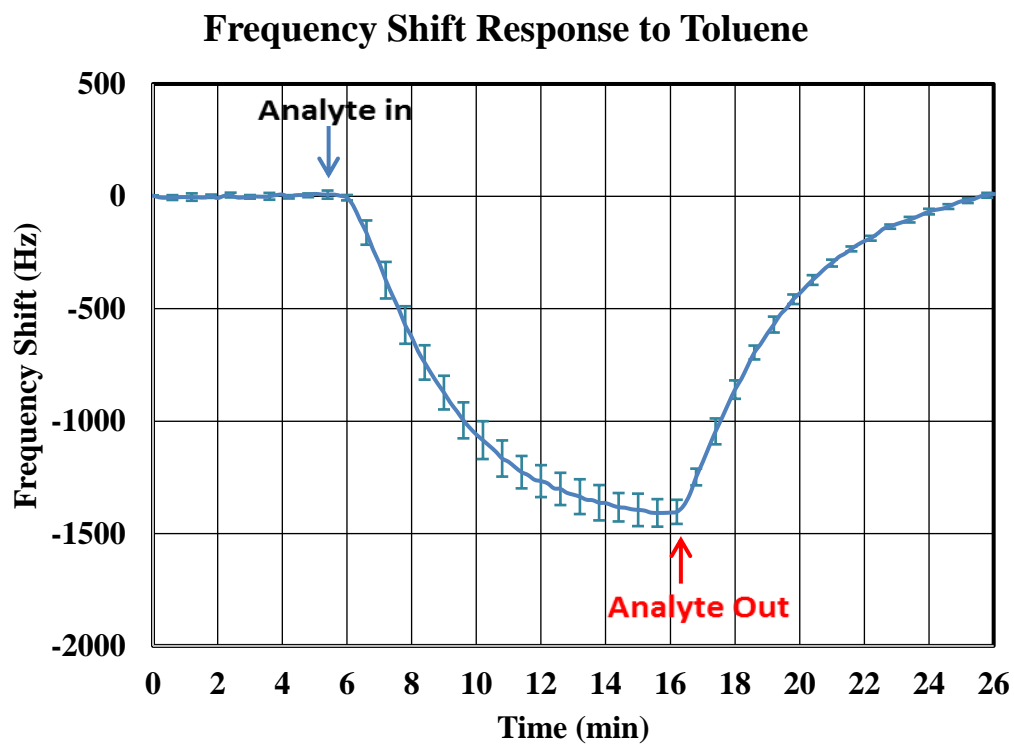


Figure 5.14: The average frequency response of SH-SAW device coated with the reproduced 1.25 μm -thick ($h = 0.031 \lambda$) 17.5% DIOA-PS coating normalized to a concentration of 1 ppm (1 mg/L) toluene in water with error bars representing the standard deviation of the measurements.

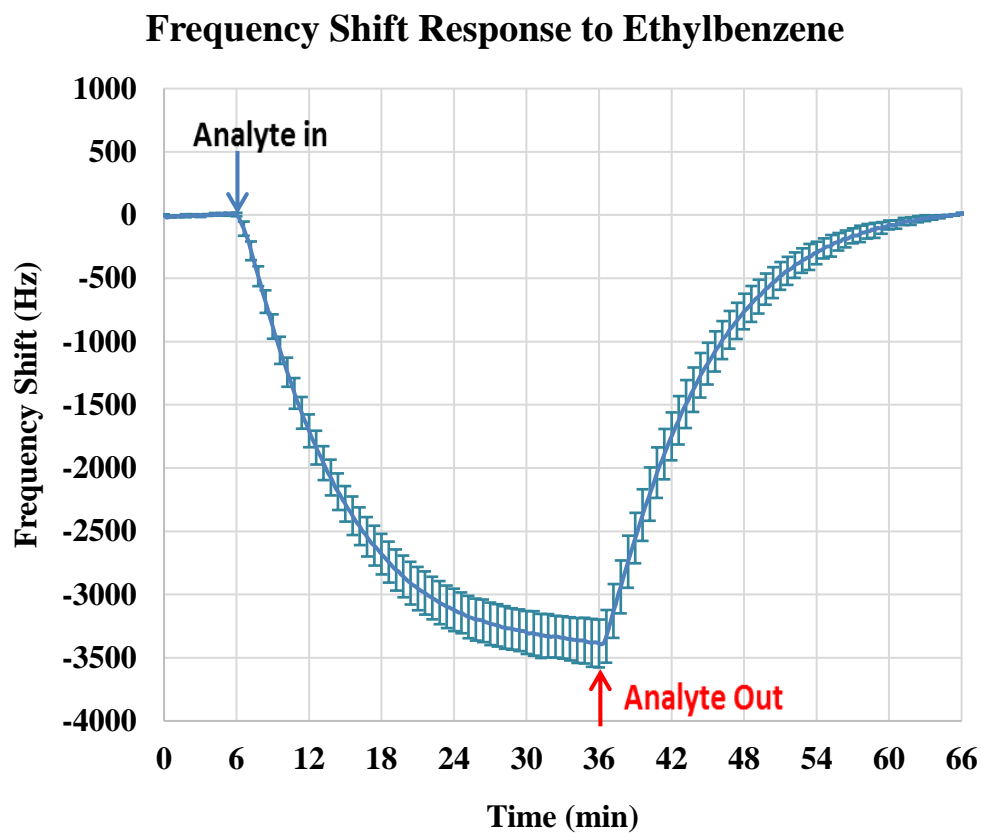


Figure 5.15: The average frequency response of SH-SAW device coated with the reproduced 1.25 μm -thick ($h = 0.031 \lambda$) 17.5% DIOA-PS coating normalized to a concentration of 1 ppm (1 mg/L) ethylbenzene in water with error bars that represent the standard deviation of the measurements.

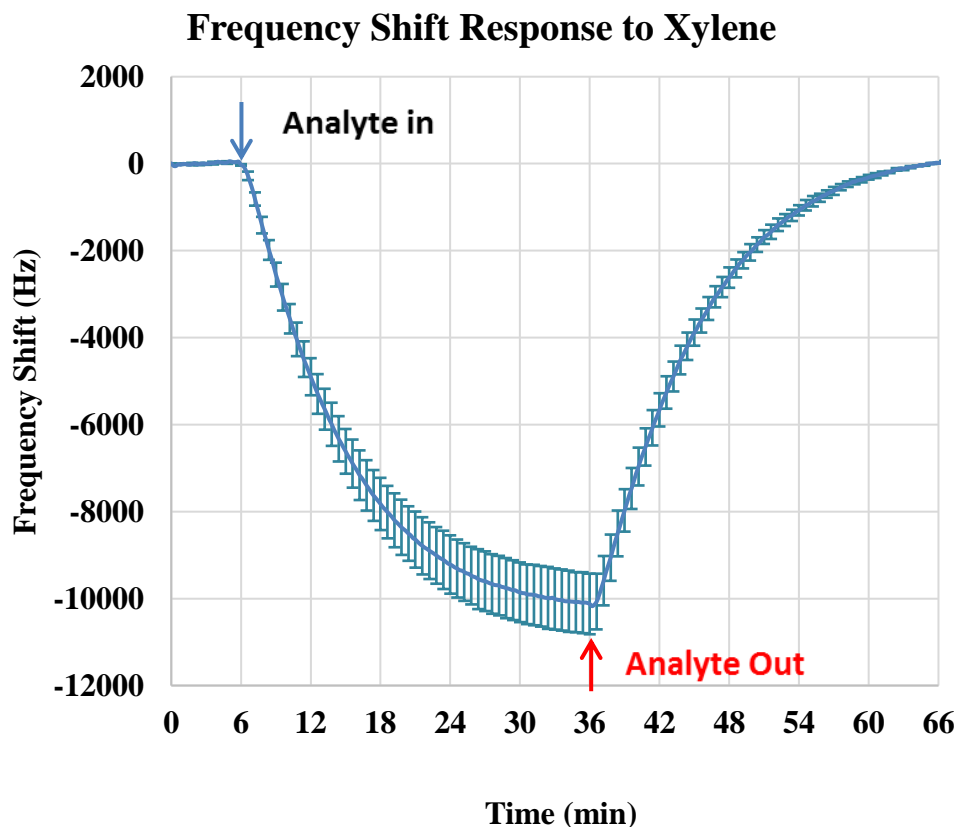


Figure 5.16: The average frequency response of SH-SAW device coated with the reproduced 1.25 μm -thick ($h = 0.031 \lambda$) 17.5% DIOA-PS coating normalized to a concentration of 1 ppm (1 mg/L) xylene in water with error bars representing the standard deviation of the measurements.

To determine the sensitivity, the frequency shift versus concentration curves were plotted for each chemical. Frequency shift was extracted from the baseline corrected data by using a MATLAB fitting program and the concentration was found from individual GC-PID measurements. Time constants for each BTEX compound were also extracted together with the frequency shifts. The time constants for benzene, toluene, ethylbenzene and xylene for 1.25 μm -thick 17.5% DIOA-PS coating are 100.7, 237.6, 576.2 and 648 seconds, respectively.

The slope of frequency shift versus analyte concentration curves represents the sensitivity for each chemical for the repeated 1.25 μm -thick 17.5% DIOA-PS coating. Fig.'s 5.17, 5.18 and 5.19 show the sensitivity curves for toluene, ethylbenzene and xylene respectively.

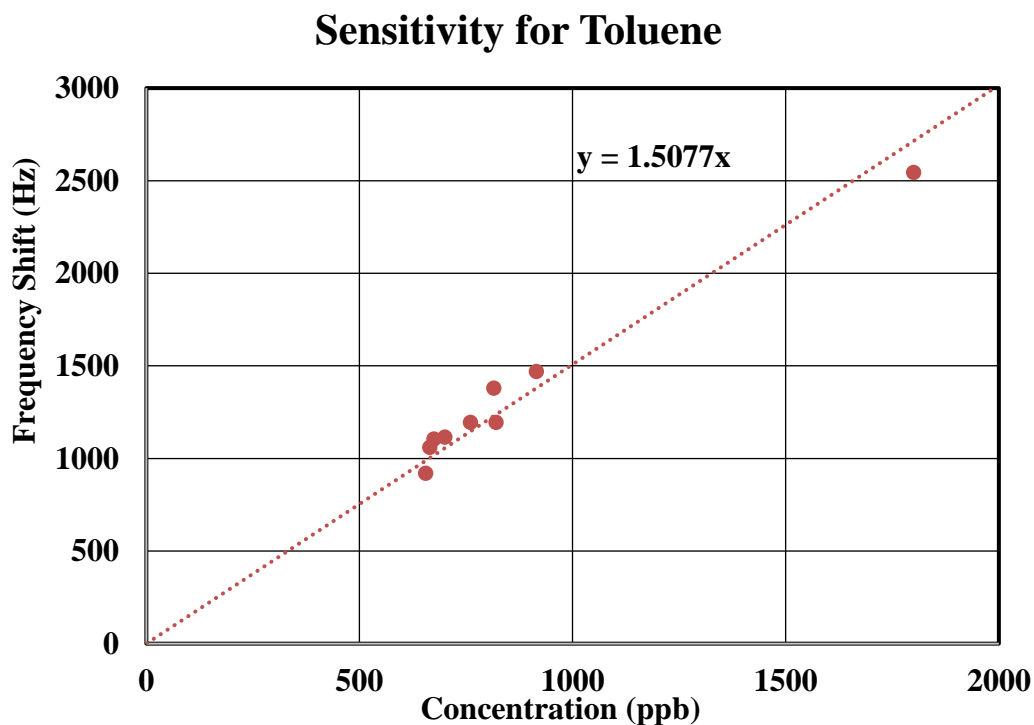


Figure 5.17: Measured frequency shift vs toluene concentration with a linear fit and zero intercept used for extracting sensitivity for the reproduced 1.25 μm -thick ($h = 0.031 \lambda$) 17.5% DIOA-PS coated SH-SAW sensor.

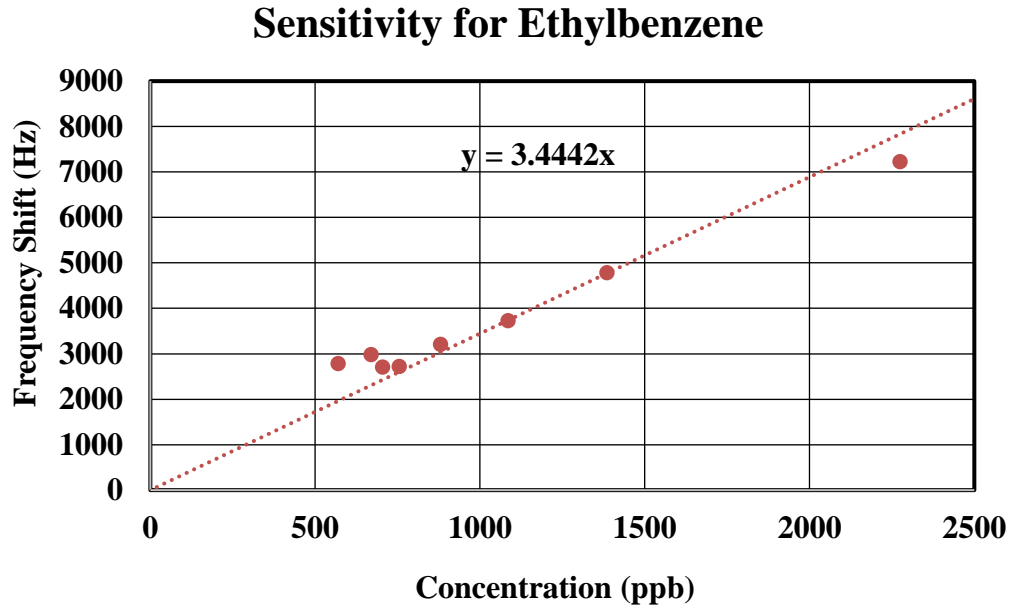


Figure 5.18: Measured frequency shift vs ethylbenzene concentration with a linear fit and zero intercept used for extracting sensitivity for the reproduced 1.25 μm -thick ($h = 0.031 \lambda$) 17.5% DIOA-PS coated SH-SAW sensor.

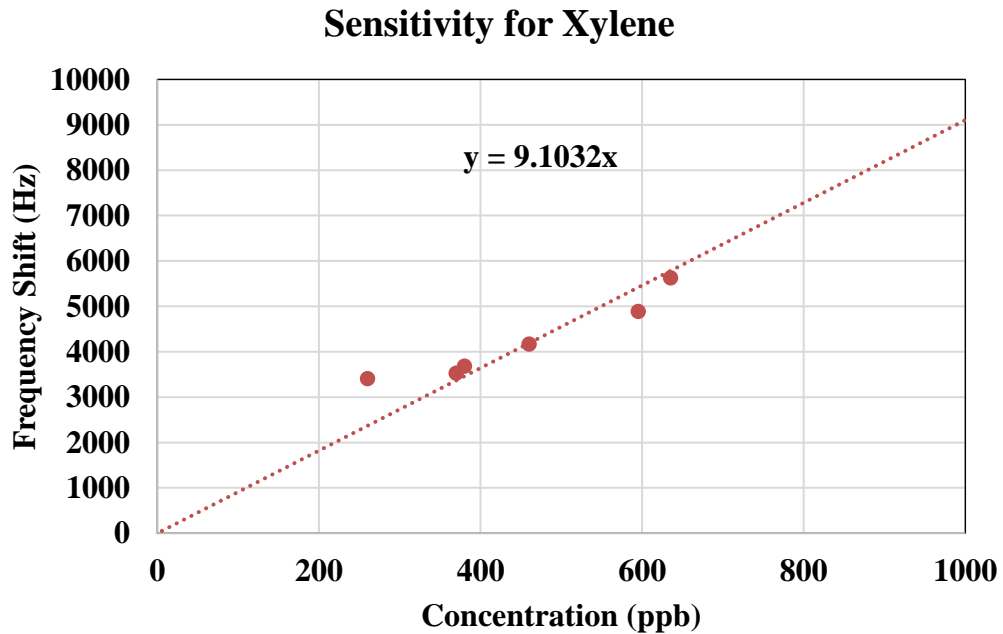


Figure 5.19: Measured frequency shift vs xylene concentration with a linear fit and zero intercept used for extracting sensitivity for the reproduced 1.25 μm -thick ($h = 0.031 \lambda$) 17.5% DIOA-PS coated SH-SAW sensor.

5.5 DIOA-PMMA and DINCH-PMMA

A second polymer, PMMA, was investigated for plasticizer-polymer coatings. This polymer has already been combined with some plasticizers for the purpose of liquid-phase hydrocarbon sensing in the literature [66], [67]. However, the long-term stability was not studied, and no DINCH-PMMA blends had been investigated. PMMA has a similar glass transition temperature compared to PS. DINCH-PMMA and DIOA-PMMA were studied for benzene detection using a SH-SAW sensor coating. The results for various plasticizer percentages and coating thicknesses for benzene concentrations ranging up to 5 ppm are summarized below in Table 5.

Table 5: Sensitivity to benzene for various coatings of DINCH-PMMA and DIOA-PMMA with several coating thickness.

Coating	Thickness	Loss	Sensitivity to Benzene
23% DINCH-PMMA 6% in TCE	0.6 μm	19 dB	Not significant
30% DINCH-PMMA 9% in TCE	1.5 μm	27 dB	Not significant
35% DINCH-PMMA 8% in TCE	1.0 μm	25-29 dB	Not significant
30% DINCH-PMMA 6% in Chloroform	0.5-0.9 μm	25 dB	Not significant
35% DINCH-PMMA 6% in Chloroform	0.7-1 μm	23 dB	Not significant
30% DINCH-PMMA 7% in Chloroform	1.0 μm	25-30 dB	Not significant
30% DINCH-PMMA 6.5% in Chloroform	0.6 μm	20 dB	Not significant
25% DIOA-PMMA 6.5% in Chloroform	0.9 μm	23 dB	Not significant
30% DIOA-PMMA 6.5% in Chloroform	0.95 μm	25 dB	Not significant

The results show that DINCH and DIOA plasticized PMMA are not very sensitive to benzene. Sensitivity to benzene is generally lower than that to the other aromatic compounds for polymer coated SH-SAW devices. Response of the DINCH-PMMA coating (e.g. 0.6 μm -thick 30.0%) to ethylbenzene was also investigated, and a significant sensitivity was found, ruling out the possibility that the coating is glassy. The observed low sensitivity of PMMA-plasticizer blends to BTEX analytes may instead be related to the

slightly high RED value listed in Table 1 for miscibility of PMMA and benzene. It is concluded that polystyrene is a better choice for this application due to its chemical structure giving it greater affinity to BTEX.

5.6 Ideal Plasticizer Percentage of Sensor Coatings

The ideal percentage of plasticizer in a polymer-plasticizer blend as well as the coating itself depends on the application. In an application where a low detection limit is very important, a coating with high sensitivity is ideal. In a different application where continuous monitoring is more important than the detection limit, long-term stability of the coating is most important. If a coating can be found which has high sensitivity and long-term stability it would be the ideal coating. Unfortunately for DIOA-PS coating blends, sensitivity and long-term stability have approximately an inverse relationship. The thin coating (0.7 μm) showed the longest (more than 3 months) stability but lowest sensitivity and the thick coating (1.25 μm) showed the highest sensitivity with only one month of stability, so there is a tradeoff between long term stability and sensitivity depending on the application. Also, for all coatings, sensitivity increases with coating thickness up to a certain thickness. For DIOA-PS blends, thickness has an impact not only on the sensitivity but also on the stability of the coating. Stability and repeatability of DIOA-PS coating blends depend on the mixing ratio of DIOA and PS as well as the thickness of the coating. Several experiments were conducted with various combinations of coating thicknesses and DIOA-PS mixing ratios to determine stability of the coating and repeatability of the sensor response (frequency shift). Based on these experiments, an

empirical figure of DIOA-PS coating stability as a function of coating thickness and plasticizer percentage was plotted and is shown below.

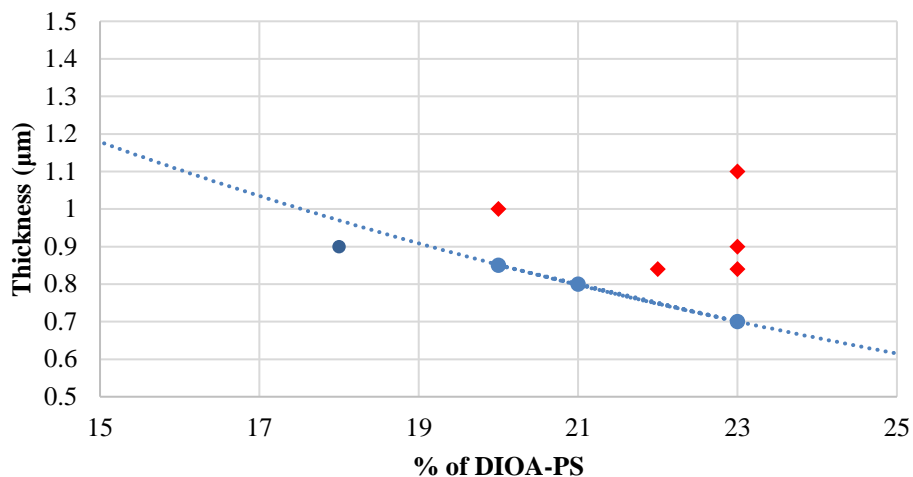


Figure 5.20: Results for coatings with various thicknesses and polymer-plasticizer (DIOA-PS) mixing ratios showing the stability of the coatings. All red points represent unstable coatings and all points on or below the dotted line are stable coatings that can produce repeatable sensor response.

In Fig. 5.20, the red points represent DIOA-PS sensor coating blends that were not stable or did not produce repeatable sensor responses. The blue points represent DIOA-PS sensor coating blends that were stable and produced repeatable sensor responses. It was expected that all the points that fall below the dotted line would produce stable DIOA-PS sensor coatings with repeatable sensor responses.

5.7 Pinhole Formation and Polymer Creep

Most sensor devices coated with polymer-plasticizer blends (DINCH-PS, DINCH-PMMA, DIOA-PS & DIOA-PMMA) showed coating degradation in various forms, including pinhole formation, polymer creep and aging of the coating over the period of measurements. In this work, it was shown that by adjusting the plasticizer's percentage in the blends as well as by adjusting the coating thickness, pinhole formation can be controlled to a certain degree, but it was not possible to eliminate it completely. Although the exact reason of pinhole formation is still unknown, some possible reasons could be contamination by organic materials on the surface of the sensor device or in the coating solution, microbubbles in the coating solution or polymer creep. Contamination can cause pinhole formation because it can affect the adhesion between the polymer coating and the surface of the device over time. In order to try to solve this contamination problem, all steps in the device cleaning procedure were done carefully and another additional cleaning step was added, but pinholes were still forming. As the devices were not cleaned and coating solutions were not prepared in a clean room environment, there may still be a possibility of contamination. To solve the microbubble problem, the coating solutions were allowed to stand for 24 hours after mixing and then used to coat the devices, but there were still pinholes. Another cause of pinhole formation could be the plasticizer-polymer mixing ratio and thickness of the coating. For DIOA-PS, with a higher percentage of DIOA in the blend, as well as higher thickness, pinholes tend to form quicker. For example, all the red points shown in Fig. 5.21 have pinhole formation occurring within about a week, but with a higher percentage of plasticizer and lower coating thickness or lower percentage of plasticizer and higher thickness the formation of

pinholes was slow. Higher percentages of plasticizer increase the mobility of the polymer chains, which can accelerate the rate of pinhole formation. It was noticed that for DIOA-PS coating blends with higher than 23 % DIOA-PS, the pinhole formation was very quick and the response of the coating was not repeatable. For thinner coatings, it was observed that the pinhole formation rate was slower and pinholes were not big enough to disturb the acoustic wave propagation decisively. In addition, the pinholes were not developed enough to reach the surface of the device and the SH-SAW was not highly attenuated. The 0.7 μm -thick 22.9% DIOA-PS coating was stable for more than 100 days. After 105 days when it was examined under a microscope, there were pinholes, but those pinholes were too small to increase the insertion loss. On the other hand, coatings with thickness of more than 1 μm have a tendency to form larger pinholes more quickly. The 17.5% DIOA-PS 1.25 μm -thick coating had the highest sensitivity but was only stable for one month. The microscopic views of the surface of the device before and after the measurements are shown below.

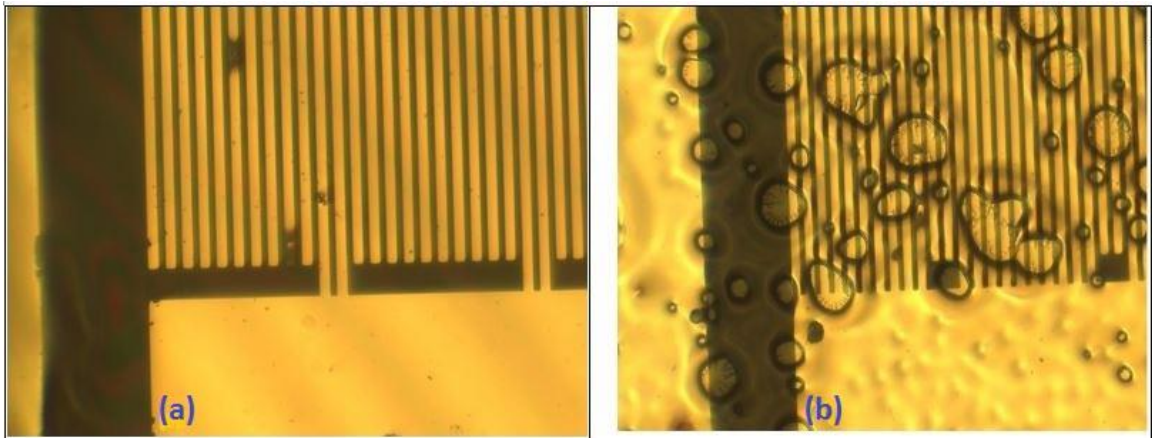


Figure 5.21: Left side (a): surface of a SH-SAW device coated with 1.25 μm -thick 17.5% DIOA-PS coating before the measurements; right side (b): surface of the same device after one month of measurements, seen under an optical microscope. Scale: the width of the IDT fingers (narrow golden lines) is about 5 μm .

There might be a possible way to solve or reduce the pinhole problem by using a more creep resistant polymer in the polymer-plasticizer blend. It is also known that an increase in molecular weight of a polymer tends to promote secondary bonding between polymer chains, thus making the polymer more creep resistant [82]. Thus, higher molecular weight and longer chain length of the polymer can be a possible solution to prevent or reduce the coating degradation. In the future, coating degradation could be further addressed by increasing polymer molecular weight or by addition of an adhesion promoter.

5.8 Improving Stability by Oxygen Plasma Treatment (OPT)

It is known that plasma treatment has the ability to modify the surface of a material in order to increase surface energy, bonding, printing, or wettability [83]. Oxygen plasma treatment is one common and low cost technique for plasma treatment because of the availability of oxygen. When oxygen gas is introduced into the plasma chamber, it is called oxygen plasma [84]. Oxygen plasma is usually used to clean a surface and along with other gases, it can be used to etch various materials. Oxygen plasma can also increase the bonding (i.e. increase cross-linking) inside the polymer materials. In a reported work [76], oxygen plasma was applied to treat a plasticized polymer film to prevent the leaching of plasticizer from the film. For DIOA-PS coatings, it was observed that when a device coated with DIOA-PS was subjected to continuous (10 to 12 hours) long-term measurement (over 30 days), the insertion loss showed a trend of improving which indicates slight leaching of plasticizer. It was decided to apply oxygen plasma treatment on the DIOA-PS coating to prevent leaching and observe the impact of the oxygen plasma treatment. In order to do that, two devices were coated with the same coating solution in the same environment at the same time. Later, one device

was treated by oxygen plasma and the other device was used without the oxygen plasma treatment. As shown in Fig. 5.22, the insertion loss of the device without the treatment of oxygen plasma changed by 2.5 dB and the loss of the device with oxygen plasma treatment was stable within ± 0.5 dB for more than 40 days. For future studies, oxygen plasma treatment can be a good choice to make stable coatings of DIOA-PS or other plasticizer-polymer coatings showing slight leaching of plasticizer.

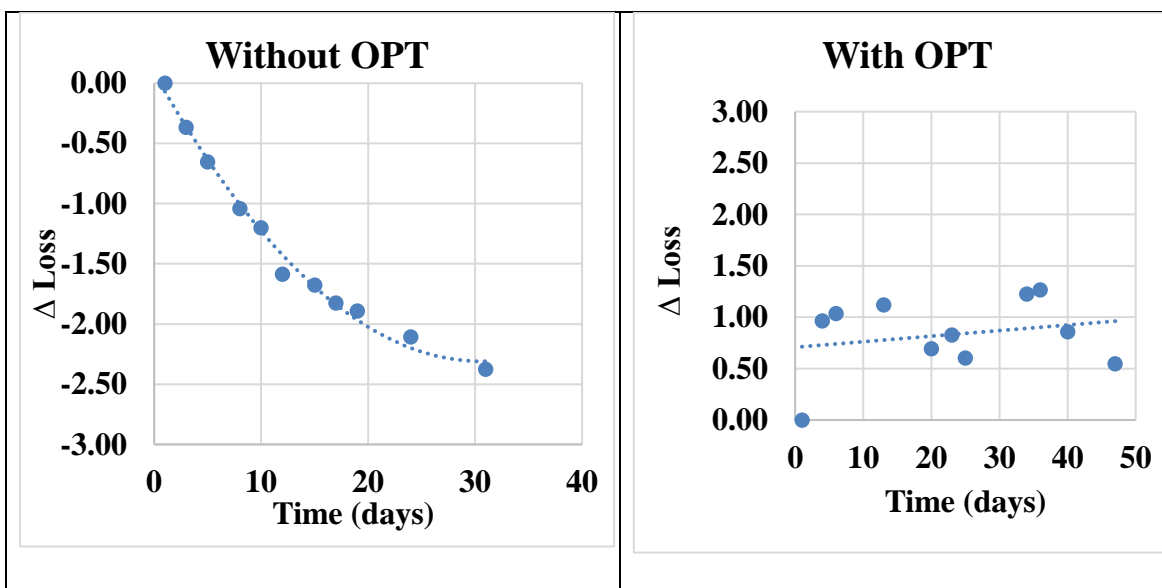


Figure 5.22: Change in insertion loss versus time, left: change in loss for a device without oxygen plasma treatment; right: change in loss for a device with oxygen plasma treatment.

5.9 Selectivity

DIOA-PS coatings were investigated for all BTEX compounds to determine the selectivity of the coatings. At first the optimum coating was determined for benzene detection and later that coating was reproduced to measure the sensitivity, selectivity and repeatability for all BTEX compounds. For DIOA-PS coatings, 17.5 % DIOA-PS with a thickness of 1.25 μm was considered the best choice for short term measurements up to about one month because it showed the highest sensitivity for benzene, and 22.9% DIOA-PS with a thickness of 0.7 μm was found to be optimal for long-term (more than 3 months) measurements. These two coatings were investigated for detection of toluene, ethylbenzene and xylene along with benzene. The Fig. 5.23 below shows the comparison of partial selectivity for polymer-plasticizer blends (1.25 μm -thick 17.5 % DIOA-PS, 0.7 μm -thick 22.9% DIOA-PS, 1.0 μm -thick 23% DINCH-PS [79]) with commercially available polymer coatings (0.6 μm -thick PECH, 0.8 μm -thick PIB [24]). For the 1.25 μm -thick 17.5 % DIOA-PS coating the sensitivity of toluene, ethylbenzene and xylene were 1.5 kHz/ppm, 3.4 kHz/ppm and 7 kHz/ppm, respectively, and for the 0.7 μm -thick 22.9% DIOA-PS PS coating the sensitivity of toluene, ethylbenzene and xylene were 515 Hz/ppm, 1.1 kHz/ppm and 1.6 kHz/ppm, respectively. For plotting the partial selectivity comparison curve, sensitivity for all BTEX compounds were normalized with respect to benzene sensitivity, analyte molecular weight and analyte solubility in water. From the Fig. 5.23, it is clearly seen that the ratios in the sensitivities to the different BTEX compounds for polymer-plasticizer blends clearly differ from those of commercially available polymer coatings, which is desirable when implementing a sensor array for identification and quantification of a mixture of BTEX compounds in water.

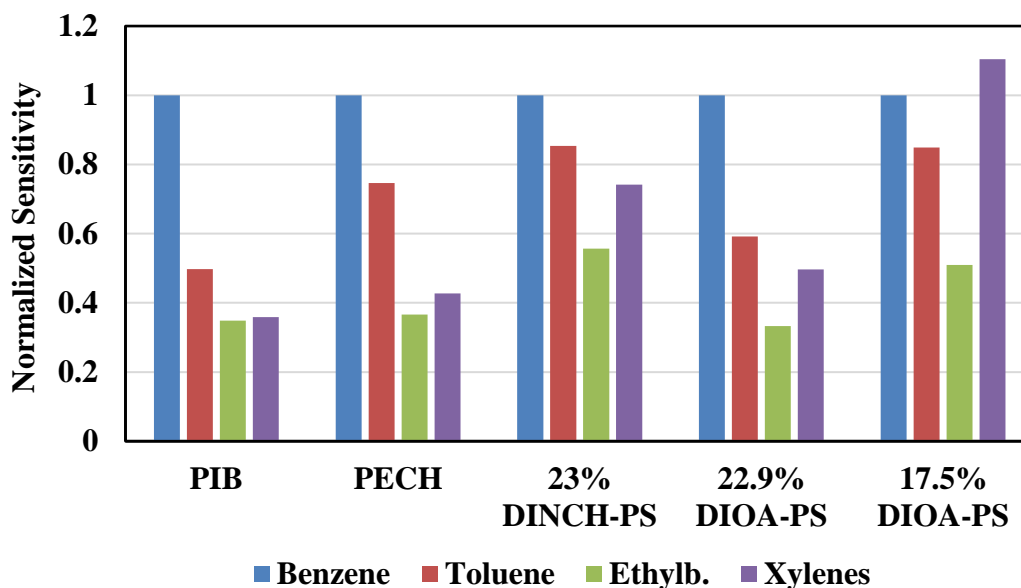


Figure 5.23: Partial selectivity comparison among various coatings (1.25 μm -thick 17.5 % DIOA-PS, 0.7 μm -thick 22.9 % DIOA-PS, 1.0 μm -thick 23% DINCH-PS, 0.6 μm -thick PECH and 0.8 μm -thick PIB). The average error on the sensitivity value is about ± 9 to 14%.

In order to determine the ability of a sensor system to distinguish among various BTEX analytes, a radial plot was created using eight input parameters, specifically the time constants and the ratios between the sensitivities measured for various polymer and polymer-plasticizer coatings. Fig. 5.24 shows the radial plot for 1.25 μm -thick 17.5 % DIOA-PS, 1.0 μm -thick 23% DINCH-PS, 0.6 μm -thick PECH and 0.8 μm -thick PIB coatings for benzene, toluene and ethylbenzene.

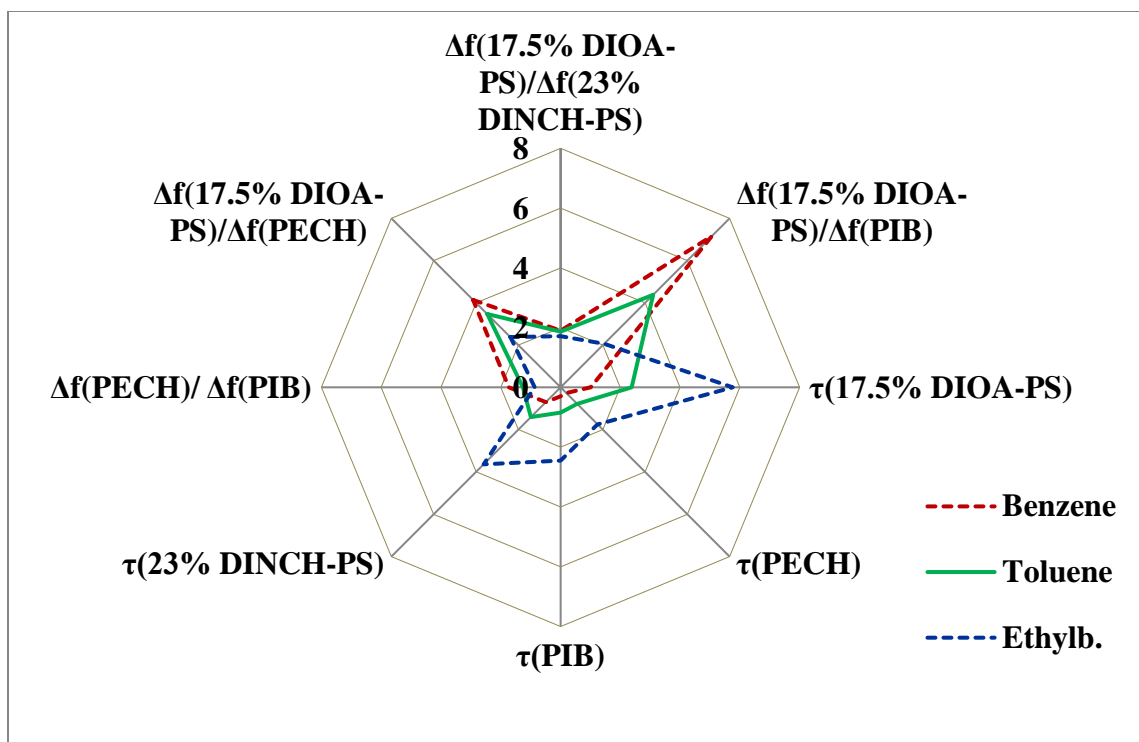


Figure 5.24: Radial plot showing the response time constant, τ (in units of 100 s), and the ratios of frequency shift, Δf of devices coated with various coatings for benzene, toluene and ethylbenzene.

By using both the steady-state (sensitivity) and transient (time constant) response information of SH-SAW sensors coated with polymer (PIB and PECH) and polymer-plasticizer blends (DIOA-PS and DINCH-PS), the radial response patterns were obtained for benzene, toluene and ethylbenzene and are shown to be easily distinguishable from each other. In the response patterns shown in Fig. 5.24, it is noticeable that the response time of benzene, toluene and ethylbenzene are better separated than the ratios of frequency shifts. Also, it can be noticed that the ratios of sensitivities of polymer-plasticizer vs. polymer coatings are better separated than those of polymer coatings or polymer-plasticizer blends. Therefore, in order to design a sensor array with many coatings for the purpose of analyte detection and identification in a mixture of analytes, it

will be better to choose at least one polymer and at least one polymer-plasticizer blend for the coatings instead of only polymers or only polymer-plasticizer blends.

5.10 Sensitivity Comparison

One of the goals for this research was to find as many suitable coatings for SH-SAW sensors as possible with high sensitivity for the BTEX compounds. The sensitivities and time constants of the investigated polymer-plasticizer blends are compared with those of the existing polymer coatings in the table below.

Table 6: Summary of the investigated coatings together with commercially available coatings showing response time constants and sensitivities for BTEX compounds

Coatings	Benzene		Toluene		Ethylbenzene		Xylene	
	τ (s)	Hz/ppm	τ (s)	Hz/ppm	τ (s)	Hz/ppm	τ (s)	Hz/ppm
PECH (0.6 μm)	26.5	110	77.6	435	174.8	1450	175	1450
PIB (0.8 μm)	29.3	63	84.2	345	244.8	1670	245	1670
23% DINCH-PS (1.0 μm)	69.6	237	140.4	810	363.9	2010	358	2520
17.5% DIOA-PS (1.25 μm)	100.7	450	237.6	1510	576.2	3445	648	9103
22.9% DIOA-PS (0.7 μm)	44.7	220	99	515	268	1110	271	1545

Frequency shift and time constant were extracted from the frequency response curve by using a MATLAB fitting program. Sensitivity is defined as frequency shift per unit concentration of a specific analyte. Furthermore, it is important to remember that time constant and response time to equilibrium (time to reach steady state) are two different parameters as defined in chapter one. Time constants for each sensor coating are different for each analyte which is important to consider when designing a sensor array. As the time constants for ethylbenzene and xylene are similar, they can be grouped together in

the analysis of multiple analyte mixtures. Note that the xylene analyte used in this work is a mixture of the three xylene isomers (m-xylene, o-xylene and p-xylene) and also contains ethylbenzene.

Fig. 5.25 shows the comparison of measured frequency shifts as a function of benzene concentration for 1.25 μm -thick ($h = 0.031 \lambda$) 17.5% DIOA-PS, 1.0 μm -thick ($h = 0.025 \lambda$) 17% DIOA-PS and 0.7 μm -thick ($h = 0.0175 \lambda$) 22.9% DIOA-PS coatings with 1.0 μm -thick ($h = 0.025 \lambda$) 23% DINCH-PS, 0.8 μm -thick ($h = 0.020 \lambda$) 20.9% DINCH-PS [5], 0.8 μm -thick ($h = 0.020 \lambda$) PIB, and 0.6 μm -thick ($h = 0.015 \lambda$) PECH coatings [85] for SH-SAW devices. A linear fit was added to each data set to represent the sensitivity and steeper slopes refer to higher sensitivity to benzene.

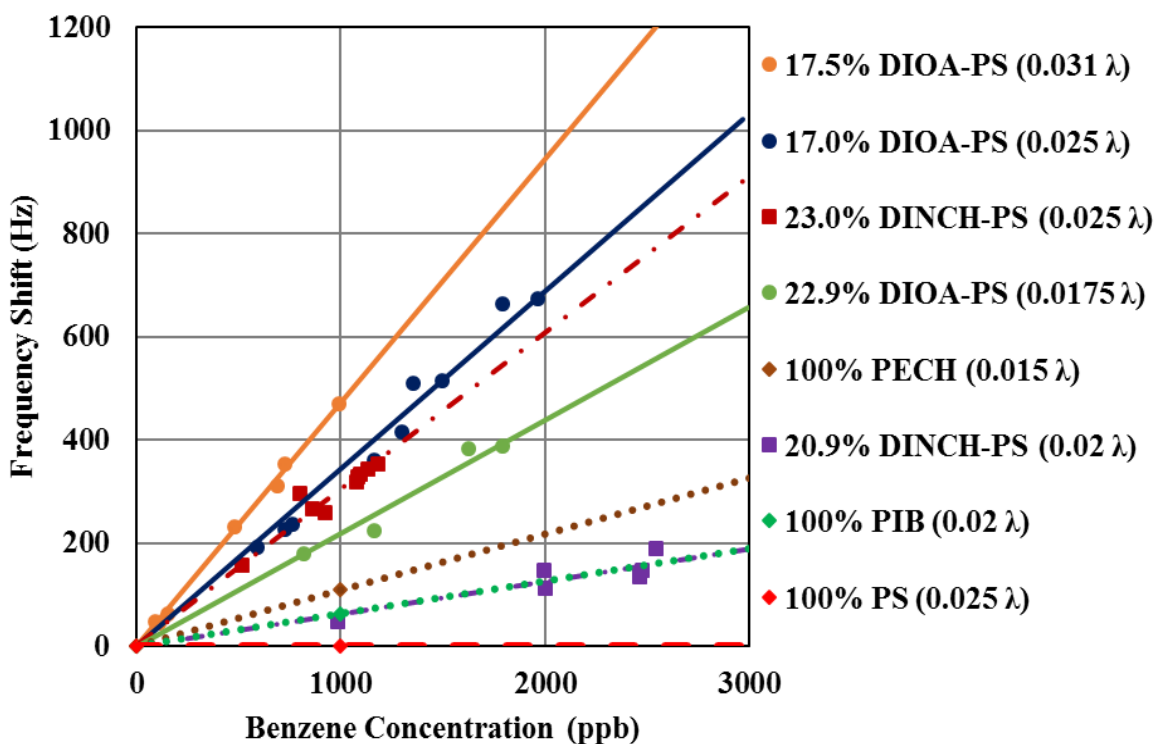


Figure 5.25: Comparison of frequency shift response as a function of benzene concentration for SH-SAW devices coated with various investigated polymer-plasticizer coatings and commercially available polymer coatings. Thickness of each coating is given in parentheses.

From Fig. 5.25, it is clear that 17.5% DIOA-PS with 1.25 μm thickness has the highest sensitivity to benzene. This coating is best for short term measurements because its stability is limited to a period of about one month. On the other hand, the polymer coatings PIB and PECH showed long-term stability but have lower sensitivity compared to polymer-plasticizer blends [85], [86]. Note that coating thicknesses are different in this comparison because the optimum thickness of each coating was used for the measurements. Optimum thicknesses are different for each coating and are determined based on sensitivity and repeatability of the sensor responses. Among commercially available polymers, unplasticized PS is not sensitive to benzene, PIB and PECH are sensitive to benzene but are relatively soft and show high acoustic-wave attenuation, thus limiting the maximum coating thickness that can be used. For the plasticizer-polymer blends, the type and percentage of plasticizer in the blend affect the glass transition temperature, the free volume, and the viscoelastic properties of the coating, and ultimately its long-term stability. The polymer-plasticizer blends allow to adjust the shear modulus of the coating by varying the polymer-plasticizer mixing ratio; this enables the use of thicker coatings with larger analyte sorption capacity and, ultimately, higher sensitivity. Note that the thicker polymer is not necessarily *acoustically* thicker, because the criterion for separating acoustically thin and thick coatings depends not on the absolute coating thickness but on the ratio of coating thickness over shear modulus of the polymer [48]. A thicker coating also leads to better electric shielding of the IDTs from the analyte sample, which is particularly important if the sample is electrically conducting (e.g., groundwater, brackish water). For these reasons, the polymer-plasticizer coatings can be used at larger thicknesses than the commercially available polymer coatings and,

therefore, can achieve higher sensitivities. Even taking into account differences in coating thickness, the plasticizer-polymer blends show greater analyte sorption capacities than the commercially available polymers, indicating they are rubbery in the low-frequency range as desired. The shear moduli of the coatings produced from plasticizer-polymer blends have not been measured, as this would be beyond the scope of this investigation.

However, tracking the insertion loss of the devices led to the conclusion that the plasticizer-polymer blends can be used with larger coating thicknesses, indicating that they have a lower loss modulus, G'' , than the commercially available polymers ($\sim 3 \times 10^8$ Pa for PIB [24]) and are glassy at the operating frequency of the sensor device. Among the commercially available sensor coatings, only PECH has good sensitivity with long-term stability for detection of benzene in groundwater. Therefore, if an array of sensors with different coatings is desired, the polymer-plasticizer blends represent valuable alternatives for such an array, permitting increased overall selectivity and accuracy.

6. SUMMARY, CONCLUSIONS AND FUTURE WORK

6.1 Summary

The goal of this research work was to investigate polymer-plasticizer blends to create suitable coatings for SH-SAW sensor devices for in-situ monitoring of BTEX chemicals in water. The results presented in chapter five show that polymer-plasticizer blends can be employed as sensitive coatings for SH-SAW sensors to detect organic compounds, particularly benzene, toluene, ethylbenzene, and xylene in water within some concentration ranges. A polymer-coated sensor platform was used, and the coating was the main focus of this research. For the coating, various polymer-plasticizer blends including DIOA-PS, DIOA-PMMA, and DINCH-PMMA were studied. Various polymer-plasticizer mixing ratios combined at various coating thicknesses were tested to characterize sensitivity, repeatability, long-term stability, selectivity and reproducibility of the coated sensor devices.

Among the investigated sensor coatings, the 1.25 μm -thick (0.031λ) 17.5% DIOA-PS coating showed the lowest detection limit (45 ppb) for benzene due to the high sensitivity (480 Hz/ppm) and low RMS noise for the sensor coating. The sensitivities of the device coated with this coating for toluene, ethylbenzene, and xylene were 1.5 kHz/ppm, 3.4 kHz/ppm, and 7 kHz/ppm respectively. This coating has been shown to be ideal for short term measurements up to one month, with negligible degradation and leaching. The sensor coating was reproduced within experimental error on multiple devices to confirm consistent sensitivity and detection limit.

The motivation for this research was described, and the problem of BTEX exposure in the environment and groundwater contamination was discussed. As potential tools for the application of in-situ groundwater monitoring, the shear horizontal surface acoustic wave (SH-SAW) sensor platform along with other sensors were described briefly. Due to the high sensitivity to surface perturbations and ability to perform well in liquid environments, the SH-SAW sensor platform was chosen for this research. The theory for an SH-SAW device was reviewed to explain the sensor response to the analyte sample. Then, the coating was discussed in detail, the polymer and plasticizer materials as coating materials were investigated, and the relative energy difference (RED) values of the polymer-plasticizer materials with the solvent and BTEX compounds were calculated from the Hansen solubility parameters of materials to predict the sensor response.

Various mixing ratios and coating thicknesses were investigated for DIOA-PS, DIOA-PMMA, and DINCH-PMMA to optimize sensitivity and long term stability. A complete description of the experimental procedure including device preparation, coating preparation, BTEX analyte sample preparation, and confirmation of sample concentration can be found in chapter iv. Experiments were conducted to evaluate the sensitivity, repeatability and stability of each coating for all BTEX chemicals, while at the same time insertion loss at the operating frequency was tracked to determine the coating degradation. After each experiment, concentration of each analyte sample was measured using a GC-PID to independently confirm the concentration. Sensitivity and detection limit for each analyte were calculated by using the concentration from GC-PID and the RMS noise computed from the frequency response.

For DIOA-PS, various percentages of DIOA (22.9%, 17%, 17.5%) in the blend were studied to find the optimal coating. Once an optimal coating in terms of sensitivity, repeatability and stability was determined for benzene, the coating was reproduced to measure the sensitivity for other BTEX compounds along with benzene. The 1.25 μm -thick (0.031 λ) 17.5% DIOA-PS coating showed the lowest detection limit (45 ppb) for benzene due to the highest sensitivity (480 Hz/ppm) and the 1.0 μm -thick (0.025 λ) 17% DIOA-PS coating showed high sensitivity (378 Hz/ppm) with one month of stability. In addition, the 0.7 μm -thick (0.0175 λ) 22.9% DIOA-PS coating showed long term stability over 100 days with good sensitivity (220 Hz/ppm).

Other polymer-plasticizer blends (DIOA-PMMA, DINCH-PMMA) were examined to find more suitable coatings for BTEX detection. Various mixing ratios and coating thicknesses for DIOA-PMMA and DINCH-PMMA were produced and tested with benzene analytes, but none of them showed significant response to benzene. Ethylbenzene was also tested to evaluate the response of those coatings, and it was found that those coatings are sensitive to ethylbenzene. The mechanical properties of the coatings were also investigated in terms of the sensor response by tracking the insertion loss of the acoustic wave device. This is because the device electrical properties are a function of the shear modulus of the coatings.

After data collection, signal and data processing were conducted for all responses collected from the vector network analyzer by using MATLAB and Excel. The frequency response was first corrected for baseline drift, and later by using a MATLAB fitting program, equilibrium frequency shift and time constant were extracted. Analyte concentrations obtained from independent measurement by GC-PID were used to

calculate the sensitivity and detection limit. The sensitivity and time constant for the investigated coated devices along with existing coatings for all BTEX compounds are summarized in table 6 in chapter 5.

6.2 Conclusions

It was determined that polystyrene (PS) is a better polymer choice than PMMA for detection of benzene using plasticized polymer coatings. Plasticized PMMA blends showed no significant sensitivity to benzene whereas the sensitivity to benzene of plasticized polystyrene was found to depend strongly on the mixing ratio of the blends. The affinity for polystyrene to benzene can be explained by the high miscibility between polystyrene and benzene. This may be related to the structure of polystyrene monomers, which include a phenyl ring, and to the fact that PS is synthesized from less polar monomers than PMMA.

Generally, the mixing ratio and thickness have been adjusted to obtain a coating that is rubbery at low frequencies, enabling large analyte sorption capacity, but glassy at the operating frequency of the sensor device, ensuring low acoustic-wave attenuation, with the former condition given greater importance for short-term measurement applications and the latter given greater importance for long-term measurements.

It was found that, by adjusting the polymer-plasticizer mixing ratio, the shear modulus of polymer-plasticizer blends can be optimized, enabling the use of thicker coatings with higher sensitivity than commercially available polymers. Higher long-term stability can also be achieved with many polymer-plasticizer blends, making them ideal sensor coatings for long-term deployment in aqueous phase. The ability to tune the

sensitivity and stability characteristics by adjustment of the plasticizer percentage and coating thickness is an attractive choice over commercially available polymers where only coating thickness can be adjusted. The final goal of this research is to use an array of sensors with different sensor coatings for increased selectivity in BTEX detection and for increased reliability in benzene identification and quantification. The results presented here indicate that both various DIOA-PS coatings along with DINCH-PS, PIB and PECH would be excellent candidates for the implementation of a sensor array. As demonstrated in Fig. 5.24, combining polymer-plasticizer coatings and unplasticized polymer coatings in a sensor array has a beneficial effect on the selectivity of the array. This is particularly important because of the very limited number of commercially available polymers identified as suitable for benzene detection in long-term aqueous-phase measurements.

The work showed that a glassy polymer (PS) can be used as a suitable coating for BTEX detection after addition of an appropriate plasticizer. It is possible to obtain a coating with the desired characteristics by choosing a suitable plasticizer with very low or undetectable leaching rate, an appropriate percentage of plasticizer and coating thickness. In addition, the plasticized polymer coatings have shown good partial selectivity for BTEX chemicals in liquid. Thus, by using these coatings along with appropriate sensor signal processing [87], it is possible to design a sensor system that can detect and quantify BTEX compounds in water with high sensitivity and selectivity in the presence of other interferences.

6.3 Future Work

For future work, polystyrene is a good choice for plasticized polymer sensor coatings for benzene detection. Because of the high sensitivity to benzene, it was thought that plasticized polystyrene will also have high sensitivity to other BTEX compounds, and this was confirmed by initial measurements presented in this work. To further enhance long term stability of the plasticized polystyrene coating blends, a higher molecular weight polystyrene sample should be investigated. In addition, other plasticizers with low leaching rates in water should be studied as additives to polystyrene to investigate sensitivity and long-term stability for BTEX detection in liquid.

During the research work of plasticized polymer coatings, one issue remains partly unsolved – the pinhole problem. To solve this problem, one possible approach will be to use polystyrene with higher molecular weight. The molecular weight of polystyrene used for this work was 35000 g/mol. It is known that an increase in molecular weight of a polymer tends to promote secondary bonding between polymer chains, thus making the polymer more creep resistant [82]. As a result, a plasticized polymer with higher molecular weight may create pinholes slower than the polymer with lower molecular weight. Polystyrene with molecular weight 280000 g/mol has been purchased, and testing of the resulting coating has started. For future study, polystyrene with various higher molecular weights will be investigated to solve the pinhole issue.

In addition, it has been found that for continuous long-term study of DIOA-PS coatings, the insertion loss shows a trend to change slightly, which indicates instability of the coating, potentially due to slow leaching of plasticizer. To solve this issue oxygen

plasma treatment (OPT) was used and for future study, this OPT will be further studied to prove the effectiveness of the treatment.

Furthermore, plasticizer with higher molecular weight and greater chain length will be investigated, mixed with polystyrene. A plasticizer, DIDA, with higher molecular weight and greater chain length, but similar structure as DIOA was found. Measurements on plasticized polymer coatings for DIDA-PS have started and will be continued. It may be possible to find more suitable coatings with DIDA-PS blends, and DIOA with higher molecular weight of PS.

Finally, to improve the adhesion of the coating, the addition of an adhesion promoter will be investigated. In addition, before coating with polymer-plasticizer blends, a very thin layer (0.1 μm) of PMMA or another polymer with good adhesion on LiTaO_3 and on gold will be applied to the device. This thin layer will act as a glue between the plasticized polymer coating and the device, which might increase the adhesion and the long-term stability of the coating in water.

REFERENCES

- [1] Bureau of Environmental Health Health Assessment Section [online] available: <https://www.odh.ohio.gov/~media/ODH/ASSETS/Files/eh/HAS/btex.ashx>
- [2] BTEX CONTAMINATION [online] available: <http://www.saveballona.org/gasoilfields/btexGC.pdf>
- [3] EPA, Laws and Regulations, "Summary of the Safe Drinking Water Act"
Online: <http://www.epa.gov/laws-regulations/summary-safe-drinking-water-act>
- [4] Jacob Fraden, "Handbook of modern sensors: physics, designs and application," 4th ed. Springer; (September 29, 2010)
- [5] Committee on New Sensor Technologies: Materials and Applications, National Materials Advisory Board, Commission on Engineering and Technical Systems, National Research Council, Expanding the vision of sensor materials, Washington, D.C. : National Academy Press, 1995
- [6] Dorozhkin, L. M. and Rozanov, I. A., "Acoustic Wave Chemical Sensors for Gases," Analytical Chemistry, vol. 56, no. 5, pp. 399-416, 2001.
- [7] Grundler, P., Chemical Sensors: An Introduction for Scientists and Engineers Leipzig: Springer, 2007.
- [8] Ballantine, D. S.; White, R. M.; Martin, S. J.; Ricco, A.J.; Zellers, E. T.; Frye, G. C.; and Wohltjen, H.; Acoustic Wave Sensors, Theory, Design, and PhysicoChemical Applications, Academic Press, San Diego, 1997.
- [9] Acoustic Wave and Electromechanical Resonators : Concept to Key Applications Authors: Campanella, Humberto
online:http://web.b.ebscohost.com.libus.csd.mu.edu/ehost/ebookviewer/ebook/bmx1YmXzMyNDUxNF9fQU41?sid=b803d691-0235-4a4b-a0c2e65ba22f9b88@sessionmgr111&vid=9&format=EB&lpid=lp_i&rid=0

- [10] Piezo Systems, Inc., History of Piezoelectricity. Online: <http://www.piezo.com/tech4history.html>
- [11] R. M. White and F. W. Voltmer, Direct Piezoelectric coupling to surface elastic waves, *Appl. Phys. Lett.* 7 (1965) 314-316
- [12] Forum, edaboard, "Difference between SAW and BAW"online: <http://www.edaboard.com/thread103938.html>
- [13] J.W. Grate et al., "Acoustic Wave Microsensors", *Anal. Chem.* 65 (1993) 940A-948A
- [14] B. Drafts, "Acoustic Wave Technology Sensors", *IEEE Trans. Microwave Theory Tech.* 49 (2001) 795-802
- [15] Michael J. Tullier: Acoustic Sensors, from Detection and Food Safety Center of Auburn University. Online: <http://www.eng.auburn.edu/files/file1007.pdf>
- [16] Humberto Campanella, "Acoustic wave and electromechanical resonators concept to key application".
- [17] McMullan, C.; Mehta, H.; Gizeli, E.; Lowe, C.R. "Modelling of the mass sensitivity of the Love wave device in the presence of a viscous liquid," *J. Phys. D.: Appl. Phys.* 2000, 33(23), 3053-3059
- [18] Grate, J.W.; Wenzel, S.W.; White, R.M.; "Flexural plate wave devices for chemical analysis," *Anal. Chem.* 1991, 63, 1552-1561
- [19] Arnold K. Mensah-Brown, "Analysis of the detection of organophosphate pesticides in aqueous solutions using polymer-coated SH-SAW Device" PhD dissertation, 2010
- [20] Yamanouchi, K. and Takeuchi, M., "Applications for Piezoelectric Leaky Surface Waves," *Proc. 1990 IEEE Ultrasonics Symposium*, 1990, 1, 11-18

- [21] Zaromb, S. and Stetter, J. R., "Theoretical basis for identification and measurement of air contaminants using an array of sensors having partly overlapping selectivities," *Sensors and Actuators*, vol. 6, no. 4, pp. 225-243, Dec.1984
- [22] Vail, J.; France, D.; Lewis, B.;"Ground Water sampling," U.S. EPA.March 6, 2013; SESDPROC-301-R3; online:
<https://www.epa.gov/sites/production/files/2015-06/documents/Groundwater-Sampling.pdf>
- [23] I.M. Cozzarelli et al.: "Progression of natural attenuation processes at a crude-oil spill site: I. Geochemical evolution of the plume", *J. Contam. Hydrol.* 53 (2001) 369– 385
- [24] F. Bender, F. Josse, A. J. Ricco, "Influence of Ambient Parameters on the Response of Polymer-coated SH-Surface Acoustic Wave Sensors to Aromatic Analytes in Liquid-Phase Detection", *Joint Conference of the IEEE IFCS and EFTF Proc.*, 2011, pages 422-427.
- [25] Josse, F.; Bender, F.; Cernosek, R.W.; "Guided shear horizontal surface acoustic wave sensors for chemical and biochemical detection in liquids", *Anal. Chem.*, 2001, 73, 5937-5944
- [26] Kondoh, J.; Shiokawa, S. "A liquid sensor based on a shear horizontal SAW device," *Electronics and Communications in Japan, Part 2*, 1993, 76 (2), 69-81
- [27] C.E. Rodgers, *Permeation of gases and vapours in polymers*, in J. Comyn (ed.), *Polymer permeability*, Elsevier, New York, 1985, Ch 2, 29-34
- [28] Engan, H. *IEEE Trans. Sonics Ultrason.* 1975, 22, 395-401
- [29] Bristol, T.W.; Jones, W.; Snow, P.B.; Smith, W. R. *IEEE Ultrason. Symp. Proc.* 1972, 343 -345
- [30] F. Bender, R.E. Mohler, A.J. Ricco and F. Josse, "Analysis of Binary Mixture of Aqueous Aromatic Hydrocarbons with Low-phase-Noise Shear Horizontal

Surface Acoustic Wave Sensors Using Multi-electrode Transducer Designs”,
Anal.Chem.2014, 86, 11464-11471

- [31] Engan, H. Electron. Lett. 1974, 10, 395-396
- [32] Z. Li, "Guided Shear-Horizontal Surface Acoustic Wave (SH-SAW) Chemical Sensors for Detection of Organic Contaminants in Aqueous Environments," Dissertation --Marquette University, Milwaukee, 2005
- [33] R. Lenisa, "Chemically Sensitive Polymer Coatings for SH-SAW Sensors for the Detection of Benzene in Water," Thesis – Marquette University, 2013.
- [34] N. Naumenko, "Multilayered Structure as a Novel Material for Surface Acoustic Wave Devices: Physical Insight," in Acoustic Waves – From Microdevices to Helioseismology, Shanghai, Intech, 2011, p. 422.
- [35] Grate, J.W.; Zellers, E. T.; "The fractional free volume of the sorbed vapor in modeling the viscoelastic contribution to polymer-coated surface acoustic wave vapor sensor responses," Anal. Chem. 2000, 72, 2861-2868
- [36] Grate, J. W.; Klusty, M.; McGill, R.A.; Abraham, M.H.; Whiting, G.; Andonian-Haftvan, J.; "The predominant role of swelling-induced modulus changes of the sorbent phase in determining the responses of polymer-coated surface acoustic wave vapor sensors," Anal. Chem. 1992, 64, 610-624
- [37] Jones, Y. K.; Li,Z.; Josse, F.; Hossenlopp, J. M. "Quantitative characterization of the partitioning of aqueous analytes into a polymer coating," Proc IEEE Internat. Conf. Sensors, 2003, 946-951
- [38] Young, R. J.; Lovell, P. A. Introduction to Polymers, Chapman & Hall, London: 1991, p. 15
- [39] "How Plastics Are Made," 2005, from American Plastics Council website: http://www.plasticsresource.com/plastics_101/manufacture/how_plastics_are_made.html [2000, May 25]

- [40] Elastomer ‘adhesiveandglue.com’. Online:
<http://www.adhesiveandglue.com/elastomer.html>
- [41] Viscoelasticity, Online: <https://en.wikipedia.org/wiki/Viscoelasticity>
- [42] Viscoelastic behavior of polymer – ResearchGate Online:
<https://www.researchgate.net/file.PostFileLoader.html>
- [43] Macioce, P. “viscoelastic damping 101” from Roush Industries, Inc. website:
<https://www.roush.com/wp-content/uploads/2015/09/Insight.pdf>
- [44] Glass transition temperature, Tech Tip23:
<http://www.epotek.com/site/files/Techtips/pdfs/tip23.pdf>
- [45] Glass Transition:
<http://faculty.uscupstate.edu/llever/polymer%20resources/glasstrans.htm#glass>
- [46] Aklonis, John J.; MacKnight, William J. , “Introduction to Polymer Viscoelasticity”, John Wiley and Sons, Inc. 1983, 2nd ed
- [47] T. R. Crompton, United Kingdom: Rapra Technology Limited, 2006
- [48] Martin, S.J.; Frye, G. C.; and Senturia, S.D., “Dynamics and Response of Polymer-Coated Surface Acoustic Wave Devices: Effect of Viscoelastic Properties and Film Response,” *Anal. Chem.* 1994, 66, 2201-2219
- [49] D. Icoz, *Understanding Molecular and Thermodynamic Miscibility of Carbohydrate Biopolymers*, Ann Arbor, MI: ProQuest LLC, 2008.
- [50] Lewis, A.F. “The frequency dependence of the glass transition,” *Polym. Lett.* 1963, 1, 649-654.
- [51] PVC, “Plasticizer” online: <http://www.pvc.org/en/p/plasticisers>

- [52] e. George Wypych, Handbook of Plasticizers 2nd Edition, Toronto: ChemTech Publishing, 2012.
- [53] E.H. Immergut and H.F. Mark, "Principle of Plasticization", Polytech Institute of Brooklyn, Brooklyn, N.Y.
- [54] J. Coompon, Characterization of plasticizer-polymer coatings, Thesis, Milwaukee, WI: Marquette University, 2015. Master's Theses (2009 -). Paper 315. http://epublications.marquette.edu/theses_open/315
- [55] D.P. Gosh, "Plasticizer in cosmetic Technology". Online: <http://www.slideshare.net/vedg007/plasticizer-class-ppt>
- [56] Sears, J. K. and Darby, J. R. (1982). Mechanism of Plasticizer Action. John Wiley & Sons, New York, NY
- [57] J. Burke, "Solubility Parameters: Theory and Application," 3 August 2011. [Online]. Available: <http://cool.conservation-us.org/coolaic/sg/bpg/annual/v03/bp03-04.html>. [Accessed 16 November 2015].
- [58] Hansen, Charles (1967), "The Three Dimensional Solubility Parameter and Solvent Diffusion Coefficient and Their Importance in Surface Coating Formulation. Copenhagen: Danish Technical Press".
- [59] C. M. Hansen, "Solubility Parameters — An Introduction," in Hansen Solubility Parameters: A User's Handbook, CRC Press LLC, 2000 .
- [60] McGill, R. A.; Abraham, M. H.; Grate, J. W. "Choosing polymer coatings for chemical sensors," Chemtech 1994, 24 (9), 27-37
- [61] McGill, R. A.; "Choosing polymer coatings for gas and liquid chemical microsensors", reprinted from SPE ANTEC Indianapolis Proceedings May 5-10, 1996, 2080-2084

- [62] Grate, J.W.; Abraham, M.H.; "Solubility interactions and the design of chemically selective sorbent coatings for chemical sensors and arrays", *Sensors and Actuators, B*, 1991, 3, 85-111
- [63] A. Hierlemann et al., Effective Use of Molecular Recognition in Gas Sensing: Results from Acoustic Wave and in Situ FT-IR Measurements, *Anal. Chem.* 71 (1999) 3022-3035
- [64] Han, Jung H. (2005). *Innovations in Food Packaging*. Elsevier. Online version available at: <http://app.knovel.com/hotlink/toc/id:kpIFP00001/innovations-in-food-packaging/innovations-in-food-packaging>
- [65] J. Kastner, D. Cooper, M. Maric, P. Dodd and V. Yargeau, "Aqueous leaching of di-2-ethylhexyl phthalate and "green" plasticizers," *Science of the Total Environment*, no. 432, pp. 357-364, 2012
- [66] B. Pejčić, E. Crooke, L. Boyd, C. Doherty, A. Hill and M. Myers, "Using Plasticizers to Control the Hydrocarbon Selectivity of a Poly(Methyl Methacrylate)-Coated Quartz Crystal Microbalance Sensor," *Analytical Chemistry*, vol. 84, p. 8564–8570, 2012.
- [67] C. White, B. Pejčić, M. Meyers and X. Qi, "Development of a plasticizer-poly(methyl methacrylate)membrane for sensing petroleum hydrocarbons in water," *Sensors and Actuators B*, no. 193, pp. 70-77, 2014.
- [68] G. Wypych, *Handbook of polymers*, ChemTec pub., 2012.
- [69] Accudyne Test, HSP parameteres,
Online:https://www.accudynetest.com/solubility_table.html
- [70] Pirika, HSP application notes, Online:
<https://www.pirika.com/NewHP/PirikaE/TiO2.html>
- [71] Hansen Solubility Parameter, email communication with Dr Charles Hansen

- [72] Z. Li, Y. Jones, J. Hossenlopp, R. Cernosek and F. Josse, "Analysis of liquid-phase chemical detection using guided shear horizontal-surface acoustic wave sensors," *Analytical Chemistry*, vol. 77, pp. 4595-4603, 2005.
- [73] "Spin Coating Theory", 2012. [Online]. Available: <http://www.cise.columbia.edu/clean/process/spintheory.pdf>. [Accessed 19 June 2013]
- [74] F. Josse at Marquette University and R. Cernosek at Sandia National Laboratories.
- [75] D. Technologies, "Hand-Held Gas Chromatography," Defiant Technologies, 2015. [Online]. Available: www.defiant-tech.com/frog-4000.php. [Accessed 17 November 2015].
- [76] Xiaoxian Zhang, Zhan Chen, "Observing Phthalate Leaching from Plasticized Polymer Films at the Molecular level", *ACS, Langmuir* 2014, 30, 4933-4944.
- [77] T. Newman, F. Josse, A. Mensah-Brown and F. Bender, "Analysis of the Detection of Organophosphate Pesticides in Aqueous Solutions Using Polymer-Coated SH-SAW Sensor Arrays," in *European Frequency and Time Forum & International Frequency Control Symposium (EFTF/IFC)*, Prague, 2013.
- [78] IUPAC, "Time Constant," Online: <http://goldbook.iupac.org/T06376.html> [Accessed October 2016].
- [79] Alderson, Laura Jeanne, "Investigation of the Use of a Plasticizer-Polymer Sensor Coating with Improved Long-Term Stability in the Liquid Phase" (2016). Master's Theses (2009 -). Paper 345. http://epublications.marquette.edu/theses_open/345
- [80] A Micro-GC Based Chemical Analysis System, Defiant Technologies, Inc., 2014; [www.defiant-tech.com/pdfs/Pittcon 2014 A Micro-GC Based Chemical Analysis System.pdf](http://www.defiant-tech.com/pdfs/Pittcon%202014%20A%20Micro-GC%20Based%20Chemical%20Analysis%20System.pdf).

- [81] Voinova M.V.; Rodahl M.; Jonson M.; Kasemo B., Viscoelastic Acoustic Response of Layered Polymer Films at Fluid-Solid Interfaces: Continuum Mechanics Approach. *Physica Scripta*. Vol. 59, 391-396, 1999
- [82] M.A. Meyers, K.K. Chawla, "Mechanical Behavior of Materials", Cambridge University Press, New York, 2nd edition, 2009, p. 690
- [83] Plasma Tech, "Plasma Surface Treatment," Online:
<http://www.plasmaetch.com/plasma-surface-treatments.php>
- [84] Plasma Tech, "Oxygen Plasma treatment" online:
<http://www.plasmaetch.com/oxygen-plasma-treatment.php>
- [85] F. Bender, R. E. Mohler, A. J. Ricco, F. Josse, "Identification and Quantification of Aqueous Aromatic Hydrocarbons Using Acoustic Wave Sensors", *Anal. Chem.* 2014, 86, 1794-1799
- [86] F. Bender, F. Josse, R. E. Mohler, A. J. Ricco, "Design of SH-Surface Acoustic Wave Sensor for Detection of ppb Concentrations of BTEX in Water," *IEEE IFCS*, PP.628-631,2013
- [87] Sothivelr, K.; Bender, F.; Josse, F.; Ricco, A. J.; Yaz, E. E.; Mohler, R. E.; Kolhatkar, R. Detection and Quantification of Aromatic Hydrocarbon Compounds in Water Using SH-SAW Sensors and Estimation-Theory-Based Signal Processing. *ACS Sens.* 2016, 1, 63-72.